Scuola di Ingegneria Civile, Ambientale e Territoriale

Corso di Studio in Ingegneria Civile

Laurea Magistrale in Ingegneria Geotecnica

Numerical modelling of ground movements induced by tunnel excavation: the use of simple constitutive models for the short-term response of stiff clays

Candidata: Andrea Benedetta Perrone

Matricola: 784349

Relatore: Prof. Giancarlo Gioda

Correlatore: Dott. Ing. Marco Redaelli

Anno Accademico 2015-2016

Index

Abstract **8**

1 Introduction **9**
1.1 Prediction of ground movements due to tunnel excavation 9
1.2 Available analytical methods for green-field conditions 10
1.2.1 Fine-grained and coarse-grained soils 10
1.2.2 Gaussian settlement trough 11
1.2.3 Surface settlement trough: volume loss and the parameter *K* 12
1.2.4 Subsurface settlement profile 13
1.3 FEM and its limitations 14
1.4 This study 17
1.4.1 Motivation and research questions 17
1.4.2 Scope 17
1.4.3 Methodology 18
1.4.4 Resources 18

2 Case Histories **19**
2.1 Jubilee Line Extension tunnels at St. James's Park 19
2.1.1 Introduction 19
2.1.2 Geology 20
2.1.3 Hydrogeology 22
2.1.4 Geotechnical characterisation 23
2.1.4.1 Engineering description and geotechnical properties 23
2.1.4.2 Made Ground 23
2.1.4.3 Alluvium 24
2.1.4.4 River Terrace Gravel 25
2.1.4.5 London Clay 26
2.1.4.6 Lambeth Group 31
2.1.4.7 Summary 33
2.1.5 Construction and ground-movements monitoring 34
2.1.5.1 Overview 34
2.1.5.2 Excavation machine 34
2.1.5.3 Construction methodology 35
2.1.5.4 Observed displacements 36
2.2 Fleet Line tunnel at Green Park 38
2.2.1 Introduction 38
2.2.2 Monitoring 38
2.2.3 Ground profile 40

3 Numerical Analysis - Jubilee Line Extension **43**
3.1 Introduction 43
3.1.1 Overview 43
3.1.2 Ground model 43
3.1.3 Meshes 43
3.2 Calculations for the Westbound Tunnel 45
3.2.1 Introduction 45
3.2.2 Stress relief method 48
3.2.3 Alternative implementation of stress relief 51
3.2.4 Use of softened zones 56
3.2.5 Sensitivity to initial stress ratio 56
3.3 Calculations for the Eastbound Tunnel 61
3.3.1 Introduction 61
3.3.2 Stress relief method 62

3.3.3 Alternative implementation of stress relief 67
3.3.4 Use of softened zones 71
3.3.5 Sensitivity to initial stress ratio 71
3.4 Summary 75
3.4.1 Westbound tunnel 75
3.4.2 Eastbound tunnel 75

4 Numerical analysis - Fleet Line at Green Park 77
4.1 Introduction 77
4.1.1 Overview 77
4.1.2 Ground model 77
4.1.3 Plate parameters 79
4.2 Calculations for the Fleet Line tunnel 80
4.2.1 Key assumptions 80
4.2.2 Calculated settlement at ground surface 80
4.2.3 Calculated settlement at depth 84
4.3 Summary 84

5 Conclusions 85
5.1 Introduction 85
5.2 Key findings 85
5.2.1 Case histories 85
5.2.2 Short-term settlement at ground surface 86
5.2.3 Settlement at depth 87
5.2.4 Summary 87
5.3 Limitations 87
5.4 Recommendations 87
5.4.1 Recommendations to the users of the proposed approach 87
5.4.2 Recommendations for future studies 88

References 89

Appendix A 93
A.1 Introduction 93
A.2 The Finite Element Method 93
Outline 93
Discretization 94
Displacement approximation 94
Requirement for a general solution 95
Numerical integration 95
Global equations 95
Boundary conditions 96
A.3 Application to geomechanics 96
Overview 96
Elasto-plasticity 97
Elastic-plastic calculations 97
Yield function 97
Plastic potential and flow rule 97
Non-linear solution methods 97
A.4 Implementation in PLAXIS 2D 99
Overview 99
Basic equations of continuum deformation 99
Elements 100
Integration method 100
Use of method and software in this thesis 100

List of Figures

Figure 1. Three-dimensional shape of surface trough and tunnel co-ordinate system (after Yeates 1985) 9

Figure 2. Gaussian settlement trough (source: Mair 2006) 11

Figure 3. Form of surface and subsurface settlement profile (Mair et al. 1993) 13

Figure 4. Summary of the results obtained by Dolezˇalova´ (2002). 15

Figure 5. 3D mesh used by Franzius et al. (2005) to study the Westbound tunnel of the Jubilee Line Extension. 15

Figure 6. Suite of results obtained by Franzius et al. (2005) with isotropic constitutive models. 16

Figure 7. Suite of results obtained by Franzius et al. (2005) with anisotropic constitutive models. 16

Figure 8. Jubilee Line Extension route, source: Page (1995). 19

Figure 9. JLE tunnels between Westminster and Green Park, plan view (source: Standing & Burland 2006) 20

Figure 10. Geological cross-section for the JLE tunnels between Green Park and Bermondsey (source: Burland et al. 2001). 21

Figure 11. Typical pore water pressure distribution in central London (source: Burland et al. 2001). 22

Figure 12. River Terrace Gravel grading envelope (source: Withers et al. 2001). 26

Figure 13. Longitudinal section across St James's Park and Westminster showing divisions of London Clay (source: Burland & Standing 2006). 27

Figure 14. Casagrande soil classification chart with results categorised by London Clay division source Standing and Burland (2006). 28

Figure 15. Profiles from each of the five boreholes across St James's Park 28

Figure 16 Undrained Young's modulus prepared by Burland & Kalra (1987). 29

Figure 17. Coefficient of earth pressure at rest k'_0 with depth 30

Figure 18. Envelope of E_u/S_u ratios vs. axial strain for the Lambeth Group. 31

Figure 19. Plan view and cross section of the JLE route (source: Davies 2000). 34

Figure 20. Open-face shield with backhoe (Mair & Dimmock 2007) 35

Figure 21. Cross-section of the precast concrete expanded tunnel lining, source: Davies, 1999 35

Figure 22. The method used in correspondence of the section instrumented for high precision monitoring (Mair & Dimmock 2007). 36

Figure 23. Instrumented section and tunnel position, source Burland and Standing (2006). 37

Figure 24. Vertical displacements profile above the Eastbound tunnel 37

Figure 25. Vertical displacements profile above the Westbound tunnel. 37

Figure 26. Example of shield used for tunnelling in stiff clays in the 1970s. 39

Figure 27. Monitoring system at Green Park (source: Attewell and Farmer 1974). 39

Figure 28. Ground conditions at Green Park (source: Loganathan & Poulos 1998); note that "this study" result refer to the work of Loganthan & Poulos (1998) and that "observed data" represent only one of several available data sets. 40

Figure 29. Ground parameters at tunnel level according to Longanathan & Poulos (1998) and observed settlements. 41

Figure 30. Vertical displacements at depth as a function of face advancement. 41
Figure 31. Maximum settlement and ultimate settlement at depth. 42
Figure 32. FEM for the Eastbound JLE tunnel at the instrumented section of St James's Park. 44
Figure 33. FEM for the Westbound JLE tunnel at the instrumented section of St. James's Park..... 45
Figure 34. WBT, Gaussian settlement trough based on the interpretation proposed by Standing & Burland (2006). 46
Figure 35. WBT, Gaussian settlement trough based on the interpretation adopted in this study. 47
Figure 36. WBT, stress relief method, k_0 = 1.25, deformed mesh. 48
Figure 37. Stress relief method, k_0 = 1.25, principal stresses around the tunnel..... 49
Figure 38. Stress relief method, k_0 = 1.25, principal stresses near the surface..... 49
Figure 39. Stress relief method, k_0= 1.25, plastic points. 50
Figure 40. Stress relief method, k_0 = 1.25, total displacements..... 50
Figure 41. Stress relief method, k_0 = 1.25, vertical displacements. 51
Figure 42. Stress relief method, k_0 = 1.25, vertical displacements at ground surface..... 51
Figure 43. Alternative method, k_0 = 1.25, vertical displacements at ground surface. 52
Figure 44. Alternative method, k_0 = 1.25, principal stresses around the tunnel..... 53
Figure 45. Alternative method, k_0 = 1.25, principal stresses around the tunnel..... 53
Figure 46. Alternative method, k_0 = 1.25, total displacements..... 54
Figure 47. Alternative method, k_0 = 1.25, vertical displacements. 54
Figure 48. Alternative method, k_0 = 1.25, plastic points. 55
Figure 49. Settlement profile: comparison between stress relief and alternative method. 55
Figure 50. Plastic zones employed in the analysis with softened material (reduction of stiffness and/or strength if the host formation): (a) traditional stress relief method; (b) alternative implementation (radial pressure)..... 56
Figure 51. Settlement profile: sensitivity to initial total stress ratio in stiff clays. 57
Figure 52. Stress relief method, k_0 = 0.5, deformed mesh..... 58
Figure 53. Stress relief method, k_0 = 0.5, principal stresses around the tunnel..... 58
Figure 54. Stress relief method, k_0 = 0.5, principal stresses near the surface..... 59
Figure 55. Stress relief method, k_0 = 0.5, plastic points. 59
Figure 56. Stress relief method, k_0 = 0.5, total displacement. 60
Figure 57. Stress relief method, k_0 = 0.5, vertical displacement. 60
Figure 58. Gaussian settlement trough based on the interpretation proposed by Standing & Burland (2006) for the instrumented section data. 61
Figure 59. Gaussian settlement trough based on the interpretation adopted in this study..... 62
Figure 60. Stress relief method, k_0 = 1.25, deformed mesh..... 63
Figure 61. Stress relief method, k_0 = 1.25, principal stresses around the tunnel..... 63
Figure 62. Stress relief method, k_0 = 1.25, principal stresses near the surface..... 64
Figure 63. Stress relief method, k_0 = 1.25, plastic points. 64
Figure 64. Stress relief method, k_0 = 1.25, total displacements..... 65

Figure 65. Stress relief method, k_0 = 1.25, vertical displacements. 65
Figure 66. Stress relief method, k_0 = 1.25, vertical displacements at ground surface..... 66
Figure 67. Alternative method, k_0 = 1.25, vertical displacements at ground surface. 67
Figure 68. Alternative method, k_0 = 1.25, principal stresses around the tunnel..... 68
Figure 69. Alternative method, k_0 = 1.25, principal stresses near the surface..... 68
Figure 70. Alternative method, k_0 = 1.25, total displacements..... 69
Figure 71. Alternative method, k_0 = 1.25, vertical displacements. 69
Figure 72. Alternative method, k_0 = 1.25, plastic points. 70
Figure 73. Settlement profile: comparison between stress relief and alternative method. 70
Figure 74. Settlement profile: sensitivity to initial total stress ratio in stiff clays. 72
Figure 75. Stress relief method, k_0 = 0.5, deformed mesh..... 72
Figure 76. Stress relief method, k_0 = 0.5, principal stresses around the tunnel..... 73
Figure 77. Stress relief method, k_0 = 0.5, principal stresses near the surface..... 73
Figure 78. Stress relief method, k_0 = 0.5, plastic points. 74
Figure 79. Stress relief method, k_0 = 0.5, total displacement. 74
Figure 80. Stress relief method, k_0 = 0.5, vertical displacement. 75
Figure 81. Analytical interpretation 77
Figure 82. FEM for Fleet Line tunnel in Green Park. 79
Figure 83. k_0 = 0.5, deformed mesh. 80
Figure 84. k_0 = 0.5, principal stresses around the tunnel. 81
Figure 85. k_0 = 0.5, principal stresses near the surface. 81
Figure 86. k_0 = 0.5, plastic points. 82
Figure 87. k_0= 0.5, total displacements. 82
Figure 88. k_0= 0.5, vertical displacements. 83
Figure 89. k_0 = 0.5, vertical displacements at ground surface. 83
Figure 90. Maximum settlement comparison at depth. 84

List of Tables

Table 1. Recommended values of coefficient K. 12
Table 2. Recommended equations for i. 13
Table 3. Schematic geological sequence in the London basin (simplified from Skipper et al. 2009). 21
Table 4. Geotechnical parameters of the Made Ground. 24
Table 5. Index properties of the Alluvium (CLAY). 25
Table 6. Geotechnical parameters of the Alluvium (CLAY). 25
Table 7. Geotechnical parameters of the River Terrace Gravel. 26
Table 8. Index properties of the London Clay. 29
Table 9. Geotechnical parameters of the London Clay. 30
Table 10. Geotechnical parameters of the Lambeth Group Clay. 32
Table 11. Summary of geotechnical parameters. 33
Table 12. Geotechnical parameters. 46
Table 13. Ground model for Green Park. 78
Table 14. Geotechnical parameters for Green Park. 78
Table 16. Key characteristics of the three case studies. 86

Abstract

This study discusses the possibility to calculate realistic green-field ground displacements induced by tunnelling in stiff clays with finite element analyses that do not employ advanced constitutive models. The focus is on the short-term response, which is generally associated with the largest differential settlements and distortions and is, therefore, the most impacting in pre-existing structures.

There tunnels have been selected as case studies and back-analysed though 2D finite element calculations: the Westbound and Eastbound tunnels of the Jubilee Line Extension at St. James's Park (London , UK) and the Fleet Line tunnel at Green Park (also in London).

2D plane strain calculations ware carried out for the case histories, initially with a fully realistic set of geotechnical parameters. All materials were modelled with linear elastic-perfectly plastic (LE/PP) constitutive models. The effect of plasticity in the ground was investigated by first identifying the plastic zones associated with the analyses with LE/PP models, then replacing the materials in these zones with a soil with lower mechanical properties. The settlement profiles obtained from analyses with a full set of realistic parameters did not match the data observed on site. Moreover, the introduction of softened zones did not improve the performance of the models.

Subsequently, the sensitivity to changes in the initial stress filed was investigated by reducing the ratio between horizontal and vertical total stress in the stiff clays. It was found that a stress ratio artificially reduced to $k_0 = 0.5$ in the stiff clays results in the calculation of realistic settlement profiles for the three cases considered. For the Fleet Line tunnel a good match between calculated and observed settlements at depth was also found.

The analysis of three case histories is not sufficient to demonstrate that the approach is universally valid. However, the low sensitivity of the settlement trough to variations in soil strength and stiffness suggests that the presented approach may be a first step toward the realistic numerical modelling with simple constitutive models of tunnelling-induced ground movements.

1 Introduction

1.1 Prediction of ground movements due to tunnel excavation

The current, ever increasing urban growth and development results in a congested subsoil with a number of underground constructions and services competing for space.

In order to allow the development of the underground space without impacting in an adverse manner the existing built environment, it is essential to accurately predict the settlements due to excavations. Of the various forms of underground excavations in urban areas, tunnels represent a particularly pervasive type.

When a tunnel is excavated movements take place in the surrounding ground; one of the results is the distortion of the ground surface in a deflected shape generally indicated as “settlement trough”. The subsoil between the ground surface and the tunnel is also subject to a similar deformation patters which, however differs from the one observed at the surface in terms of magnitude and extent in space of the settlement. The vertical displacement profile of any horizontal level between ground surface and tunnel is commonly indicated as “settlement trough at depth”.

Analytical models, based on the fitting of appropriate mathematical functions to data observed in past cases, are available to predict, with a good degree of confidence, the spatial extent and magnitude of tunnelling-induced settlement for a soil mass free from other structures (Page & Skipper 2000). These models are both analytical, in that they have an exact closed-form solution, and empirical, in that they are based on the observation of the ground response in past cases (no attempt is made to describe the physical process behind that response).

The complete absence of other structures, which is a pre-requisite for the use of this class of analytical/empirical models, is generally referred to as “green field” conditions (Peck 1969; Schmidt B. 1969; (Attewell et al. 1986).

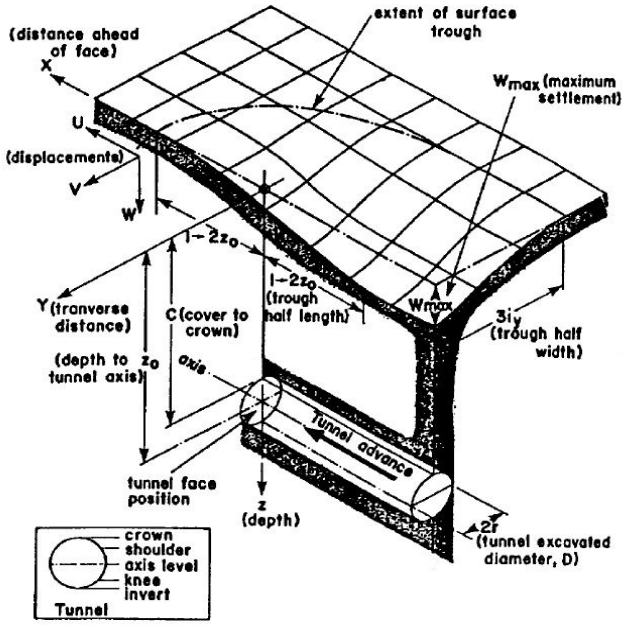

Figure 1. Three-dimensional shape of surface trough and tunnel co-ordinate system (after Yeates 1985)

Despite performing well in green field conditions, the analytical/empirical models are not suitable to study those cases of practical relevance in which the presence of existing structures and infrastructures interacts with the soil to modify the overall ground movement. It would be therefore highly desirable to

have an alternative analysis approach, possibly explicitly modelling the soil behaviour, which could deal with the interaction between the ground affected by tunnelling and pre-existing structures of arbitrary size and stiffness. In this respect, an obvious choice is the use of numerical methods for the analysis of continua, and in particular of the finite element method (Zienkiewicz 1977), which has been successfully employed to study a broad variety of soil-structure interaction problems in the context of geotechnical engineering at both academic and industrial level.

The first step in the use of the finite element method (FEM) to predict the impact of tunnelling on existing structure needs necessarily to be the demonstration that the method provide realistic results in the simpler green field case. So far, however, the credible modelling of tunnelling-induced settlement troughs with finite elements has proven surprisingly difficult. In fact, despite the availability of advanced constitutive models and three-dimensional (3D) numerical tools, FEM analysis regularly return troughs which are much wider and flatter then the observed data (Attewell *et al.* 1986; Doležalová 2002; Franzius *et al.* 2005).

Quite recently, some very refined and complex constitutive models have been able to achieve a good approximation of specific case histories. For example the three-surfaces kinematic hardening constitutive model, incorporating stiffness degradation and soil texture destructuration, proposed by Gonzalez *et al.* (2012) was able to accurately reproduce the short-term settlements observed immediately after the excavation of a tunnel in over-consolidated clay under St. James's Park, in London (UK).

The complexity of these constitutive models, however, places them well beyond the understanding of the vast majority of practicing geotechnical engineers. Moreover, the calibration of the large number of parameters required by this type of models is very challenging. The combination of complex formulation and challenging calibration makes this type of very advanced models extremely difficult to use in practice.

The aim of the present study is to systematically review the results which can be obtained via finite element analysis in order to identify the simplest possible methodology usable by geotechnical practitioners to obtain satisfactory results.

Encouraging evidence is provided by the observation that to force the models to approach the observed data is to adopt an artificially low coefficient of earth pressure at rest k'_0. This modification emphasises the "squatting" of the tunnel and produces a narrower, deeper trough which is closer to the observed data.

A positive precedent also lies in the work of Gioda & Locatelli (1999) who efficiently back analysed settlements generated by a tunnel in sand by using a simple elasto-plastic model in which the modulus of elasticity and the friction angle of the sand decreased with increasing plastic shear strains.

1.2 Available analytical methods for green-field conditions

1.2.1 Fine-grained and coarse-grained soils

Tunnelling in soft ground generates significant ground movements, which are manifest at the surface in a trough centred over the tunnel and extending in front of the advancing face, as shown in Figure 1.

In fine-grained soils (clays and silts) two distinct phases of ground movements are commonly recognised:

- an instantaneous movement, which takes place as the tunnel is excavated, associated with the undrained response of the soil

- a long term, time-dependent movement, which develops after the tunnel construction due to consolidation of the soil and to viscous phenomena.

In coarse-grained soils (sands and gravels) the permeability is sufficiently high to ensure a drained response of the material and all movements take place immediately during construction.

Settlements caused by tunnelling have been widely researched, and empirical formulae have been proposed, in the case of short-term response of fine-grained soils (sometimes called “cohesive” soils) and in the case of coarse-grained soils (sometimes called “granular” soils) as summarised by Lake *et al*. (1996).

The evaluation of long-term displacements in fine-grained soils, comparatively, has so far received less attention (Mair 2006). This may depend on two main reasons. First, it is difficult and costly to arrange the long lasting monitoring campaigns required to cover the duration of the consolidation process (and potential viscous processes of even longer duration). Second, it is believed that the slow dissipation of the pore pressure does not emphasize the angular distortion that results from differential settlements the main cause of damage on pre-existing structures (Attewell & Farmer 1974). In the authors view the study of long term movements in fine-grained soils subject to tunnelling is a topic of great relevance; however, since the main focus of this study is the definition of practical numerical approaches, a deliberate choice was made to limit the present work to those cases in which the best practice, in terms of analytical models for green-field conditions is already established and adopted in engineering practice.

1.2.2 Gaussian settlement trough

Many authors, in the past decades, proposed solutions to the problem of estimating green field settlements above a tunnel. Peck (1969) and Schmidt (1969) recognised that the shape of the settlements trough above a tunnel, in a transverse section, is well represented by the probability density function of a Normal distribution (also known as Gaussian distribution). The works of Hansmire & Cording (1972, 1975), Boscardin & Cording (1989), Atkinson & Potts (1977) and Attewell (1978), confirmed and adopted the Gaussian shape and advanced the understanding of how the tunnel geometry and excavation technique, as well as the nature of the ground, affects the maximum settlement observed above the tunnel and the width of the through. Nowadays, a number of analytical solutions, empirically calibrated against different set of real data are available to the practicing engineer for fine-grained, coarse-grained and layered soils. The analytical solutions of these empirical models can be easily implemented in a spreadsheet. Dedicated commercial computer programs, like X*disp* (Oasys 2013) are also available.

Having adopted the shape of the probability density function of a Normal distribution, a Gaussian settlement profile is described by the equation:

$$S = S_{max} e^{-\frac{y^2}{2i^2}} \qquad (1.1)$$

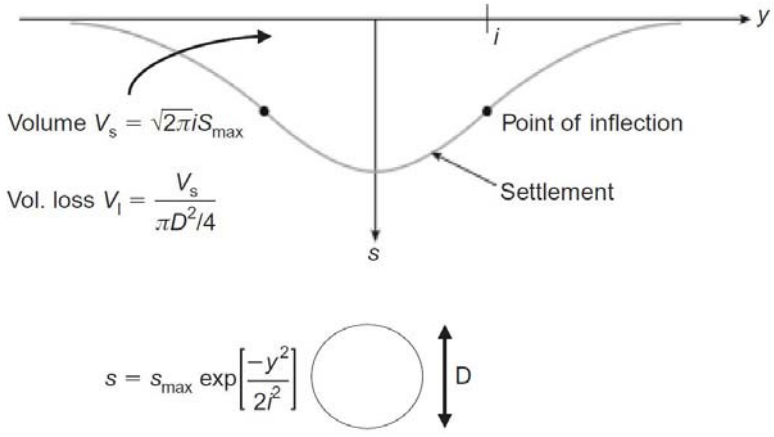

Figure 2. Gaussian settlement trough (source: Mair 2006)

where

S is the surface settlement at any distance from the tunnel centre line

y is the transverse distance from the tunnel centre line

S_{max} is the maximum settlement, which occurs above the tunnel central line

i is the trough width parameter,

The parameter *i* represents the distance of the point of inflection from the tunnel centre line. With reference to the formulation of the probability density function, *i* is the standard deviation of the normally-distributed random variable.

1.2.3 Surface settlement trough: volume loss and the parameter *K*

The fundamental parameter that underlies all empirical methods of estimating tunnelling settlement is the volume loss. Volume loss can be defined as the ratio of the volume of the settlement trough V_s over the theoretical volume of the tunnel V_o, when short-term equilibrium has been attained. It is usually defined in a two dimensional sense and expressed as a percentage. In the case of excavation in fine-grained soils, where undrained conditions can be assumed in the short-term, the settlement trough volume coincides with the additional volume of the excavated ground removed. This equality is not strictly true for coarse-grained soils, whose specific volume can change while deforming.

Integrating the area over the Normally-distributed tough, the volume per unit length of the settlement trough is obtained as:

$$V_s = \sqrt{2\pi} \cdot i \cdot S_{\max} \tag{1.2}$$

The theoretical volume per unit length of the ideal tunnel is

$$V_0 = \frac{\pi D^2}{4} \tag{1.3}$$

where *D* is the diameter of the circular excavation.

Additional soil volume removal during excavation is unavoidable due to the fact that soil is a deformable medium. Further loss of volume is associated with the deformation of the lining under the ground loading and by imperfections in the construction techniques which vary from case to case.

Different expressions for the width parameter have been proposed, generally as a function of the depth of tunnel axis, z_0. In practice it is often sufficiently accurate to assume:

$$i = K \cdot z_0 \tag{1.4}$$

Commonly recommended values of the coefficient *K* can be found in the literature, on the basis of empirical studies. Some examples are reported in the following table, which collects suggestions from different authors (O'Reilly & New 1982, Boscardin & Cording 1989).

Table 1. Recommended values of coefficient K.

Soil	**Range for *K***
Stiff clay	0.4 to 0.5
Soft clay	0.6 to 0.7
Glacial deposits	0.5 to 0.6
Coarse-grained	0.2 to 0.3

More accurate expressions for *K* have been proposed by different authors, for a variety of conditions, by interpolating data from different datasets. A few examples are reported in the table below.

Table 2. Recommended equations for i.

Author	**Equation for *K*** (***i* and z_0 in metres**)	**Ground conditions**
O'Really & New (1982)	$i = 0.43z_0 + 1.1$	fine-grained soil
	$i = 0.28z_0 - 0.12$	coarse-grained
Selby (1988)	$i = 0.43z_2 + 0.28z_1 + 1.1$ *	clay overlain by sand
	$i = 0.28z_2 + 0.43z_1 + 0.1$ *	sand overlain by clay
(*) Note: z_1 = thickness of upper layer; z_2 = thickness of tunnel layer		

1.2.4 Subsurface settlement profile

It is often assumed that the vertical displacement profile at any level between the tunnel and the ground surface also follows a Gauss bell shape. Although the availability of subsurface measurements is more limited, the available data seem to support this claim. (Mair *et al.* 1993) have shown, through the interpretation of field data and physical modelling in centrifuge, how the how the width of the settlement profiles and the magnitude of the maximum settlement vary with depth above tunnels constructed in clays. Eq. (1.4), originally written for surface settlements, can be extended to the subsurface by writing:

$$i_z = K_z \cdot (z_0 - z) \tag{1.5}$$

where *z* is the generic depth being considered, as sketched in Figure 3.

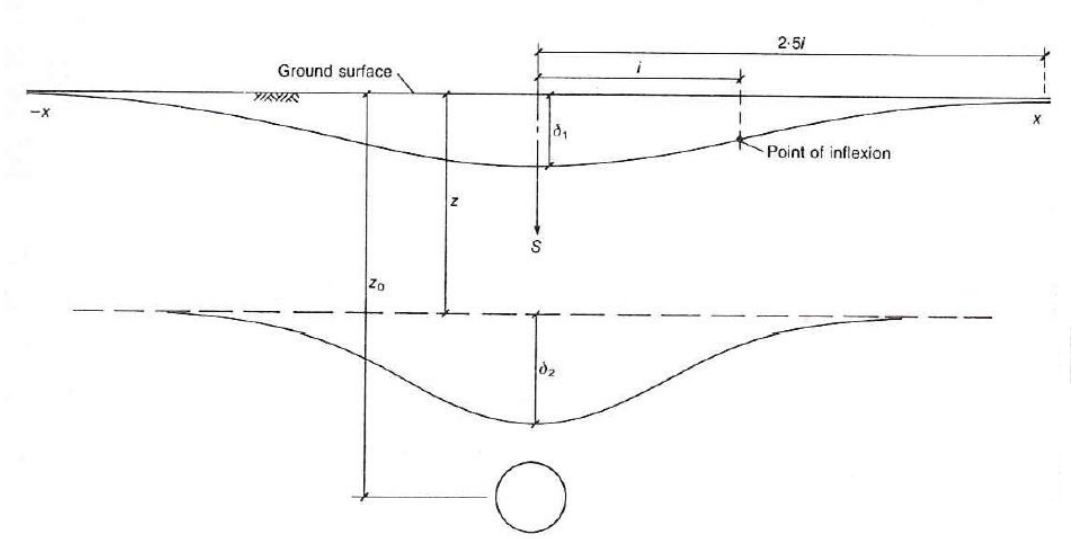

Figure 3. Form of surface and subsurface settlement profile (Mair et al. 1993)

Filed measurements indicate that *K* is not uniform, instead it increases with depth (for this reason, the often neglected subscript "z" is added here to *i* and *K* in Eq. 1.5). On the basis of several case histories in over-consolidated clays (Mair *et al.* 1993) proposed the following equation for K_z

$$K_z = \frac{0.175 + 0.325\left(1 - z/z_0\right)}{1 - z/z_0} \quad (1.6)$$

Finally it is worth recalling that (New & Bowers 1994) proposed an alternative, refined interpretation of surface and subsurface settlement in their interpretation of the ground movements induced by the construction of the Heathrow Express tunnel. This method assumes displacements are directed towards a 'ribbon' of volume loss taking place at the tunnel invert level and is also known as the 'ribbon sink' method. It is useful in the case of particularly shallow tunnels.

1.3 FEM and its limitations

The finite element method has been successfully applied to several geotechnical problems (Zaman *et al*. 2000; Potts & Zdravkovic 2001; Bull 2003) and the method is becoming a usual design tool in the consulting industry in its 2D, and occasionally 3D, implementation. Several authors, however, have noted that, when this numerical method is used to simulate ground movement above tunnels, the calculated settlement profile is invariably wider and flatter than the one observed in the field. The difference appears particularly severe for sites with high horizontal stresses, hence a high coefficient of heart pressure at rest k_0 (Franzius *et al.* 2005).

Addenbrooke *et al*. (1997) presented a suite of two-dimensional analyses including both linear elastic and non-linear elastic pre-yield models, combined with the Mohr–Coulomb failure criterion. They concluded, studying the Jubilee Line Extension beneath St James's Park (London) that, for a realistic value of k_0 = 1.5, the predicted surface settlement profile was far too wide when geo-mechanical parameters appropriate for the local soil were adopted in the constitutive models. Their study also showed that introducing soil anisotropy did not significantly improve the. Comparable observations were made by Gunn (1993). In contrast, Simpson *et al*. (1996), by conducting a plane strain study of the Heathrow Express trial tunnel, suggested that soil anisotropy gives better surface settlement predictions for over-consolidated clay. However, only limited details about the applied soil model were given.

Lee & Ng (2002) suggested that moving from 2D to 3D modelling can significantly improve the analysis results. However, the statement by Lee & Ng (2002) that 3D FE modelling leads to better surface settlement predictions than corresponding 2D analyses is in sharp contrast to the findings of several other authors (Guedes & Santos Pereira 2000, and Doležalová 2002).

Guedes & Santos Pereira (2000) presented a suite of elastic analyses with a range of different assumed values for k_0 in which virtually identical settlement profiles were obtained from 2D and 3D models. Doležalová (2002) confirmed similar finding in a more comprehensive study which included the use of linear elastic/perfectly plastic and non-linear elastic/perfectly plastic constitutive laws. A summary of these results is shown in Figure 4.

Franzius *et al.* (2005) presented a series of both 2D and 3D FE analyses of tunnel construction in London Clay (see Figure 5). Advanced constitutive models based on both isotropic and anisotropic non-linear pre-yield elasticity were adopted. The results show that, even for a high degree of soil anisotropy, the transverse settlement trough remains consistently too shallow. More realistic results were only obtained by combining unreasonably high anisotropy with a very low-k_0 regime. A summary of results obtained by Franzius *et al*. (2005) is shown in Figure 6 and Figure 7.

Recently, Gonzalez *et al.* (2012), have been able to achieve a good approximation of the same case history with a very complex the three-surfaces kinematic hardening constitutive model, incorporating stiffness degradation and soil destructuration.

The complexity of this constitutive model, however, places it well beyond the understanding of the vast majority of practicing geotechnical engineers. Moreover, the calibration of the model parameters by this

type of models is challenging. The combination of advanced formulation and challenging calibration makes this type of very advanced models extremely difficult to use in practice.

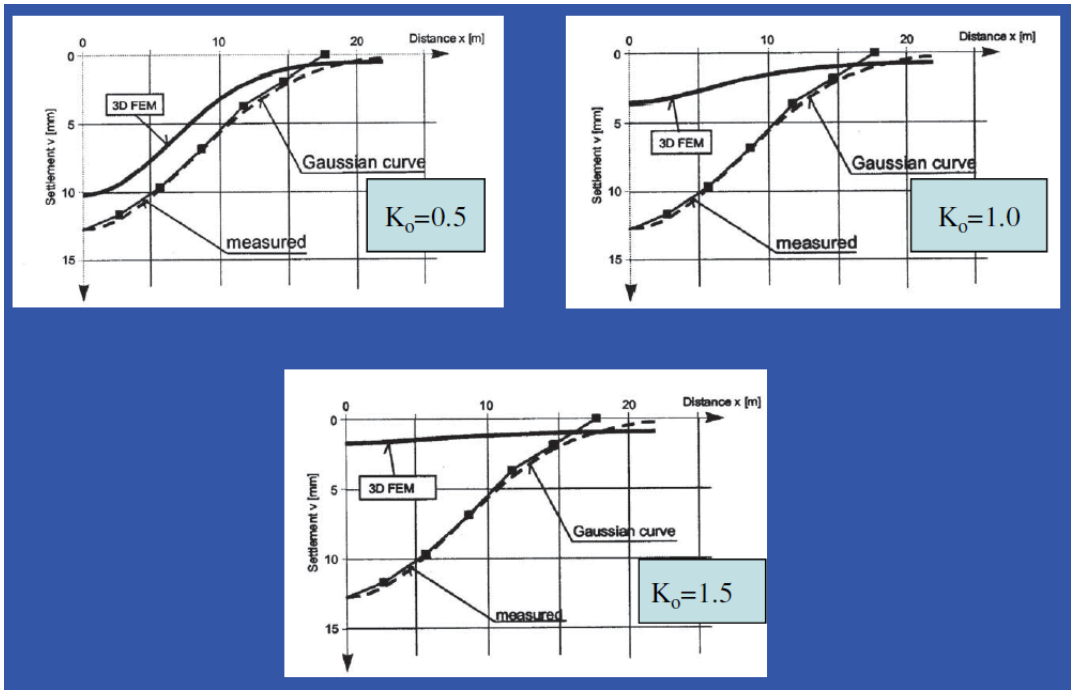

Figure 4. Summary of the results obtained by Dolez˘alova´ (2002).

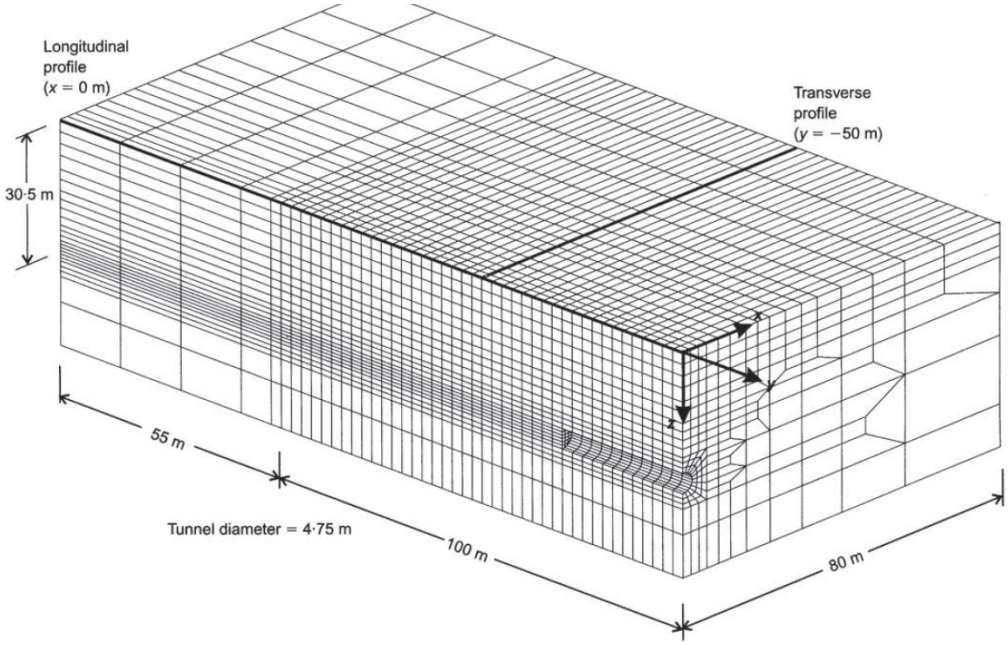

Figure 5. 3D mesh used by Franzius et al. (2005) to study the Westbound tunnel of the Jubilee Line Extension.

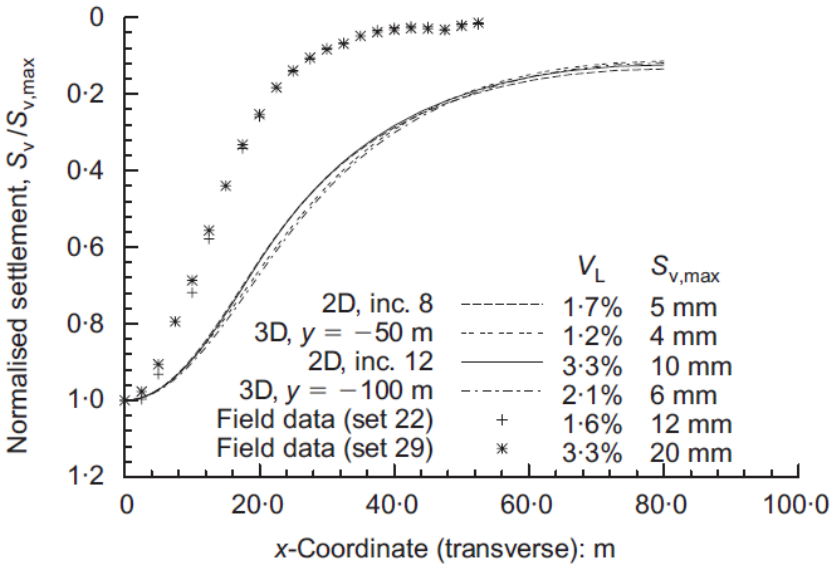

Figure 6. Suite of results obtained by Franzius et al. (2005) with isotropic constitutive models.

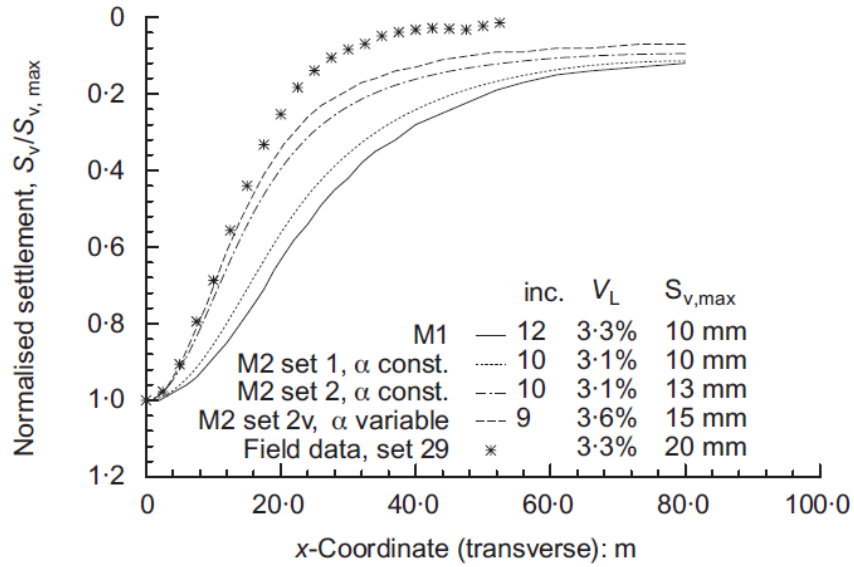

Figure 7. Suite of results obtained by Franzius et al. (2005) with anisotropic constitutive models.

1.4 This study

1.4.1 Motivation and research questions

The academic community has addressed the problem of numerical modelling of ground movement induced by tunnelling in soil by developing progressively more refined and complex constitutive models. This effort, which has become more intense in the last decade, incurred repeatedly in unexpected difficulties. Only very recently, some extremely complex constitutive models have shown encouraging results, although their validation has been mostly confined to specific cases, rather than extended to the full range of situations that can be encountered in practice.
In the meantime, these advanced constitutive models have reached a level of complexity that is well beyond the understanding of practicing geotechnical engineers. Furthermore, the calibration of the numerous parameters required by the advanced models, often deprived of a clear physical meaning, is a substantial challenge, hard to tackle with the amount of information typically available in commercial projects.

This study aims at exploring the possibility of reproducing satisfactory green-field ground displacements with a finite element analysis without resorting to extremely advanced constitutive models. The approach consists in pragmatically prioritising the achievement of reasonable results with a simple tool over the elegance and theoretical correctness of the tool itself. In this contest, the sensitivity of the results, in terms of settlement, to the coefficient of earth pressure at rest k'_0 can be seen more as an opportunity more than as a limitation. Once the attempt of developing an all-purpose FE model is set aside and only the simulation of credible ground movements is sought, the following research questions become conceivable an of interest:

“Is it possible to match the observed field data with a FE calculation which adopt a linear-elastic/perfectly-plastic (LE/PP) soil and using an artificially reduced k_0 as a calibration parameter?”

“If so, by how much is it necessary to reduce the actual k_0? Is it possible to draw a systematic rule valid across the range of possible practical cases?”

“If not, what is the simplest of the more refined constitutive models which could achieve satisfactory results with artificially low values of k_0?”

These research questions can be repeated for progressively more refined constitutive models. If care is taken in proceeding to only gradual increase in complexity at each step and a full, pragmatic exploration of the calibration options is carried out at each step, the chances of discovering a methodology which produces satisfactory results with the relative simplicity appealing to the consulting industry are maximised.

1.4.2 Scope

This works is focussing on the short-term response to tunnelling of over-consolidated clays, in particular on the transverse settlement trough that is generated at each cross-section once the tunnel face has advanced past it sufficiently for the cross-section to be outside the transient condition experienced immediately in front and immediately behind the tunnel face. Although a worthy subject in itself, this study does not discuss the longitudinal settlement profile in this transition zone, sometimes named “bow wave” in the industry terminology.

No attempt is made to study the long-term response of the ground associated with consolidation, change in drainage conditions and viscous processes. The long-term condition is generally considered less critical than the sort-term one, which is generally associated with the largest differential settlements and distortions and is, therefore linked to the most severe conditions for pre-existing structures and infrastructures.

The analyses present here are limited to stiff, overconsolidated clays and do not cover neither the case of soft, normally-consolidated fine-grained soils nor the case of coarse-grained soils. Stiff clays are the prevailing geotechnical condition for a number of urban conglomerates worldwide and represent a good starting point for a set of studies that, ideally, should cover, in the future, other geotechnical setting, thanks to the contribution of other authors.

1.4.3 Methodology

There tunnels in stiff clay have been selected as case studies and back-analysed though 2D finite element calculations. The case studies were selected amongst situations where a satisfactory monitoring programme was in place and reliable sit measurements were available to support credible back-analysis. The site measurements from all the considered case histories are freely available and have been previously published; so no data confidentiality or data property issues are associated with this work.

2D plane strain FE back-analyses ware carried out for the three case histories, initially with a fully realistic set of geotechnical parameters, and subsequently with artificially reduced horizontal stresses in the stiff clays to check the sensitivity of the models to this change.

Only undrained conditions, which are associated with the short-term response of the material, were considered for the fine-grained soils, which include the over-consolidated clays at depth for all the case histories and shallower, normally consolidated clay deposits in some of the cases.

All materials were modelled with linear elastic-perfectly plastic (LE-PP) constitutive models: in total stress and with Tresca's criterion as yield condition for the undrained fine-grained soils; in effective stress and with Mohr-Coulomb's failure criterion as yield condition for the coarse-grained soils, which always respond in drained manner even in the short-term.

The stress relief method (Panet & Guenot 1982, Schikora & Fink 1982), which is a way to introduce consequences of the actual 3D situation in the simpler model, was adopted to control the area loss in the 2D model.

The effect of plasticity in the ground was investigated by first identifying the plastic zones associated with the analyses with LE/PP models, then by replacing the materials in these zones with a soil with lower mechanical properties (stiffness and/or strength).

The sensitivity to changes in the initial stress filed was investigated by reducing the ratio between horizontal and vertical total stress in the stiff clays.

As satisfactory back-analyses were obtained with the LE/PP models, there was no need to progress to the use of more advances constitutive models.

The analysis of three case histories is not sufficient to demonstrate that the approach is universally valid for any stiff clay. However, considering the low sensitivity of the settlement trough to variations in soil strength and stiffness (parameters which do not appear in the analytical solutions based on Gaussian, or other, distributions), it is reasonable to expect that the approach developed here would enable realistic calculations of settlement for most stiff clays. This study may therefore represent a useful first step in the development of a methodology for the numerical modelling of short-term tunnelling induced ground movements in stiff clays.

1.4.4 Resources

Priority has been given to commercial computation codes. In particular, the software Plaxis has been selected for its diffusion in the geotechnical industry. The research was carried out by the author, A. Perrone for her MSc dissertation, in the context of an academia/industry cooperation between Politecnico di Milano and the British geotechnical division of CH2M HILL. The work has been facilitated by Dr Marco Redaelli (CH2M HILL and University of Leeds). Mr Peter Wright (CH2M HILL, Tunnelling Regional Manager for Europe) has provided tunnelling expertise and specialist support throughout this work.

2 Case Histories

2.1 Jubilee Line Extension tunnels at St. James's Park

2.1.0 Introduction

In the mid-1990s the Jubilee Line of the London Underground was extended from Green, in central London, to Stafford, in East London, as shown in Figure 8. A stretch of particular interest with regards to ground movement control and settlement monitoring is the one connecting Waterloo to Green Park via Westminster. In this section the two 4.85m external diameter tunnels, which were constructed with expanded concrete segments, pass alongside the Big Ben clock tower one above the other, then they continue towards the Queen Elizabeth II (QEII) Conference Centre, were they start to diverge. Figure 8 shows a plan view of the tunnels alignment. An instrumented section for ground movement monitoring, also indicated in Figure 9, was set up between the QEII centre and the lake in St. James's park. The resulting data offer insight into the effect of two tunnels that were bored at different depths and experienced different volume losses during construction. It is also one of the few situation where the route encountered genuine green-field conditions. At St. James's Park the tunnels were excavated in a thick stratum of London Clay; this location constitutes an ideal case to study the response to tunnelling of heavily over-consolidated clays.

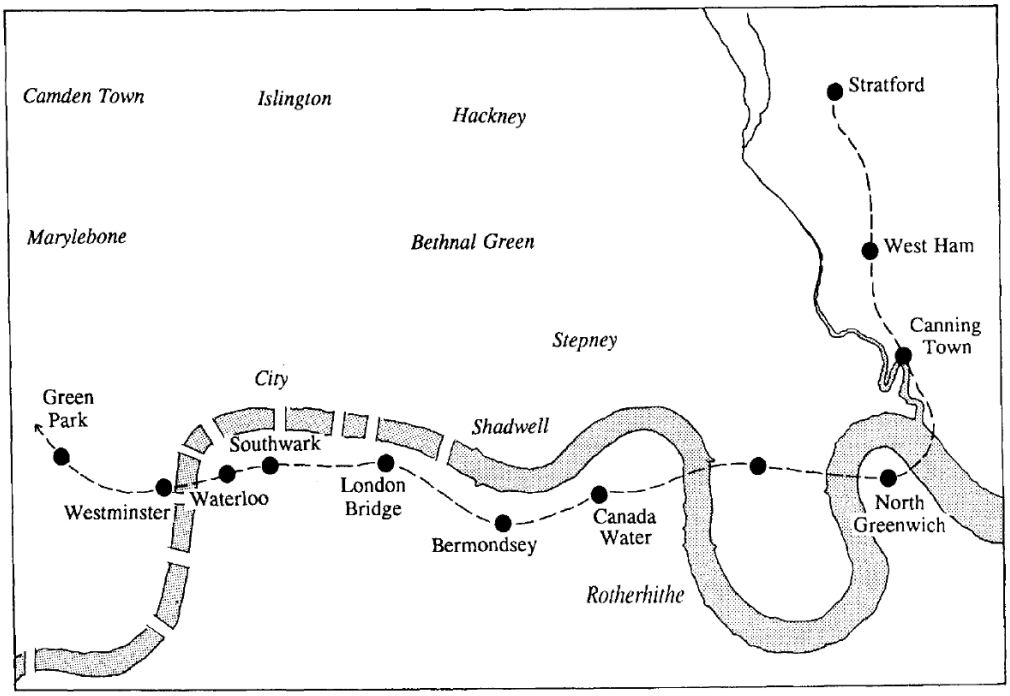

Figure 8. Jubilee Line Extension route, source: Page (1995).

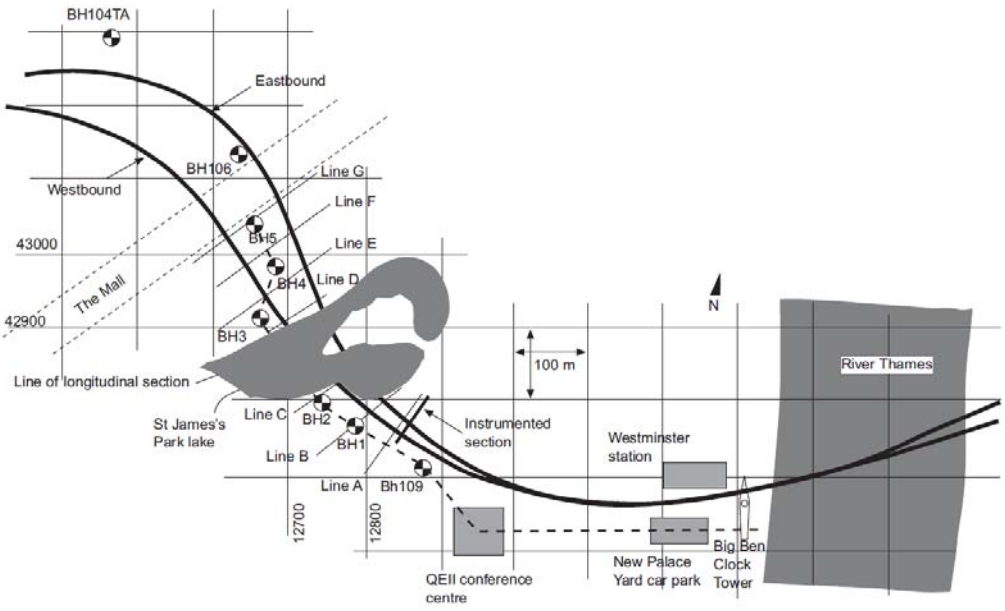

Figure 9. JLE tunnels between Westminster and Green Park, plan view (source: Standing & Burland 2006)

2.1.1 Geology

The near surface geology of the London Basin is remarkably complex (Skipper *et al*. 2009) and only the aspect that are relevant to the engineering practice, and in particular to tunnelling, are recalled here. Chalk from the Upper Cretaceous underlies more recent geological formations across central London. Above the Chalk, the Thanet Sand Formation and the more recent Lambeth Group (both from the Palaeocene) are found. Above the Lambeth Group, the Thames Group (Eocene) is found. The Quaternary deposits are River Terrance Deposits and Alluvium. Made Ground covers the natural geology all over London. A simplified scheme of the London Basin geology is also shown in Table 3.

The Lambeth Group is a complex sequence of formations that, in engineering terms, generally results in alternating fine-grained and coarse-grained soils (Page & Skipper 2000). Across London, the vast majority of the Thames group is generally constituted by the London Clay Formation, with the older Harwich Formation being of very small thickness or absent.
Considering that the River Terrace Deposits are essentially Gravel, the nomenclature adopted in Figure 10 is obtained. It is worth noting that elevations in the figure are referred to the Project Datum (PD) that is 100m under the usual British vertical reference Ordnance Datum (OD).The geological cross-section shows six different units of engineering relevance. For the present case study, the relevant part of the cross section is at the left hand side of the figure, between Green Park and Westminster. At St. James's Park the following geological units are encountered:

- Made Ground and Alluvium (variable thickness, in the order of a few meters)
- Terrace Gravels (variable thickness, in the order of a few meters)
- London Clay (variable thickness, in the order of 40m)
- Lambeth Group (unknown thickness, estimated in the range of 15-20m)

The base of the Lambeth Group under St. James's Park is uncertain and the thickness of the Thanet Beds and elevation of the Chalk top are unknown. However, these features are sufficiently remote from the JLE tunnels to be of little engineering significance in the specific case.

The position of the shallower Eastbound tunnel and of the deeper Westbound tunnel are clearly visible in Figure 10.

Table 3. Schematic geological sequence in the London basin (simplified from Skipper et al. 2009).

Geological sequence in the London Basin			
Made Ground			
Quaternary		Alluvium	
		River Terrace Deposits	
Paleogene	**Eocene**	Thames Group	London Clay Formation
			Harwich Formation
	Palaeocene	Lambeth Group Formation	Woolwich Formation
			Reading Formation
			Woolwich Formation
			Reading Formation
			Upnor Formation
		Thanet Sand Formation	
Cretaceous	White Chalk Subgroup		

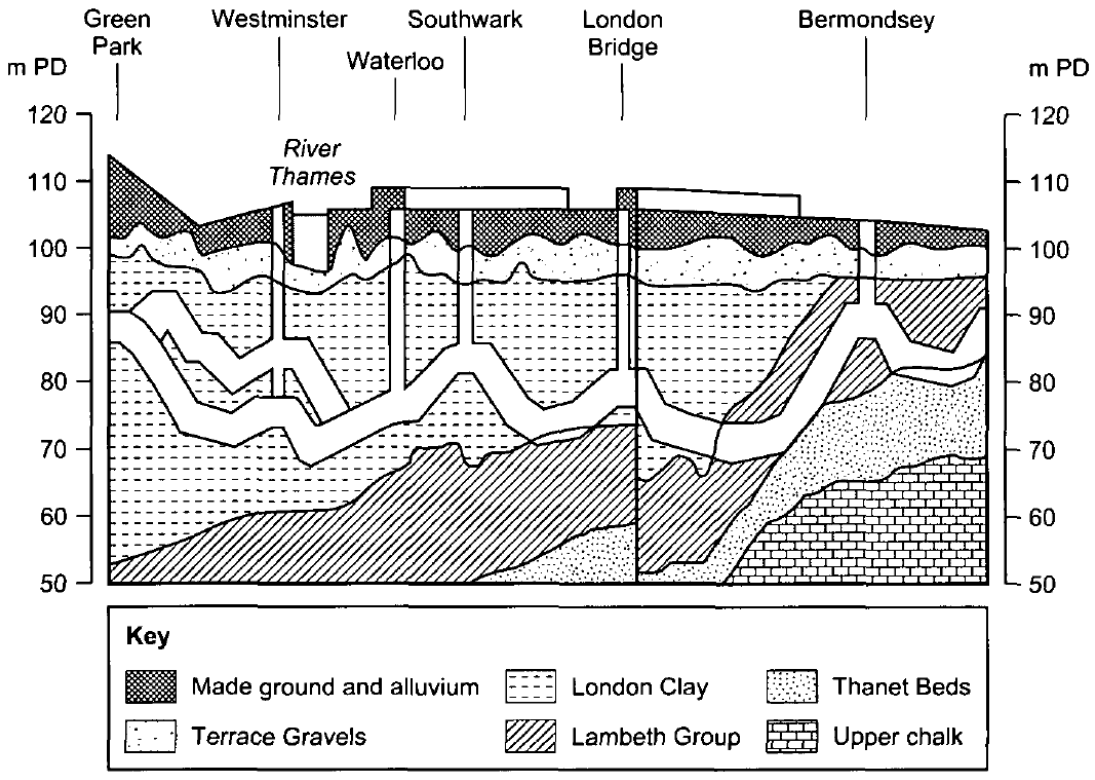

Figure 10. Geological cross-section for the JLE tunnels between Green Park and Bermondsey (source: Burland et al. 2001).

2.1.2 Hydrogeology

The hydrology of the London area in controlled by two aquifers, named the upper and lower aquifer (Simpson *et al.* 1989). In the central and western part of the London area, where a thick stratum of low permeability London Clay is present, the upper and lower aquifers are well separated and the deeply buried lower aquifer has little influence on the engineering works (Burland *et al.* 2001).

The upper aquifer is unconfined and consists of the Alluvium and Terrace Gravel. The elevation of the piezometric surface is around 100mPD, where PD indicates the "Project Datum", which is 100m below the "Ordnance Datum". The aquifer has widespread connectivity with the river Thames and is somehow affected by its tidal movement for an amplitude of about 1-2m.

The lower aquifer is confined and consists of three strata: the Upnor Formation (the lowest, highly permeable part of the Lambeth Group), the Thanet Sand and the Chalk (Simpson *et al*. 1989; Burland *et al*. 2001).

The piezometric level in the lower aquifer is generally in proximity of the base of the Lambeth Group. The pore water pressure distribution, therefore, drops to almost zero near the base of the Lambeth Group. In the London Clay and the pore water pressure distribution is shows an hydrostatic or slightly lower gradient in the upper part of the layer, then exhibits a marked reduction toward the base of the London Clay and through the upper part of the Lambeth Group. As shown in Figure 11, this situation is deduced by observation is the field and can be explained with a constant underdrainage of the London Clay – upper Lambeth Group aquitard, as confirmed by numerical modelling carried out with the ICFEP finite element software by Higgins *et al*. (1996).

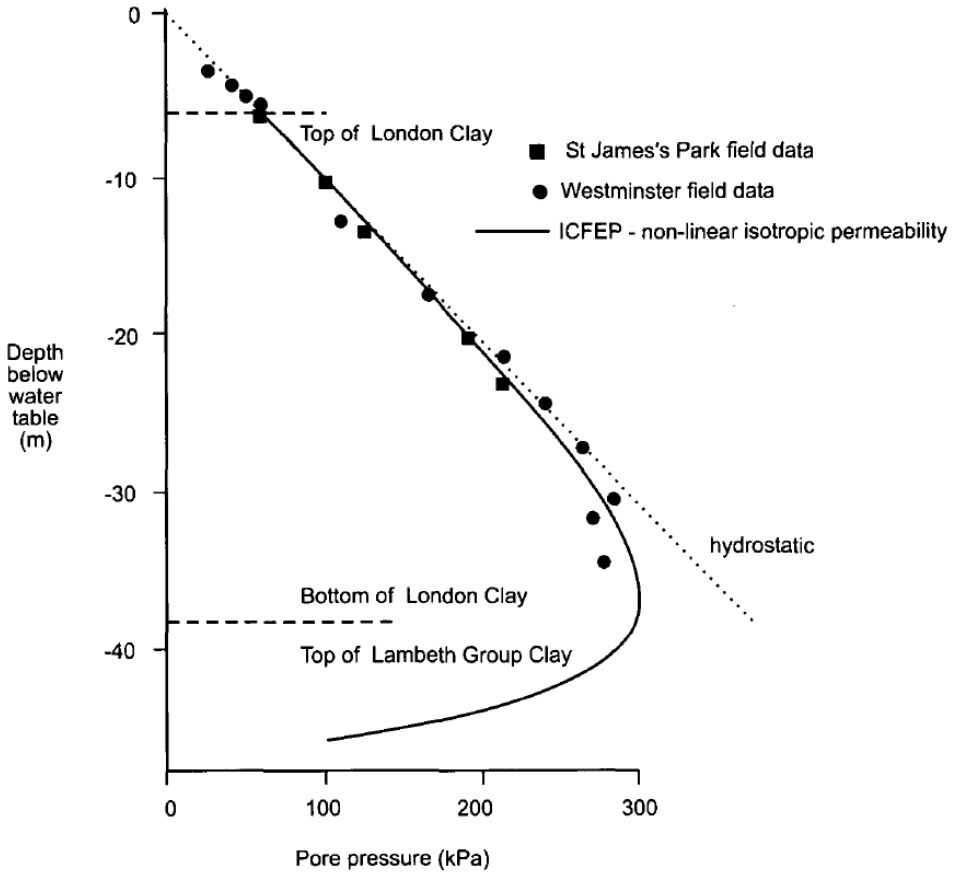

Figure 11. Typical pore water pressure distribution in central London (source: Burland et al. 2001).

2.1.3 Geotechnical characterisation

2.1.4.1 Engineering description and geotechnical properties

The following sections classify the geotechnical units found at St. James's Park are according to their geotechnical properties, in line with the British Soil Classification System (BS 5930).

For the fine-grained soils, the following index properties are discussed:

LL	liquid limit
PL	plastic limit
PI	plasticity index; *PI = LL - PL*

The text also discusses the basic geotechnical parameters of each unit, in particular:

γ_{sat}	saturated unit weight
S_u	undrained shear strength (for fine-grained soils only)
c'	effective cohesion
ϕ'	effective angle of shearing resistance
E_u	undrained Young's modulus
E'	drained Young's modulus
ν'	drained Poisson's ratio
K'_0	coefficient of earth pressure at rest

The undrained Poisson's ratio is consistently assumed to be equal (or very close to) 0.5, due to the inerent inability of soils to rapidly change volume in undrained conditions.

Since this work focuses on the short-term response to tunnelling, and neither consolidation nor seepage analyses are required, the coefficient of permeability of the material is not discussed.

2.1.4.2 Made Ground

The Made Ground is extremely variable in nature. It general can consist of a mix of concrete, rubble, brick, gravel and sand often in a clay matrix. At St. James's' Park the coarser fraction of materials of anthropic origin appears to be small and the predominance of the clay matrix suggests it could be reasonably treated as a fine-grained soil, although with very heterogeneous properties.

The parameters listed in the table below have been selected as a representative of the Made Ground behaviour in this work. In this respect, the presented values are "characteristic" values, in the terminology adopted by Eurocode 7 (EN 1997). A suggested range of variation is also reported in the table, in square parenthesis, to provide an idea of the possible variability. The estimates are based on the design parameters at entre route scale (Withers *et al*. 2001) adjusted with the information available for the specific site (Burland & Standing 2006; Wongsaroj *et al*. 2007).

Table 4. Geotechnical parameters of the Made Ground.

Parameter			Value
γ_{sat}	(kN/m^3)	unit weight, saturated	17 [15-19]
S_u	(kPa)	undrained shear strength	30 [15-70]
c'	(kPa)	effective cohesion	0
ϕ'	(°)	angle of shearing resistance	28 [22-35]
E_u	(MPa)	Young's modulus, undrained	12 [5-30]
E'	(MPa)	Young's modulus, drained	10 [4-26]
ν'	(-)	Poisson's ratio, drained	0.3
k'_0	(-)	coeff. earth pressure at rest	0.5 [0.4-0.6]

2.1.4.3 Alluvium

The Alluvium is constituted by the recent fluvial deposits of the river Thames and its small tributary Tyburn, which is now artificially channelled in a buried conduct. There is a degree of variability in the lithology, however the predominant descriptions are:

soft light grey-green to dark brown, very silty, sandy CLAY, with rare carbonaceous material and occasional shell gravel

and

soft to firm dark grey to black organic silty CLAY

For the purposes of calculations, the above lithologies have been grouped together and characterised with one set of parameters reported below. The estimates have been obtained, similarly to what already done with the Made Ground, by filling the gaps in the locally available information with averages valid at entire route scale.

Table 5. Index properties of the Alluvium (CLAY).

Parameter			Value
w	*(%)*	natural moisture content	37 [18-55]
LL	(%)	liquid limit	55 [40-70]
PL	(%)	plastic limit	20 [15-25]
PI	(%)	plasticity index	35 [25-45]

Table 6. Geotechnical parameters of the Alluvium (CLAY).

Parameter			Value
γ_{sat}	(kN/m^3)	unit weight, saturated	18 [16-20]
S_u	(kPa)	undrained shear strength	35 [25-50]
c'	(kPa)	effective cohesion	0
ϕ'	(°)	angle of shearing resistance	26 [22-30]
E_u	(MPa)	Young's modulus, undrained	9 [5-15]
E'	(MPa)	Young's modulus, drained	[4-13]
ν'	(-)	Poisson's ratio, drained	0.3
k'_0	(-)	coeff. earth pressure at rest	0.6 [0.5-0.8]

2.1.4.4 River Terrace Gravel

The River Terrace Gravel at St' James's park is at the lowest elevation for a deposit of its kind along the entire route. The Gravel presents considerably variations in particle size distribution in the lateral and vertical direction and can occasionally become a Sand. The envelope of grading is presented in Figure 12

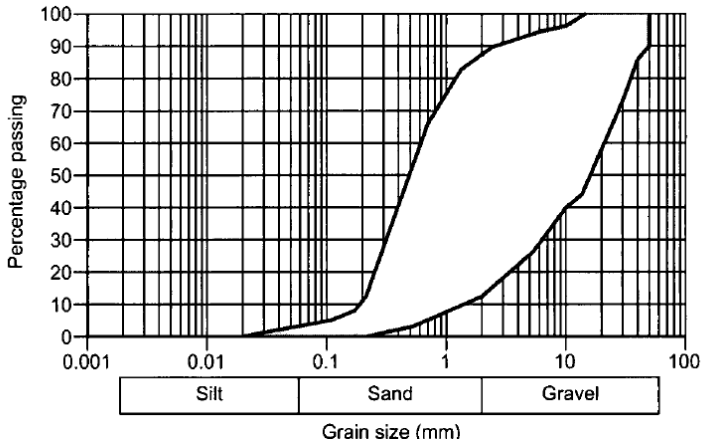

Figure 12. River Terrace Gravel grading envelope (source: Withers et al. *2001).*

The description of the River Terrace Grave is:

medium dense to dense, orange brown, very sandy, sub-angular to sub-rounded, fine to coarse, GRAVEL, with occasional cobbles

The geotechnical parameters of the River Terrace Gravel are (Withers *et al.* 2001, Addenbroke *et al.* 1997, Wongaroj *et al.* 2007)

Table 7. Geotechnical parameters of the River Terrace Gravel.

Parameter			Value
γ_{sat}	(kN/m^3)	unit weight, saturated	19.5 [19-20]
c'	(kPa)	effective cohesion	0
ϕ'	(°)	angle of shearing resistance	35 [32-40]
E'	(MPa)	Young's modulus, drained	75 [50-120]
ν'	(-)	Poisson's ratio, drained	0.25
K'_0	(-)	coeff. earth pressure at rest	0.4 [0.3-0.5]

2.1.4.5 London Clay

The London Clay is a marine clay that, across the London area attained thicknesses sometimes in excess of 100m and then underwent significant erosion by uplift and the fluvial/glacial activity associated with the River Terrace deposits. In the geology of the London Clay five units, indicated with the letters from A to E, can be identified (King 1981) and each unit can be further subdivided into two or three parts according to sedimentary cycles recognisable from subtle variations in lithology and fossils. At St. James's Park units A2, A3 and B are present (Standing & Burland 2000). In engineering projects, however, one or at most two geotechnical units are generally recognised as this is sufficient for a correct characterisation of material strength and stiffness. A detailed ground investigation arranged by the

Imperial College was carried out a few years after the JLE construction. The detailed interpretation of the data showed that, although there are subtle geotechnical differences among the subunits (Standing & Burland 2000), the main difference is between the basal unit A2 and the remaining London Clay. The basal unit, in fact, contains more silt and sand than the upper layers. The main impact of this change seems to be on the permeability that can be significantly higher for the basal layers. The present work, in agreement with other authors (Addenbroke *et al.*, Wongsaroj *et al.* 2007) considers acceptable assigning only one set of strength and stiffness parameters to the entire London Clay.

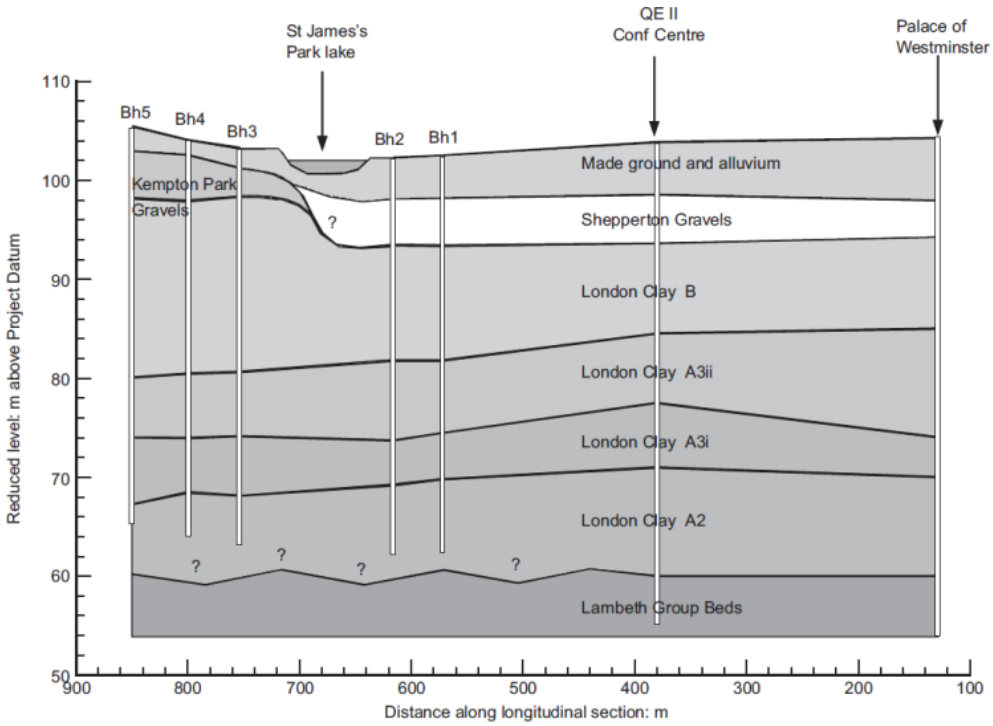

Figure 13. Longitudinal section across St James's Park and Westminster showing divisions of London Clay (source: Burland & Standing 2006).

The main body of the London Clay is a

very stiff, thinly laminated, very closely fissures, dark grey and grey-brown CLAY of very low to medium compressibility and high to very high plasticity

The plasticity chart for the samples recovered in the detailed post-construction investigation is shown in Figure 14.

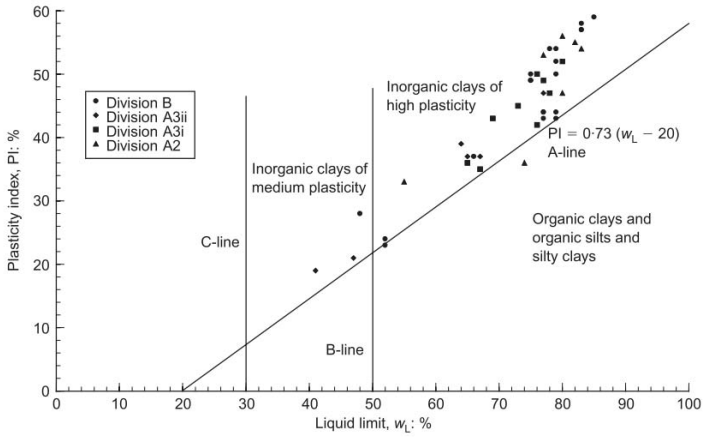

Figure 14. Casagrande soil classification chart with results categorised by London Clay division source Standing and Burland (2006).

The undrained shear strength has been obtained by interpolating the results of quick unconsolidated undrained triaxial test shown in Figure 15 (Burland & Standing 2006) and is in good agreement with assumptions made for the JLE design (Withers *et al.* 2001).

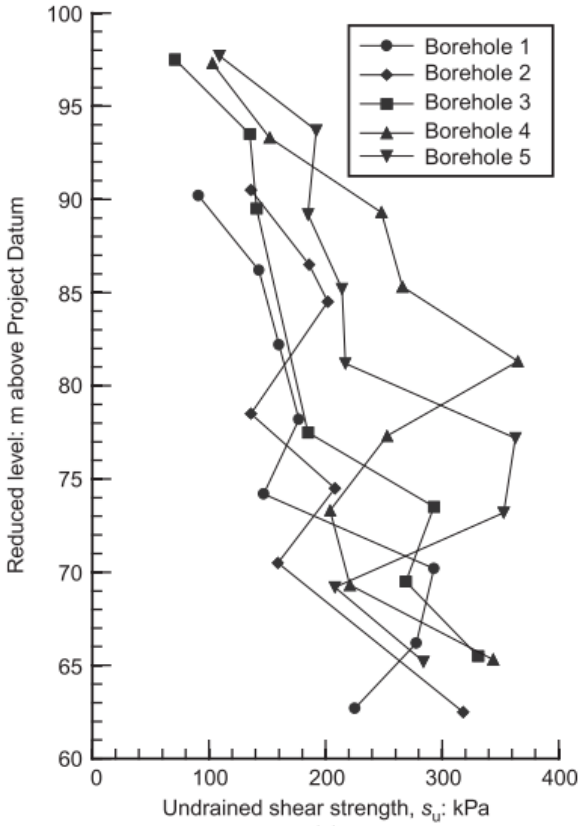

Figure 15. Profiles from each of the five boreholes across St James's Park

The effective strength parameters derive from a database of triaxial tests.

The undrained Young's modulus was estimated on the basis of the back-analyses presented by Burland & Kalra (1987) by choosing a cautious interpretation.

Due to the stress history of the London Clay, and in particular its over-consolidation and underdrainage, the coefficient of earth pressure at rest *K*0 varies with depth. The typical values are those shown in Figure 17, that refer to a nearby site at Waterloo but are representative of the entire area. An initial value as low as 0.5 is found at the top of the layer. It then increases till a maximum of 1.5 at about 5m below the top of the layer to finally decrease gradually to 1.0 or just above.

Table 8. Index properties of the London Clay.

Parameter			**Value**
w	(%)	natural moisture content	25 [20-30]
LL	(%)	liquid limit	70 [54-85]
PL	(%)	plastic limit	25 [20-30]
PI	(%)	plasticity index	45 [30-55]

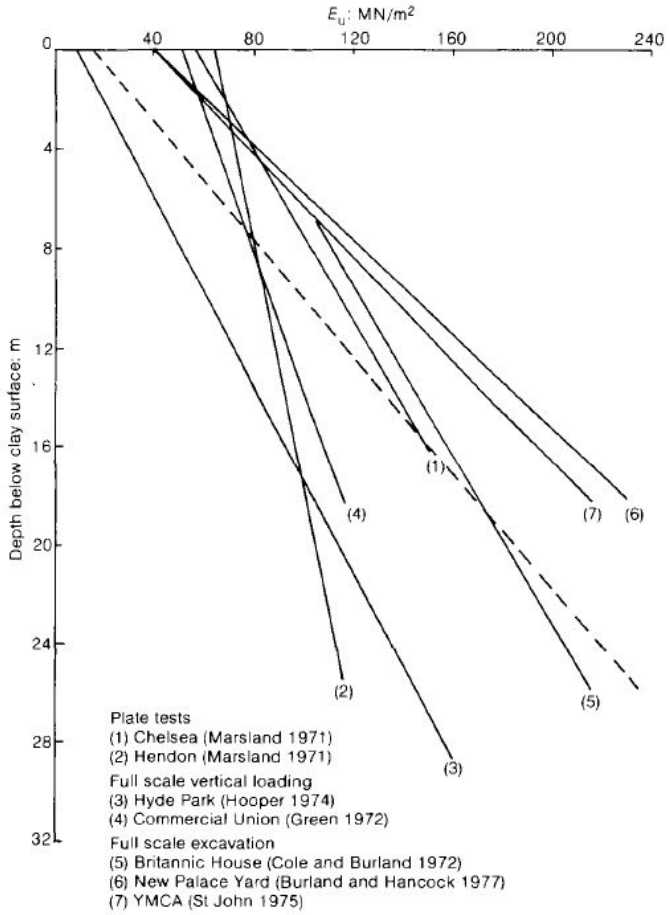

Figure 16 Undrained Young's modulus prepared by Burland & Kalra (1987).

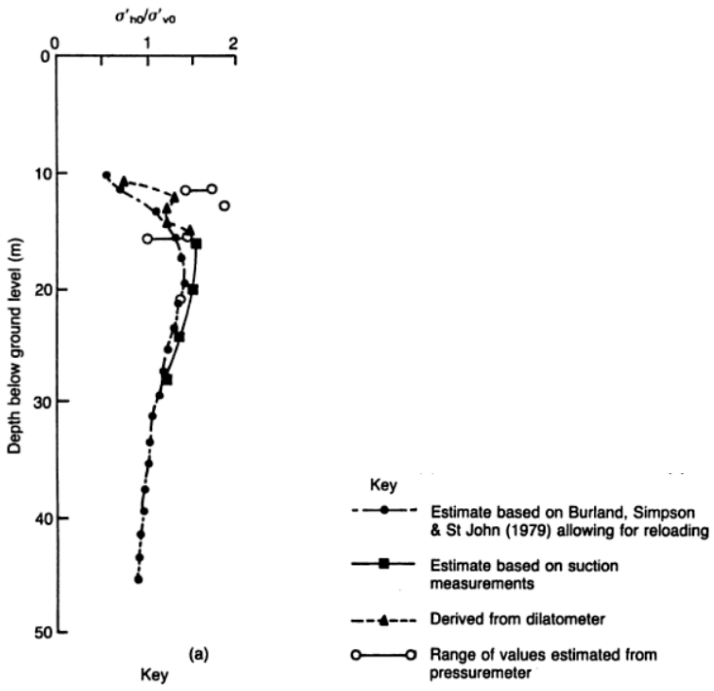

Figure 17. Coefficient of earth pressure at rest k'_0 with depth

Table 9. Geotechnical parameters of the London Clay.

Parameter			Value
γ_{sat}	(kN/m^3)	unit weight, saturated	19 [18-20]
S_u	(kPa)	undrained shear strength	50 + 8*z* [±20%]
c'	(kPa)	effective cohesion	5 [0-12]
ϕ'	(°)	angle of shearing resistance	25 [24-28]
E_u	(MPa)	Young's modulus, undrained	10+5.2 z
E'	(MPa)	Young's modulus, drained	0.8 E_u
ν'	(-)	Poisson's ratio, drained	0.2
k'_0	(-)	coeff. earth pressure at rest	depth dependant [0.5-1.5]

2.1.4.6 Lambeth Group

The Lambeth Group at this site is predominantly clay (Addenbrooke 1977, Wongsaroj *et al*. 2007). Less site-specific information is available for the Lambeth Group Clays (also known with the old name of Woolwich and Reading beds) than for the London Clay. From field testing and laboratory testing of samples from the site and from other sections of the JLE route, it has been possible to formulate sensible assumptions on the undrained and drained strength.

Figure 18 shows the very narrow envelope of E_u/S_u ratios as a functions of the strain level that was obtained from testing the Lambeth Group Clays (Withers *et al.* 2001).

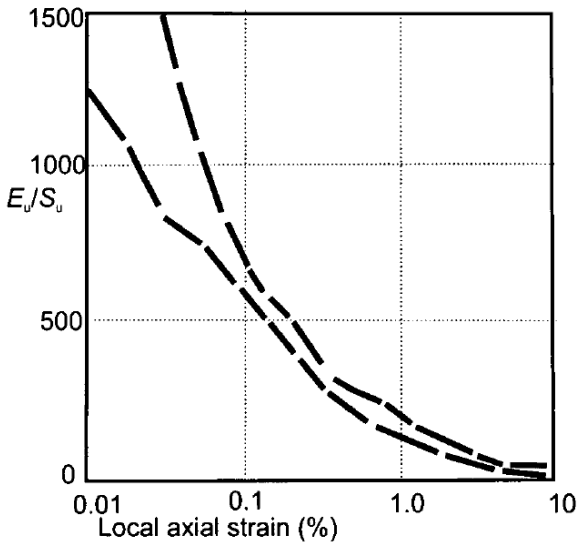

Figure 18. Envelope of E_u/S_u ratios vs. axial strain for the Lambeth Group.

For the axial strain values of less than 0.1% that are typical of tunnelling a ratio of 700 can be reasonably assumed.

Table 10. Geotechnical parameters of the Lambeth Group Clay.

Parameter			Value
γ_{sat}	(kN/m^3)	unit weight, saturated	20 [19-21]
S_u	(kPa)	undrained shear strength	280 [200-400]
c'	(kPa)	effective cohesion	10 [5-15]
ϕ'	(°)	angle of shearing resistance	30 [28-32]
E_u	(MPa)	Young's modulus, undrained	200 [140-280]
E'	(MPa)	Young's modulus, drained	0.8 E_u
ν'	(-)	Poisson's ratio, drained	0.2
K_0	(-)	coeff. earth pressure at rest	1.25 [1.0-1.5]

2.1.4.7 Summary

The geotechnical parameters for the site are summarises in the following table.

Table 11. Summary of geotechnical parameters.

Parameter			Made Ground	Alluvium	River Terrace Gravel	London Clay	Lambeth Group
γ_{sat}	(kN/m^3)	unit weight, saturated	17	18	19.5	19	20
S_u	(kPa)	undrained shear strength	30	35	/	40+6.4z	280
c'	(kPa)	effective cohesion	0	0	0	5	10
ϕ'	(°)	angle of shearing resistance	28	26	35	25	30
E_u	(MPa)	Young's modulus, undrained	12	9	/	10+5.2z	200
E'	(MPa)	Young's modulus, drained	10	8	75	40+6.2z	160
ν'	(-)	Poisson's ratio, drained	0.3	0.3	0.25		
k'_0	(-)	coeff. earth pressure at rest	0.5	0.6	0.4	1.25 * [0.5-1.5]	1.25
(*) Note: Depth dependent							

2.1.4 Construction and ground-movements monitoring

2.1.5.1 Overview

The construction of the JLE was split among a number of contractors to prevent London Underground being dictated by the contractors the end of the works and the opening time of the tunnels (Mitchell 2003).

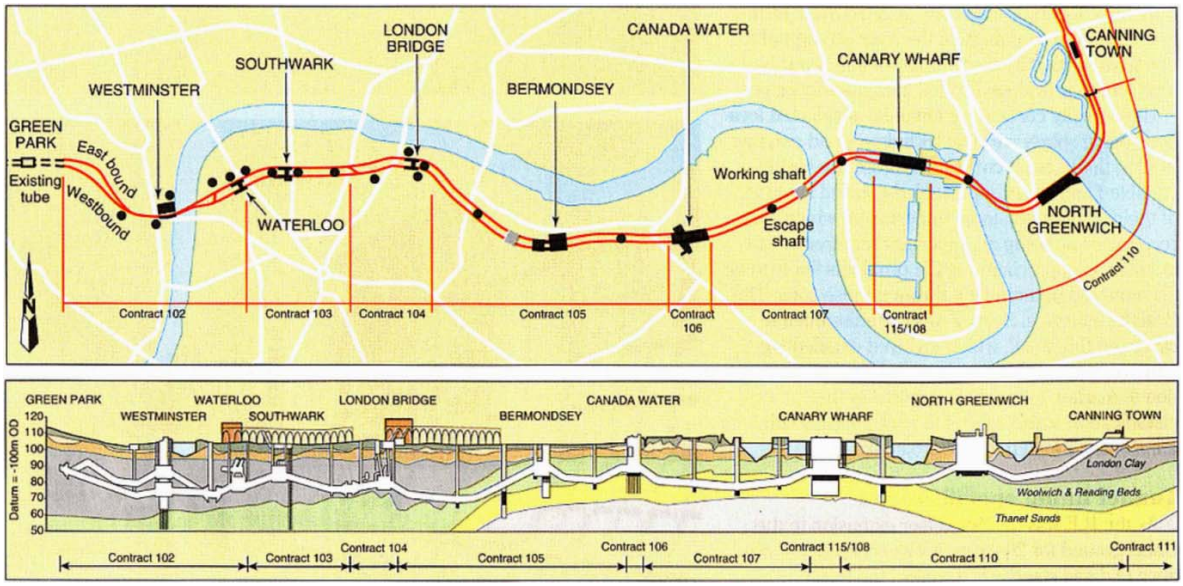

Figure 19. Plan view and cross section of the JLE route (source: Davies 2000).

The contractor in charge of the section between Green Park and Waterloo was Maunsell & Partners (Contractor 102).

On the western section of the Jubilee Line Extension most of the tunnels are in London Clay (Mair & Jardine 2001; Davies 1999). London Clay remains initially stable upon excavation because it is generally sufficiently strong and impermeable, therefore open-face tunnelling methods were used.

Incidentally, on the eastern side of the JLE, where permeable materials like the Thanet Sand where encountered both slurry and earth pressure balance machines were adopted.

2.1.5.2 Excavation machine

As the contractor found a very good quality material, stiff to very stiff clay, the tunnel has been entirely excavated with an open-face shield. A Wirth Howden open-face shield of 4.85m diameter was used with a backhoe excavating the front. A schematic representation can be found in Figure 20.

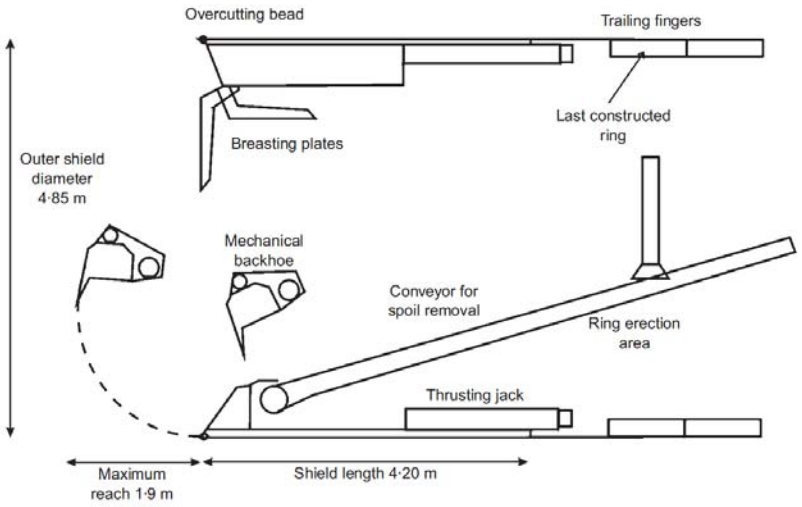

Figure 20. Open-face shield with backhoe (Mair & Dimmock 2007)

2.1.5.3 Construction methodology

To the west of London Bridge the running tunnels were designed as conventional bolted linings in either precast concrete (PCC) or in spheroidal graphite iron.

The contractor 102 changed the tunnel lining from bolted to an expanded PCC lining made up of 10 segments slightly reinforced, expanded by two wedge at the knee levels (Davies 1999), as show in Figure 21.

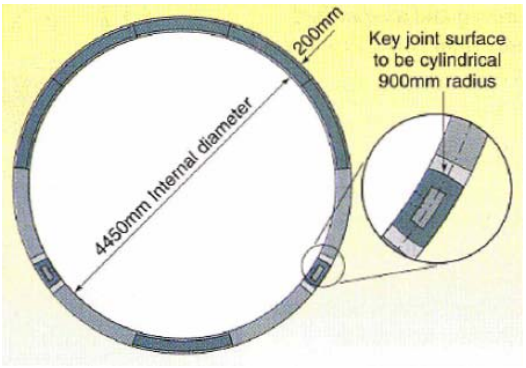

Figure 21. Cross-section of the precast concrete expanded tunnel lining, source: Davies, 1999 .

The excavation method under St. James's Park varies along the route, the lake of St James's Park represents the break between a methodology and another.

In Figure 22 is represented where each method is adopted the different procedures are briefly descripted below (Mair & Dimmock 2007):

- Standard Method: excavate 1.9m ahead of shield without forepoling or breasting patles, and to within 50 mm of extrados of shield.
- Method 1: Excavate 1.2m ahead of the shield without forepoling or breasting plates within 500 mm of extrados of shield.
- Method 2: excavate 0.8 m ahead of the shield and to within 500 mm of shield extrados, extend forepoling and breating plates, much lower half of face, retract forepoling and breasting plates, repeat excavation sequence to 1.2 m ahead the shield, then shove shield forward.

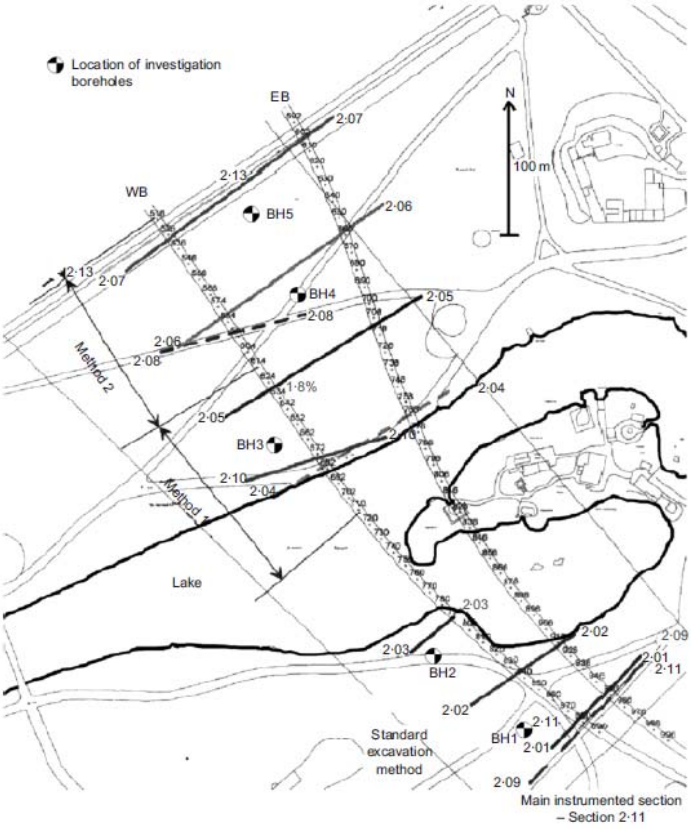

Figure 22. The method used in correspondence of the section instrumented for high precision monitoring (Mair & Dimmock 2007).

2.1.5.4 Observed displacements

The contractor installed 7 simple instrumented sections for ground displacement monitoring. An additional section, intended to return better equality data, was set up by a research team (Nyren 1998) to investigate surface and sub-surface settlements. The location of the high-precision instrumented section is visible in Figure 9.

Details of the instrumentation can be seen in Figure 23 (note the rotation, with skewed North, with respect to Figure 9).

Both tunnels were driven from the South-East to the North-West. The Westbound tunnel passes under the instrumented section in April 1995; the Eastbound tunnel in January 1996 (Nyren *et al.* 2001). The tunnels crossed the instrumented section almost perpendicularly at a horizontal distance of 21.5 m. The actual distance separating the tunnels in the ground is larger as they are located at different depths: approximately 31m below ground level the Westbound tunnel and approximately 21m below ground level the Eastbound tunnel.

The measurements of surface displacements were made on 24 surface monitoring points (SMPs), spacing 2.5m and positioned in a nearly perpendicular to both the tunnels. Each SMP comprise an extended socket embedded into a 1.5m deep concrete pillar, sleeved with stiff PVC tubing over the top 0.8m. Vertical displacements were measured on a monitoring plug screwed tightly into the extended socket at each SMP. Measurements at St. James's Park were made using two high-precision coaxial electronic theodolites with integrated electronic distance measurement and digital data acquisition capabilities, often referred to as "total stations". The surface monitoring systems use reference point affixed on the buildings near to the site but outside the zone of tunnelling influence.

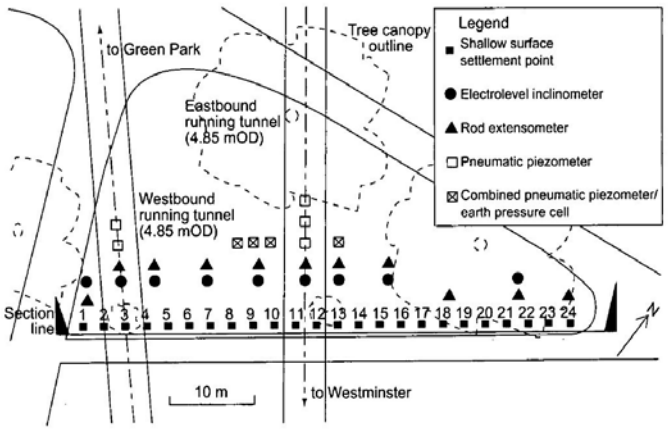

Figure 23. Instrumented section and tunnel position, source Burland and Standing (2006).

Below are reported the settlements through obtained consequentially the construction of the tunnels. As it can be noticed from Figure 25, only part of settlements through has been captured. The instrumentation was not extended enough inside of the area of influence of the tunnel, the vertical movements extend out to a distance of about 45m from the centre line of the tunnel, i.e. about 1.45 times the depth of the tunnel axis. In Figure 24 the surface displacements of the eastbound tunnel show a same asymmetry presumably due to the previous construction of the west tunnel.

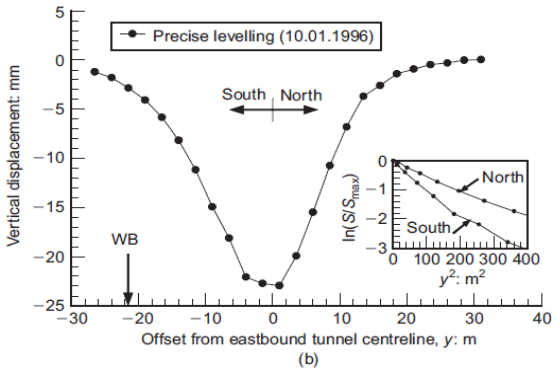

Figure 24. Vertical displacements profile above the Eastbound tunnel

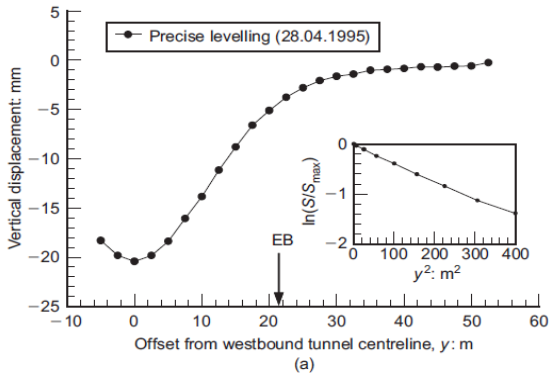

Figure 25. Vertical displacements profile above the Westbound tunnel

The maximum displacement of the westbound tunnel is 20.4 mm and it was recorded at the tunnel centre-line, while the maximum displacement recorded for the eastbound tunnel was recorded from approximately 1m offset from the centre-line of the tunnel and it was of 23.4mm.

2.2 Fleet Line tunnel at Green Park

2.2.1 Introduction

One more case history considered in this study is the settlement observed above a London Underground tunnel in proximity of Green Park Station (Attewell & Farmer 1974). The tunnel was constructed in the early 1970s as part of the Fleet Line, now renamed and representing part of the Jubilee Line. The works consisted of a hand excavation of a 4,146 m external diameter shield driven tunnel at an axis depth of 29.3 m in previously undisturbed London Clay.

The excavation process included:

- excavation of the upper part of the face to a distance of 0.6 m beneath and in advance of the shield; the upper part is then supported (or "boxed up")
- the shield is jacked forward by 0.6 m
- the lower part of the face is excavated and then boxed up

The lining was a seven-segment cast iron lining with 4.070 m external diameter and 0.6 m width.

Post-installation grouting was carried out. More precisely:

- the last complete ring after the shield jacking was isolated with packing
- the cavity between clay surface and lining was injected with water-cement grout; the injection was carried out at low pressure trough several grouting holes and starting from the lower part of the ring.

Tunnel advancement was obtained by repeating the excavation-lining-grouting sequence. A shield like the one used for the Fleet Line tunnel at Green Park is shown in Figure 27.

2.2.2 Monitoring

Vertical displacements were measured at ground surface and at depth in the soil mass above the tunnel crown. The vertical surface movements were monitored with precise levelling at stations established along three lines normal to the tunnel centreline, as shown in Figure 27.

Vertical subsurface movements were measured at magnetic rings located approximately at 6 m depth intervals.

Vertical surface movements were measured to an accuracy of ± 0.1 mm. The accuracy of vertical subsurface readings is considered to be in the range of ± 0.2 mm, thanks to repeated observation and data reduction techniques.

Horizontal movement were also recorded at the surface, via topographic measures, and at depth, using inclinometers.

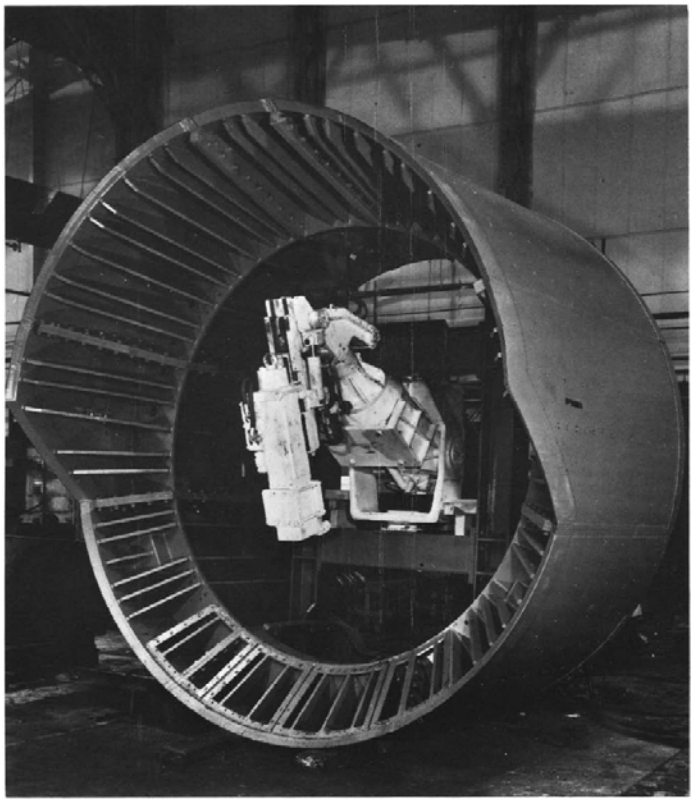

Figure 26. Example of shield used for tunnelling in stiff clays in the 1970s.

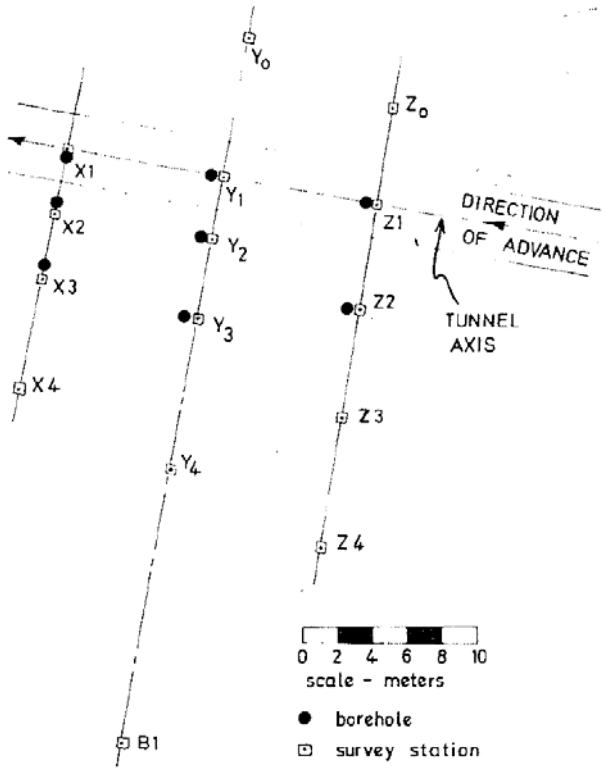

Figure 27. Monitoring system at Green Park (source: Attewell and Farmer 1974).

2.2.3 Ground profile

The geology of the site are not dissimilar to the one at St. James's Park. However, in this case the shallow ground profile is somewhat simpler, with only two meters of mixed coarse-grained soil overlying the London Clay. The Lambeth Group is deeper at this location and unlikely to have any influence on the tunnel.

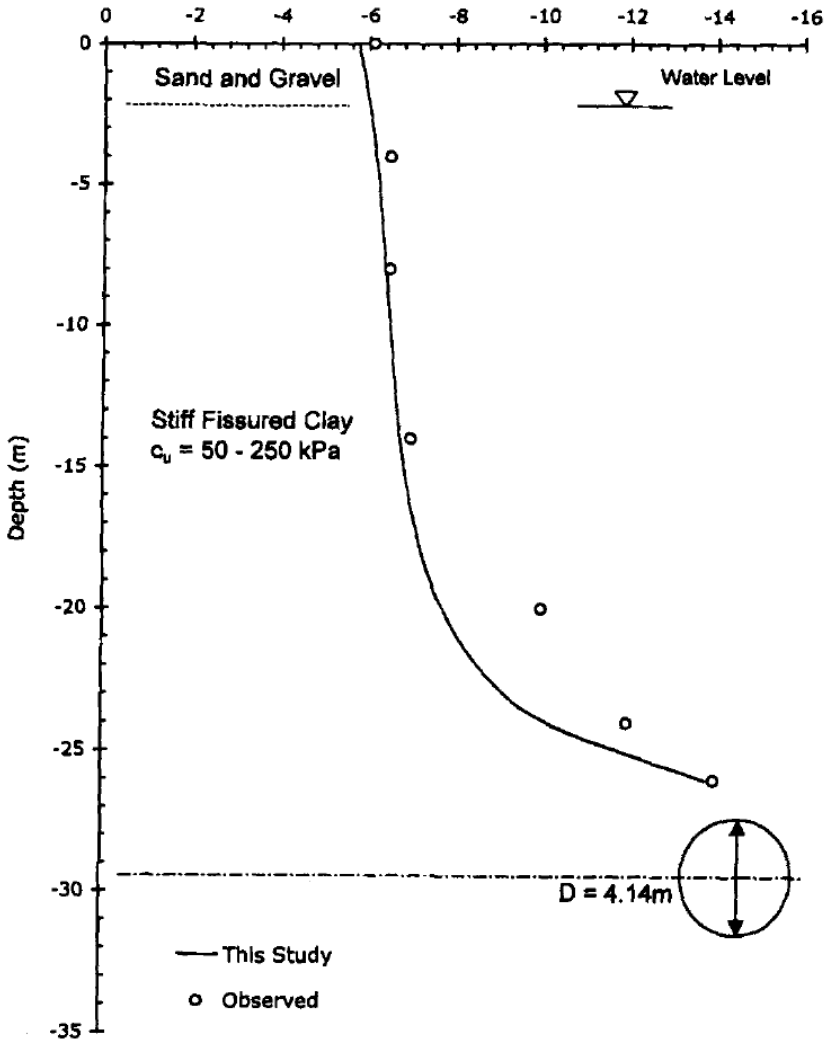

Figure 28. Ground conditions at Green Park (source: Loganathan & Poulos 1998); note that "this study" result refer to the work of Loganthan & Poulos (1998) and that "observed data" represent only one of several available data sets.

Attewell and Farmer (1974), as well as Loganathan & Poulos (1978), report strength and stiffness values of the London Clay at the site. In summary, the undrained shear strength S_u increases with depth and varies approximately between 50 KPa and 250 kPa. At the tunnel level (see also Figure 29), the undrained shear strength is estimated to be in the range of S_u = 175 kPa and the undrained Young's modulus in the range of E_u = 40 MPa

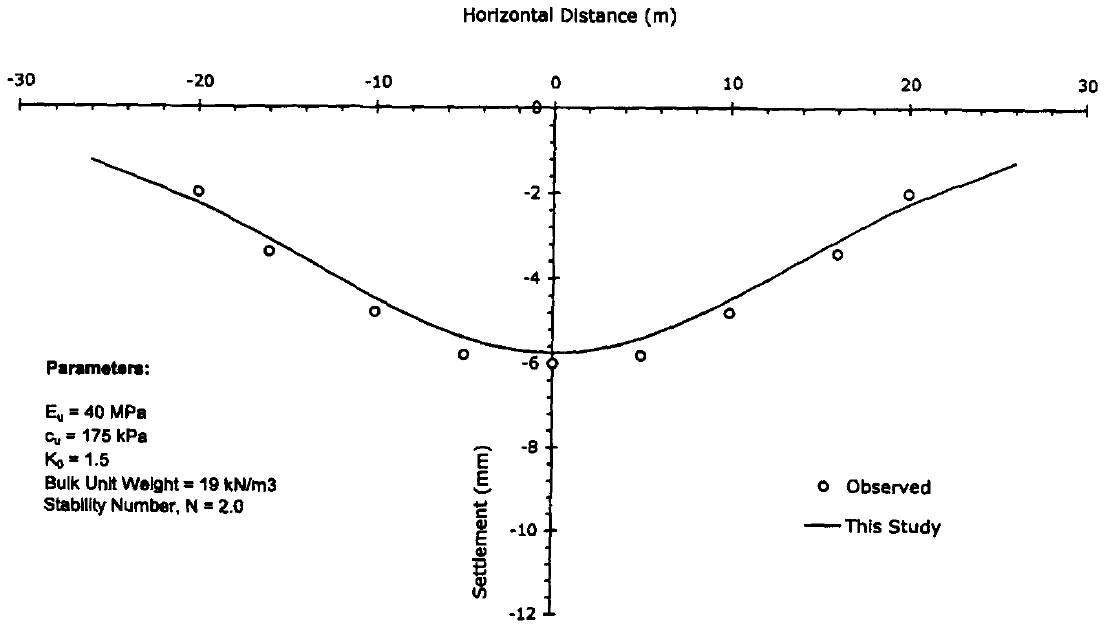

Figure 29. Ground parameters at tunnel level according to Longanathan & Poulos (1998) and observed settlements.

The maximum vertical displacement occurred over the tunnel centreline at boreholes X1, Y1, Z1. The average maximum settlement at ground surface was S_{max} = 6.1 mm. The settlement profile transverse to the tunnel is reported in Figure 29.

When observing the settlement recorded at depth plotted against the tunnel face advancement (Figure 30) it will be noticed that the records show an eventual uplift of the of the ground above the tunnel soffit after following the maximum settlement, which occurs approximately 10-20 m behind the tunnel face.

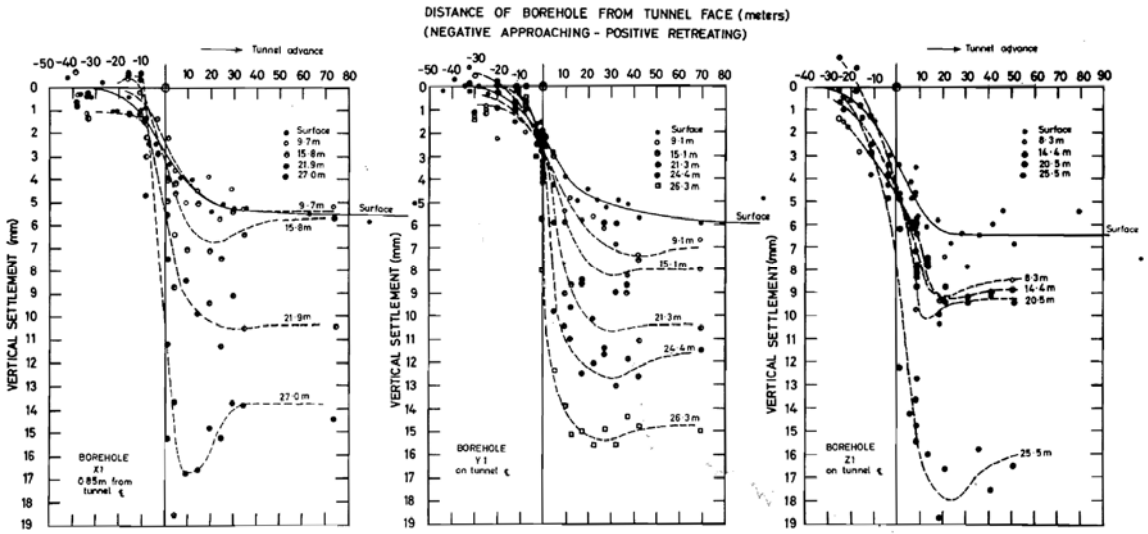

Figure 30. Vertical displacements at depth as a function of face advancement.

This uplift has been explained as a consequence of post-tailskin relaxation of lateral pressure in the clay and subsequent stiffening of the clay annulus as the setting grout resists inward deformation (Attewell and Farmer 1974, Ward and Thomas 1965).

The variation of tunnelling induced vertical displacement with depth, in terms of maximum settlement and ultimate (smaller) settlement is visible in Figure 31.

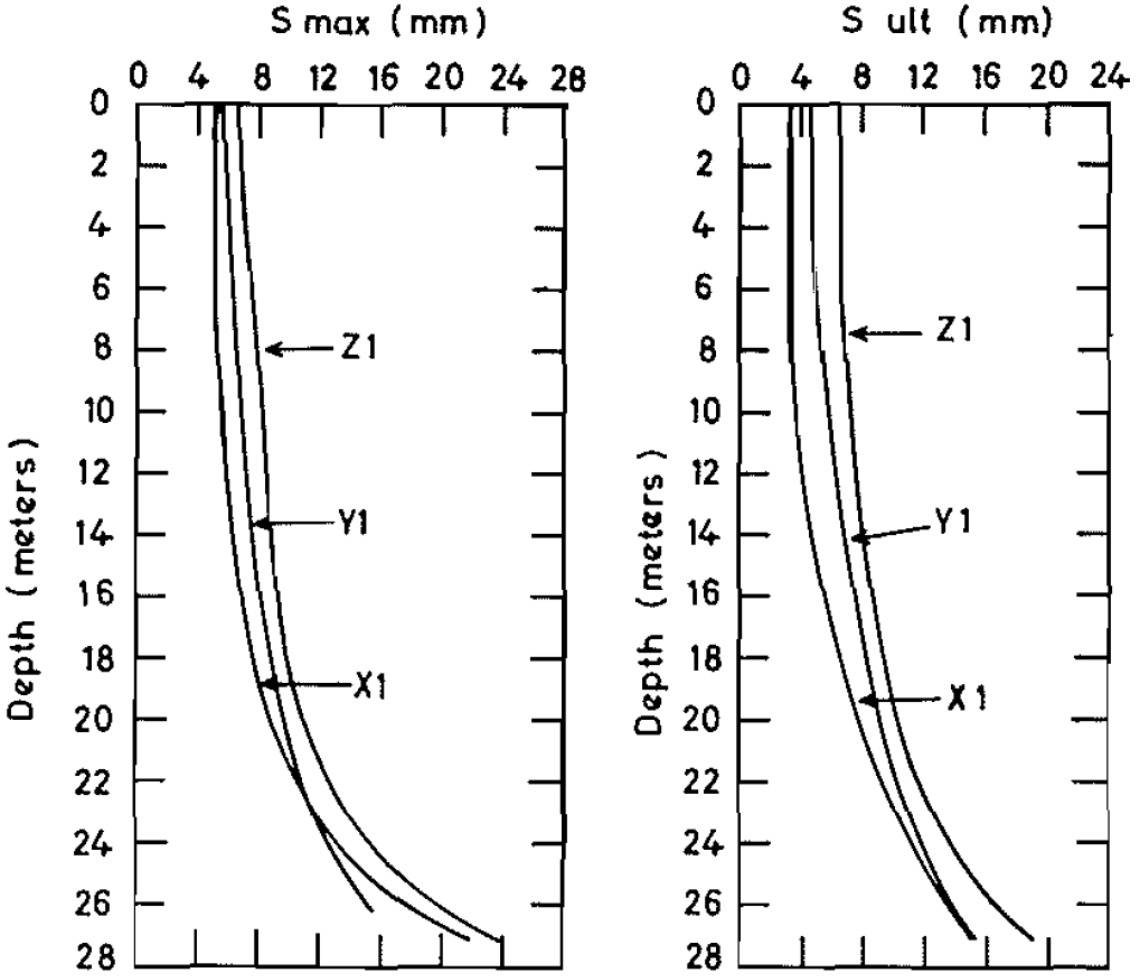

Figure 31. Maximum settlement and ultimate settlement at depth.

3 Numerical Analysis - Jubilee Line Extension

3.1 Introduction

3.1.1 Overview

First case history considered is the Jubilee Line Extension (JLE) at the instrumented section of St. James's Park. The location is of particular interest because two tunnels were constructed at different depths. They also experienced different volume losses. The tunnels are approximately 21m apart in plan when they cross the instrumented section. A small degree of interaction between the transverse settlement troughs generated by the two tunnels was observed. In the present work, however, analyses are conducted, for the sake of simplicity, with two separate meshes, each considering one tunnel in isolation.

3.1.2 Ground model

The ground model adopted in the finite element calculations is reported in Table 12. Ground model. The Made Ground (predominately fine-grained) and the Alluvium (essentially normally-consolidated Clay) have been grouped into a single layer due to the similarity of their geo-mechanical properties.

The Lambeth Group at the relevant location is predominantly fine grained and here is treated as a uniform layer of Clay. This assumption is also consistent with the work of Addenbrooke *et al*. (1997) and Wongsaroj *et al*. (2007).

Table 12. Ground model.

From (mPD)	To (mPD)	Thickness (m)	Soil
103	98	5	Made Ground & Alluvium (CLAY)
98	95	3	River Terrace Deposit (GRAVEL)
95	60	35	London Clay
60	-*	-*	Lambeth Group Clays
(*)Note: the exact thickness of Lambeth Group Clays is uncertain but it is known to extend below 50mPD, that is the mesh base in the FE model.			

The aim of the present work is to successfully simulate the short-term response of the ground to tunnelling. In these circumstances the fine-grained layers experience undrained behaviour. The only coarse-grained soil expected to respond in a drained manner in the short-term is the River Terrace Gravel.

Due to the geometry of the problem, there is no need to include in the model layers that are deeper than the Lambeth Group Clays.

3.1.3 Meshes

Two finite element meshes of 6-nodes triangular elements have been generated to study each tunnel separately. The symmetry about the vertical axis passing for the centre of the tunnel has been used to half the size of the meshes. They both represent a portion of ground that is 60m wide and 53m deep.

In the attempt of facilitating a more accurate modelling of the ground movements above the tunnel, a relatively fine mesh has been used all the way up to ground level. This is somehow different from

calculations aiming purely at estimating the structural actions in lining, in which a refinement of the mesh exclusively around the tunnel would be adopted.

Figure 33 shows the mesh for the Westbound tunnel, which is 31m below ground level (depth of tunnel axis). It comprises 1927 triangular elements (6-noded) for a total of 4017 nodes.

Figure 32 shows the mesh for the Eastbound tunnel, which is 21m below ground level (depth of tunnel axis). It comprises 2670 triangular elements (6-noded) for a total of 5508 nodes.

In both cases the nodes at the base of the mesh are fixed in the horizontal and vertical direction. The nodes at the sides of the mesh are fixed in the horizontal direction but free to move vertically.

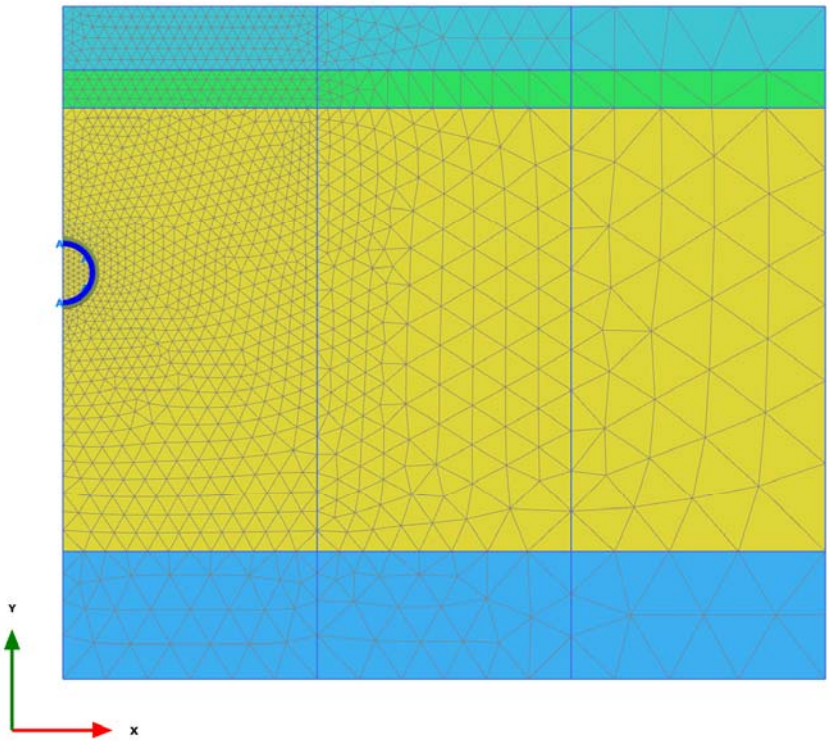

Figure 32. FEM for the Eastbound JLE tunnel at the instrumented section of St James's Park.

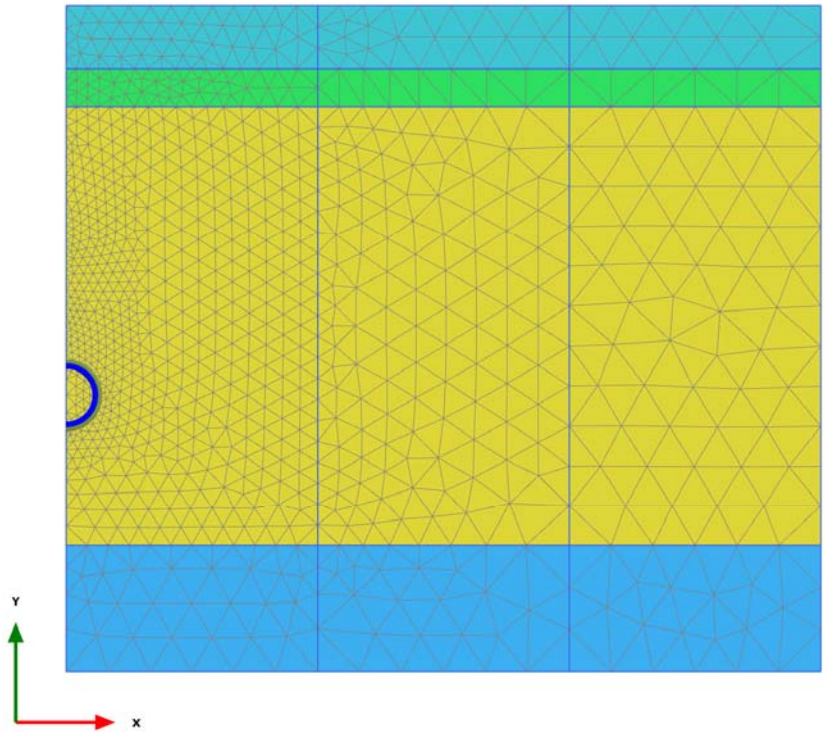

Figure 33. FEM for the Westbound JLE tunnel at the instrumented section of St. James's Park.

3.2 Calculations for the Westbound Tunnel

3.2.1 Introduction

This section presents the results of 2D plane strain finite element analysis of the Westbound Tunnel of the Jubilee Line Extension at St. James's Park. The aim is to match the short-term settlements measured at the monitoring section via precise levelling at the time of construction.

The calculations have been conducted with linear elastic-perfectly plastic (LE-PP) constitutive models. To simulate undrained conditions, the fine-grained soils have been modelled in total stress and with Tresca's failure criterion. The single coarse-grained material (River Terrace Gravel) has been modelled in effective stress with Mohr-Coulomb failure criterion. The calculations parameters are summarised in Table 12.

The Westbound tunnel is located approximately 31m below ground level (BGL). A maximum vertical displacement of 20.4 mm at the tunnel centreline was measured at the instrumented section when the tunnel had passed beyond the zone of influence. Standing and Burland (2006) declare a volume loss for this profile of 3.3% and a trough width parameter K = 0.43. Considering that the excavated diameter was 4.85m (open-face shield excavation), however, the parameters mentioned above return the Gaussian curve plotted in Figure 34. In the author's view, an interpretation based on V_L = 3.36% and K = 0.4 provides a better interpretation of the field data and has been adopted in this study (Figure 35).

Table 12. Geotechnical parameters.

Soil	γ_{sat} **(kN/m³)**	**c'** **(kPa)**	ϕ' **(°)**	S_u **(kPa)**	E' **(MPa)**	ν' **(-)**	**Eu** **(MPa)**	ν_u **(-)**
MG/Alluvium	17.5	-	-	30	-	-	10	0.49
RTD	19.5	0.1	35	-	75	0.25	-	-
London Clay	19.0	-	-	40+6.4 z	-	-	10+5.2 z	0.49
Lambeth Group	20	-	-	280	-	-	200	0.49
Note: *z* is the depth below the top of the London Clay								

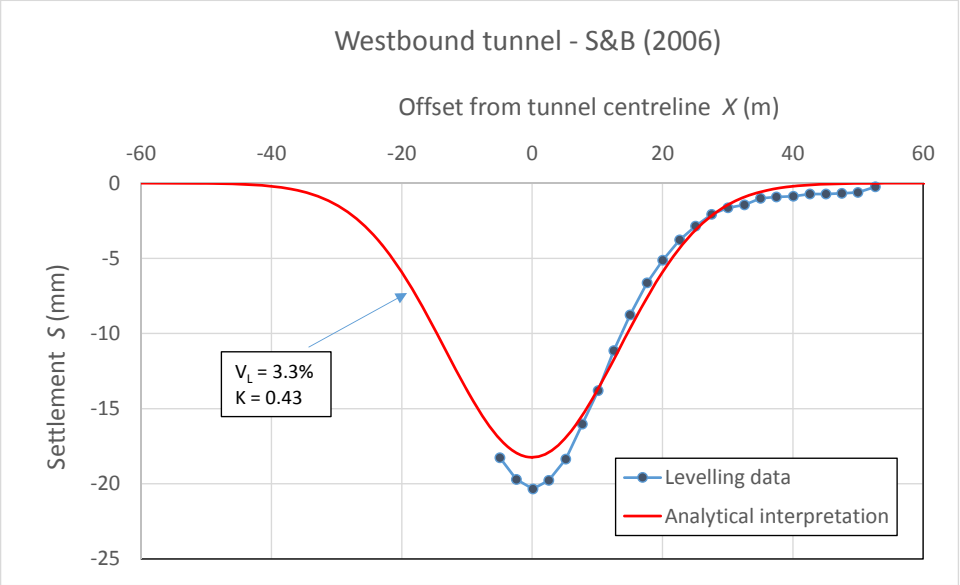

Figure 34. WBT, Gaussian settlement trough based on the interpretation proposed by Standing & Burland (2006).

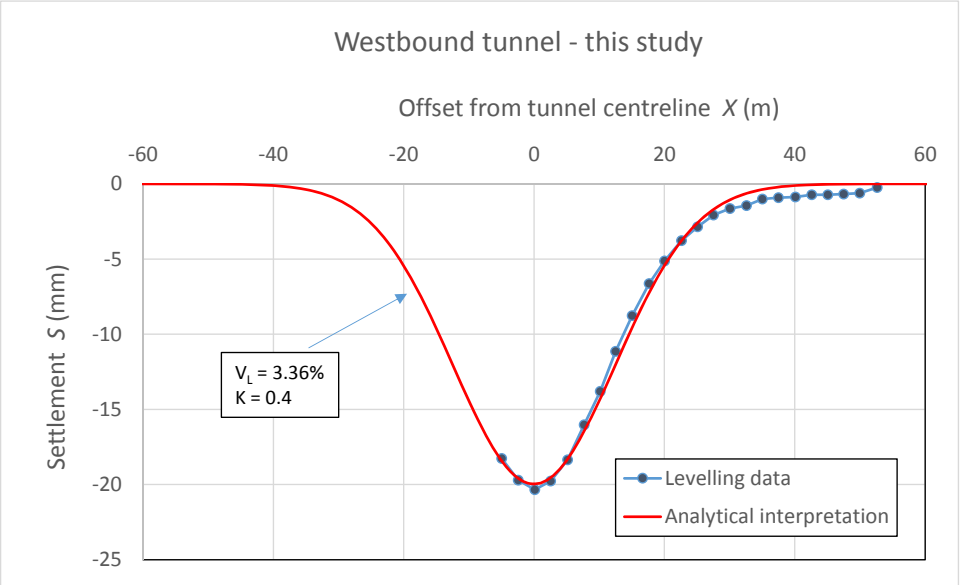

Figure 35. WBT, Gaussian settlement trough based on the interpretation adopted in this study.

It is worth pointing out that in the finite element mesh the tunnel lining is introduced as a set of beams without thickness. As the ideal lining in the model is placed at the axis position of the real lining (mid-way between outer diameter and internal diameter), the excavated area in the model is smaller than the area actually excavated on site. This implies that a correction has to be applied to the volume loss and a slightly higher value is needed in the finite element calculations. In the specific case, being the JLE lining 200mm thick, a corrected volume loss V_L^* = 3.66% is appropriate for the finite element calculations.

The lining of the JLE tunnels at St. James's Park is made of 10 expanded concrete segments. The axial stiffness of the plate representing the lining in the FE model has been calculated as

$$E_{conc} * A$$

where

E_{conc} is the Young's modulus of concrete
A is the cross sectional area per metre run

The axial stiffness of the plates governs the tunnel response in the circumferential and longitudinal direction.

The bending stiffness of the plate has been estimated taking into account the behaviour of the segmental lining as described by Muir Wood (1975):

$$I_e - I_j + \left(\frac{4}{n}\right)^2 I$$

where

I_j is the second moment of area at the joint
I is the second moment of area for the ring
n is the number of segment

A sensitivity check, in which the bending stiffness reduction due to the segmental nature of the lining was neglected, and the material was treated as monolithic inserted, has been carried out. However, the results demonstrated that the displacement field around the tunnel is virtually insensitive to the lining stiffness, provided the target volume loss is correctly imposed.

3.2.2 Stress relief method

The target volume loss - more correctly area loss, in 2D - in the finite element model has been achieved with the stress relief (or "confinement-convergence") method (Panet & Guenot 1982; Schikora & Fink 1982), in which a portion of nodal forces at the wall, equal to (1-β), is kept in place until the activation of the lining. In Plaxis this method is implemented by controlling the multiplier M_{stage}. (Brinkgreve 1998).

The stress relief parameter needed to achieve the required area loss of 3.66% has been found, by trial and error, to be

(1-β) = 0.99

The area loss in the model has been checked at each attempt with a spreadsheet that makes use of the initial coordinates and calculated displacements of the points that constitute the polygonal approximation of the tunnel wall.

The key results of calculations with an initial stress ratio in the London Clay k_0 = 1.25, which is a reasonable approximation of the true site conditions, are presented in Figure 36 to Figure 43.

It is obvious, from the comparison in Figure 42, that the calculated settlements bear no resemblance to the settlement profile observed on site.

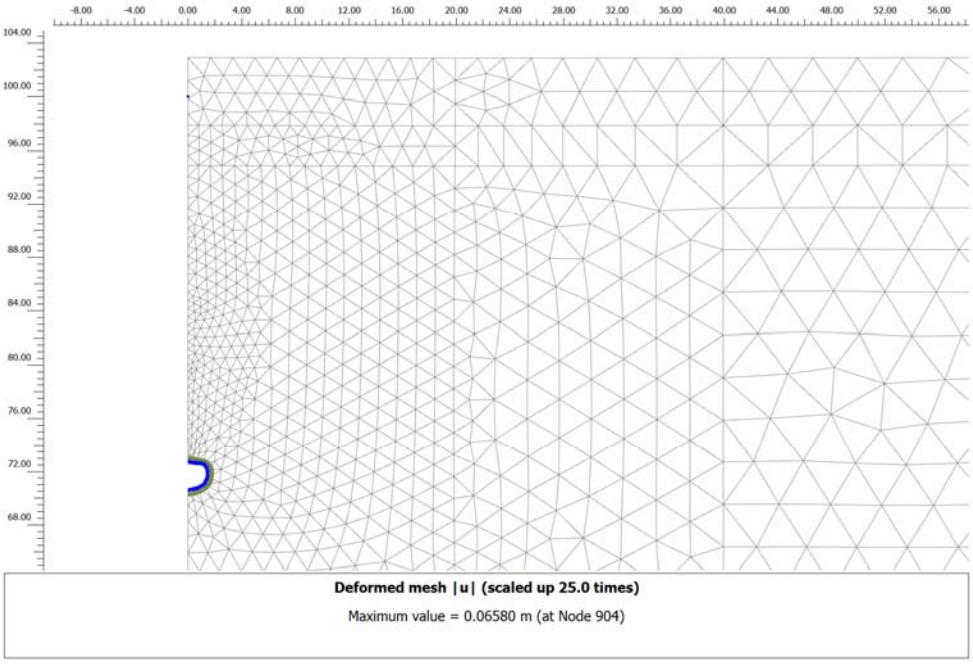

Figure 36. WBT, stress relief method, k_0 = 1.25, deformed mesh.

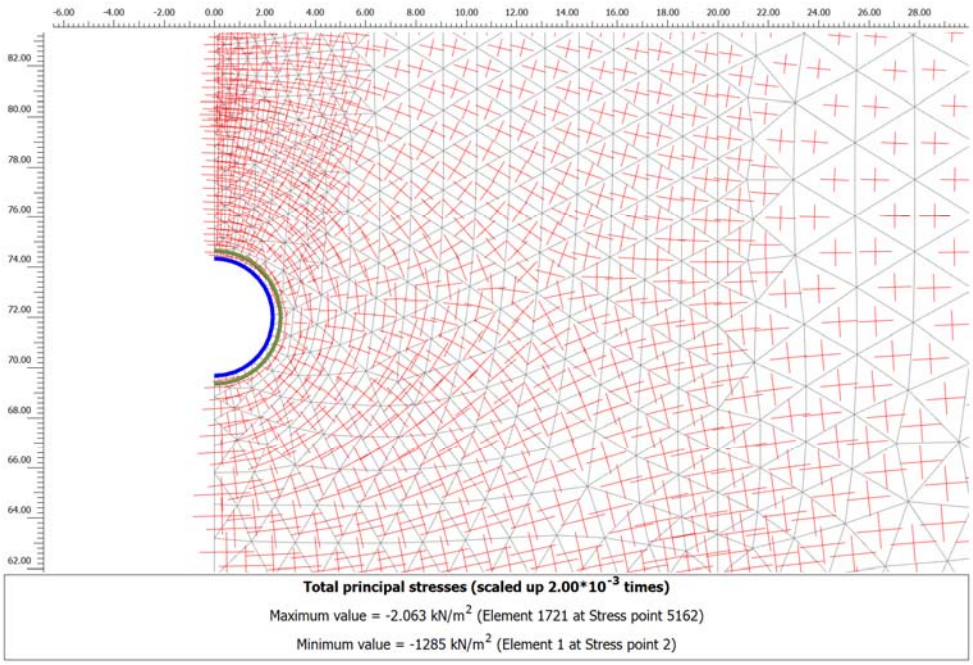

Figure 37. Stress relief method, $k_0 = 1.25$, principal stresses around the tunnel.

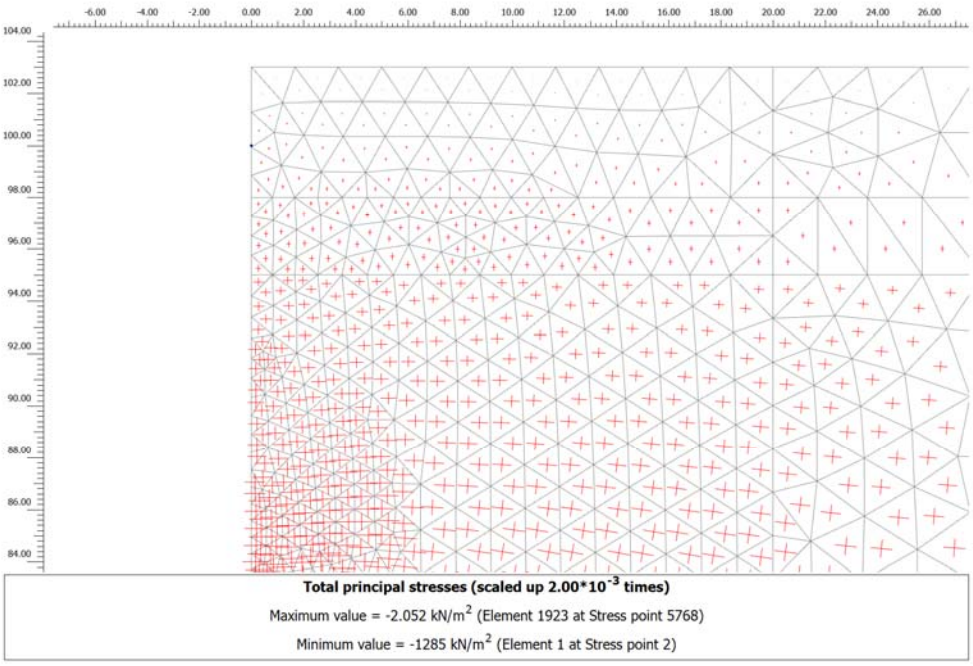

Figure 38. Stress relief method, $k_0 = 1.25$, principal stresses near the surface.

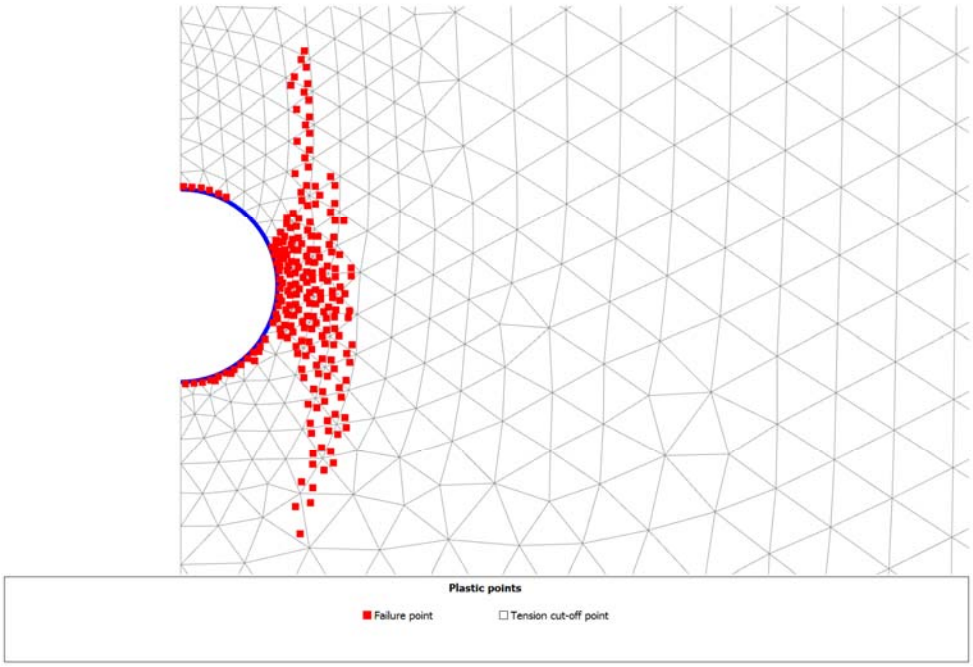

Figure 39. Stress relief method, k_0= 1.25, plastic points.

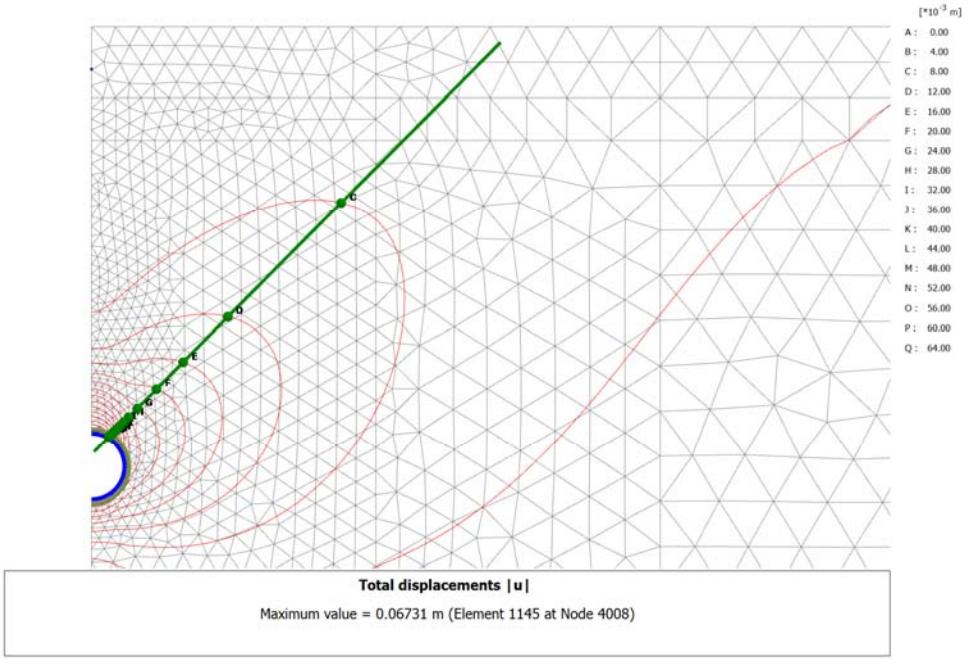

Figure 40. Stress relief method, k_0 = 1.25, total displacements.

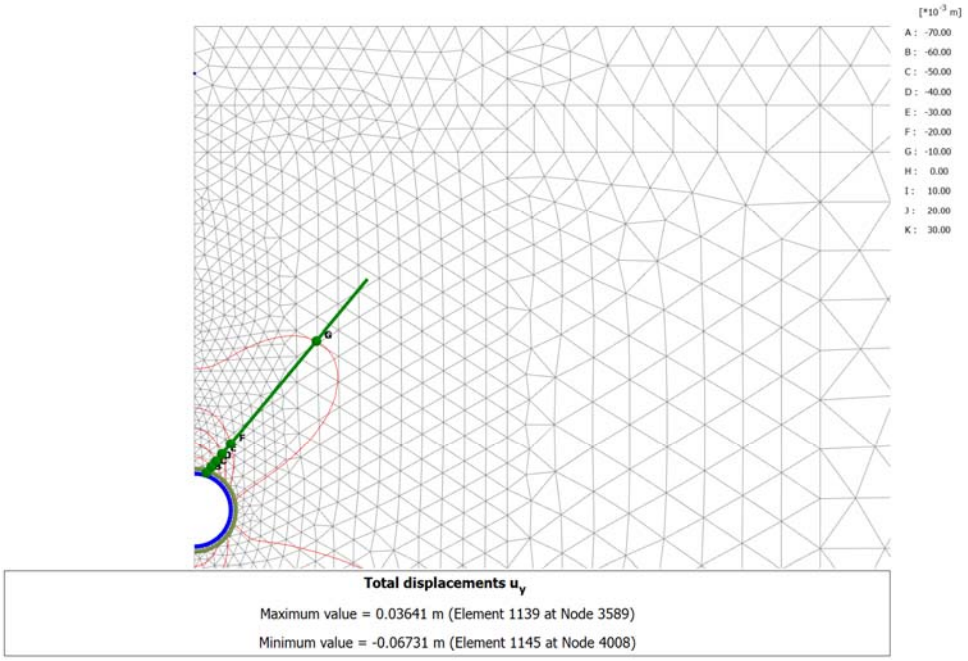

Figure 41. Stress relief method, k_0 = 1.25, vertical displacements.

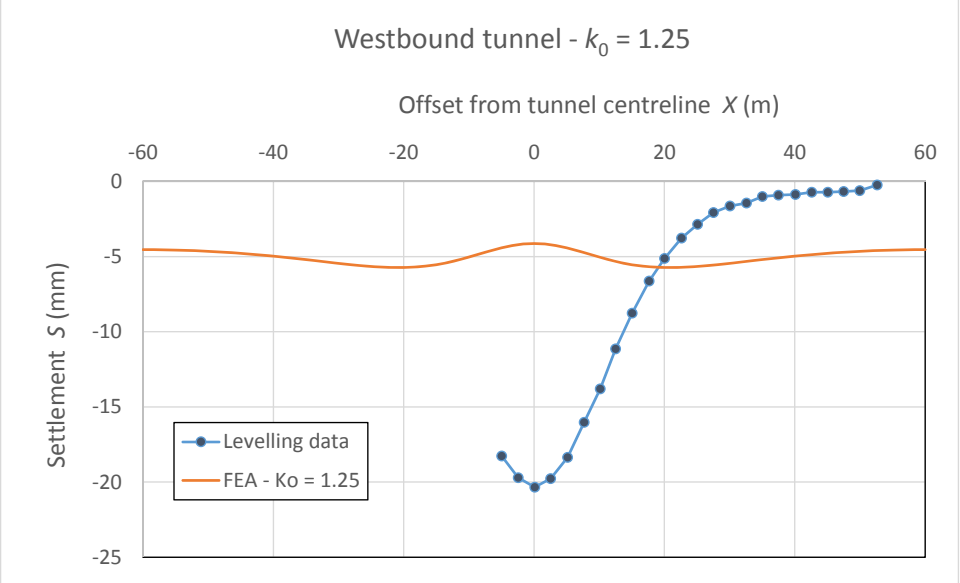

Figure 42. Stress relief method, k_0 = 1.25, vertical displacements at ground surface.

3.2.3 Alternative implementation of stress relief

In an attempt to check the influence of what is left, at the moment of the lining activation, of the anisotropy of the initial stress state. A different approach to stress relief was also considered in this work by temporarily supporting the tunnel wall with a uniform radial pressure (rather than preserving part of the out-of-balance forces from the previous phase). The aim was to verify any significant effect on the displacement field. Some influence of similar assumptions was observed in soft clays by *Likitlersuang et al.* (2013).

The key results of calculations with an initial stress ratio in the London Clay k_0 = 1.25, which is a reasonable approximation of the site conditions, are presented in Figure 43 to Figure 49.

The comparison between the settlement profiles calculated with the alternative method and with the traditional implementation of stress relief shows virtually no difference (Figure 49).

The main aspect differentiating the two situations is the variation in shape and extent of the area subject to plastic deformations. The use of traditional stress relief results in a plastic zones that extends vertically at the sided of the tunnel, in a shape that we could define “hear shaped” (Figure 48). The use of the alternative method (uniform radial pressure), instead, results in a plastic zones that is predominantly above the tunnel and has two sided uniting into a dome shape.

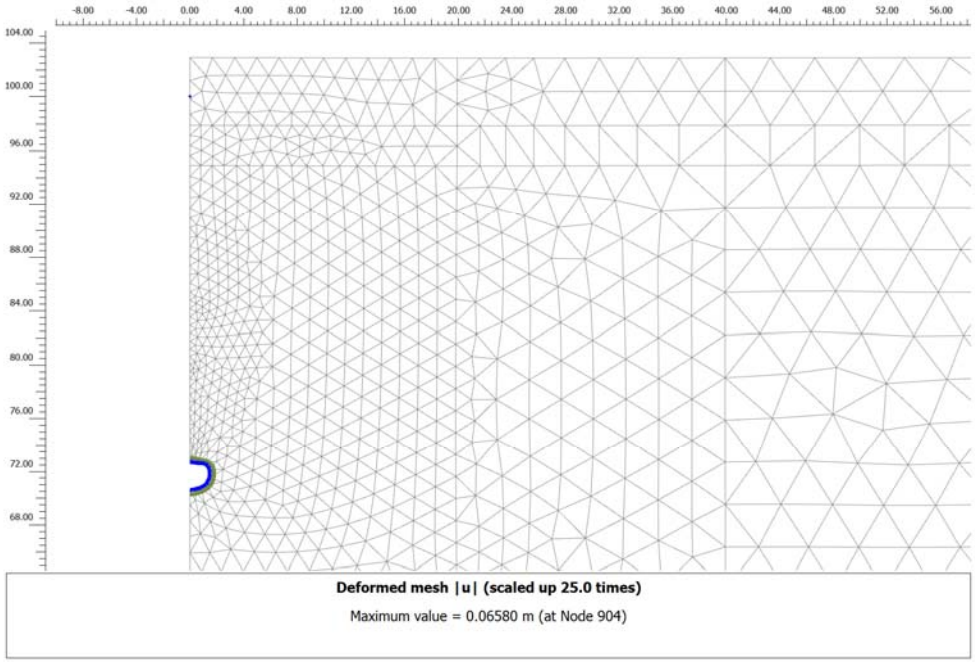

Figure 43. Alternative method, k_0 = 1.25, vertical displacements at ground surface.

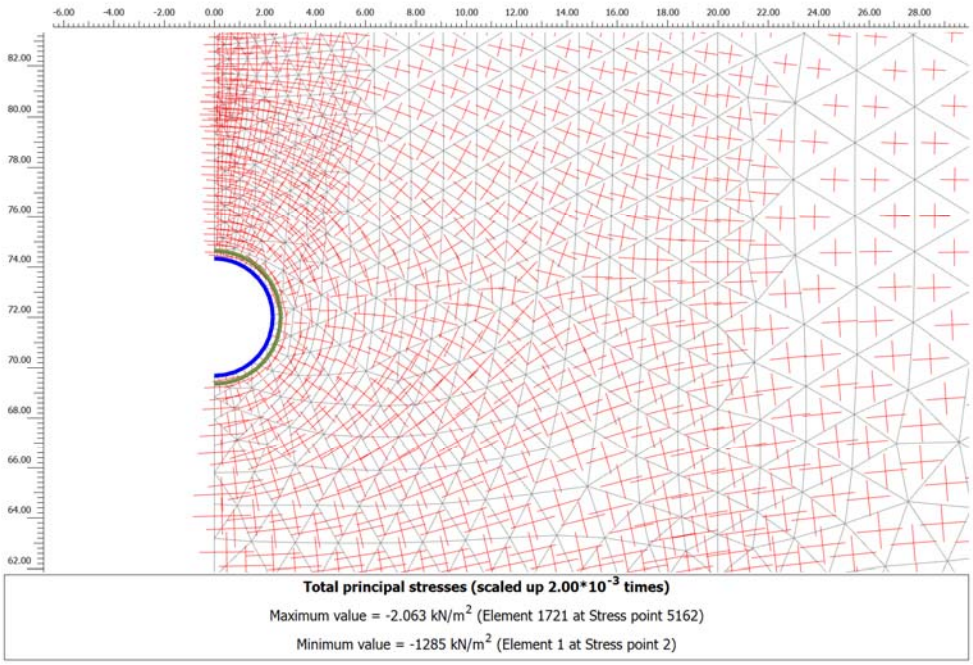

Figure 44. Alternative method, k_0 = 1.25, principal stresses around the tunnel.

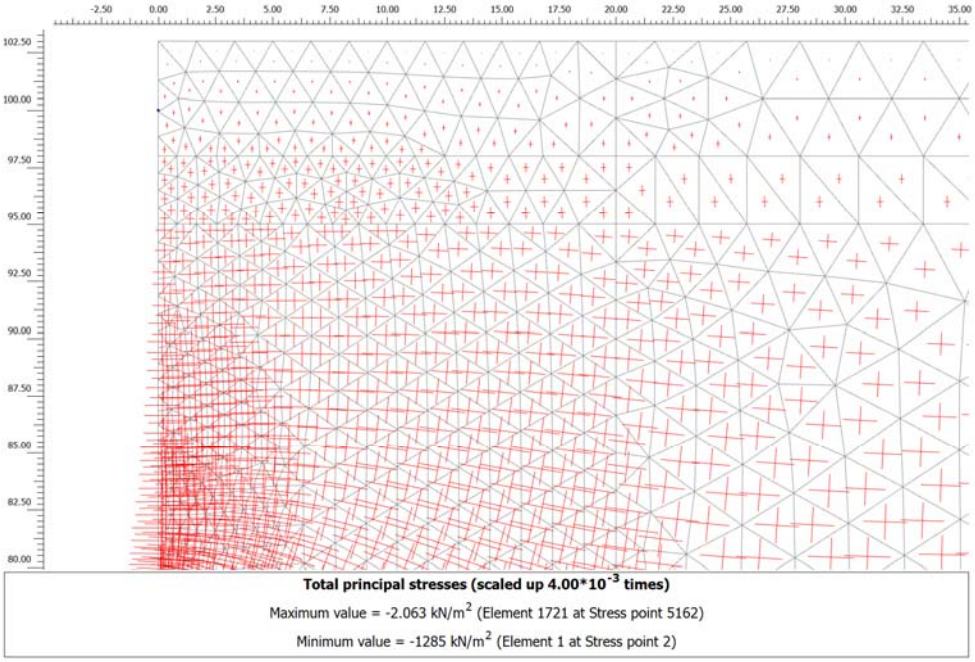

Figure 45. Alternative method, k_0 = 1.25, principal stresses around the tunnel.

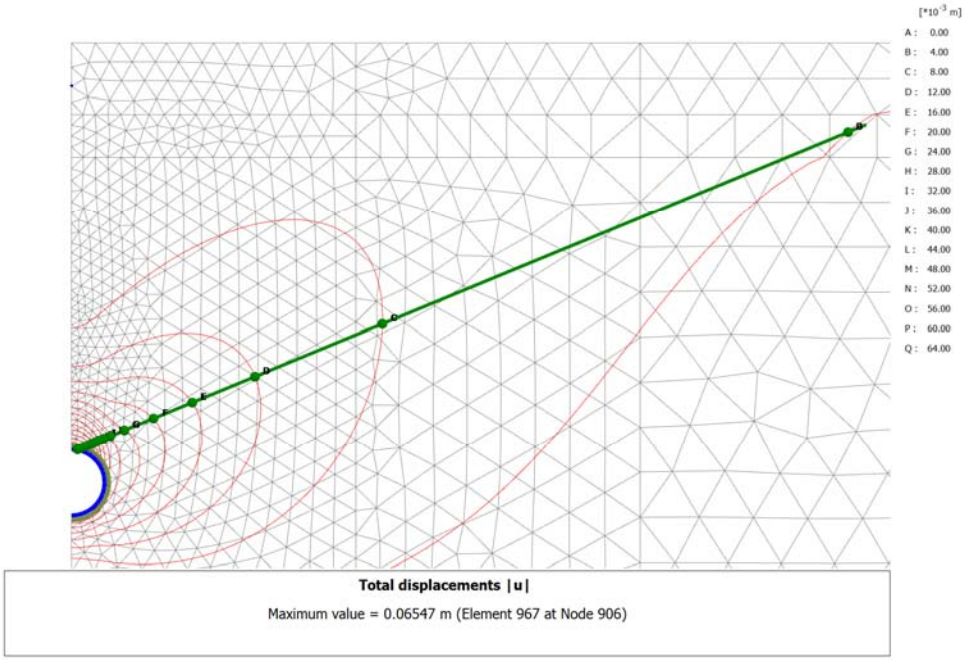

Figure 46. Alternative method, k_0 = 1.25, total displacements.

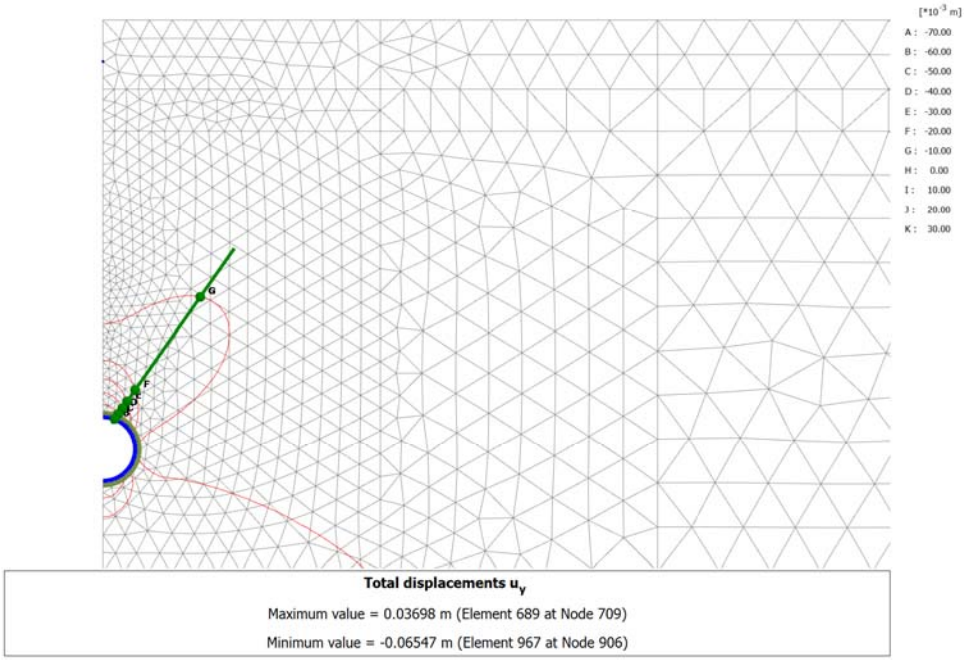

Figure 47. Alternative method, k_0 = 1.25, vertical displacements.

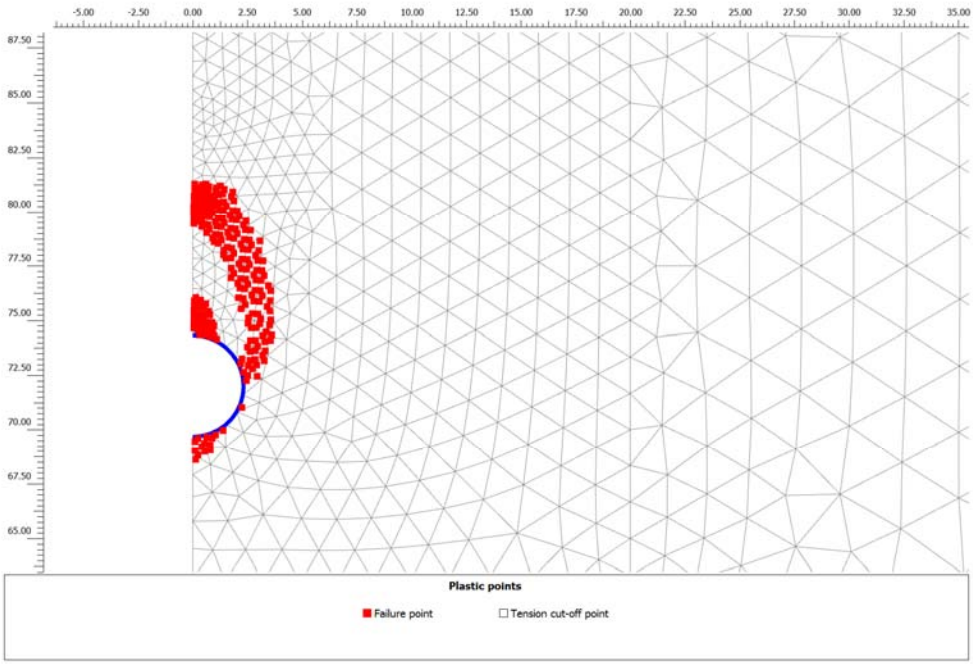

Figure 48. Alternative method, k_0 = 1.25, plastic points.

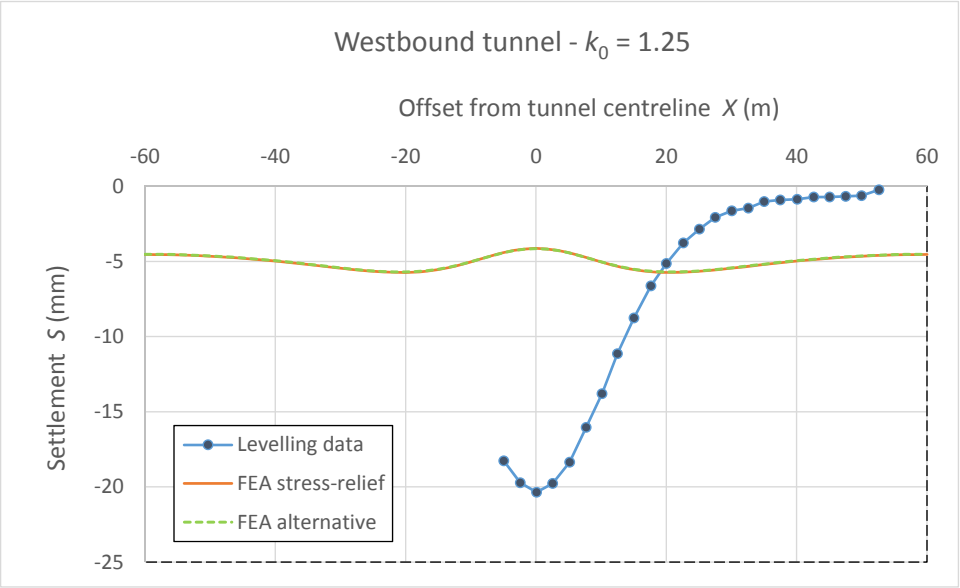

Figure 49. Settlement profile: comparison between stress relief and alternative method.

3.2.4 Use of softened zones

The attempt to use a variation of the traditional stress relief method has produced a calculated settlement profile that does not differ significantly from the one obtained with the more traditional approach and, most importantly, does not resemble the behaviour observed in reality.

However, the plastic zones obtained with the two analyses are significantly different, prompting the question of what would happen if the mechanical properties were modified in the plastic zones.

For this purposes, two meshes have been generated, in which clusters of elements inside the areas identified as subject to plasticity in the previous calculation were delimited in order to enable lower stiffness and/or strength to be assigned.

The geometry of the softened zones, pre-defined in the new analysis on the basis of what was seen in the previous iteration, are shown in Figure 50.

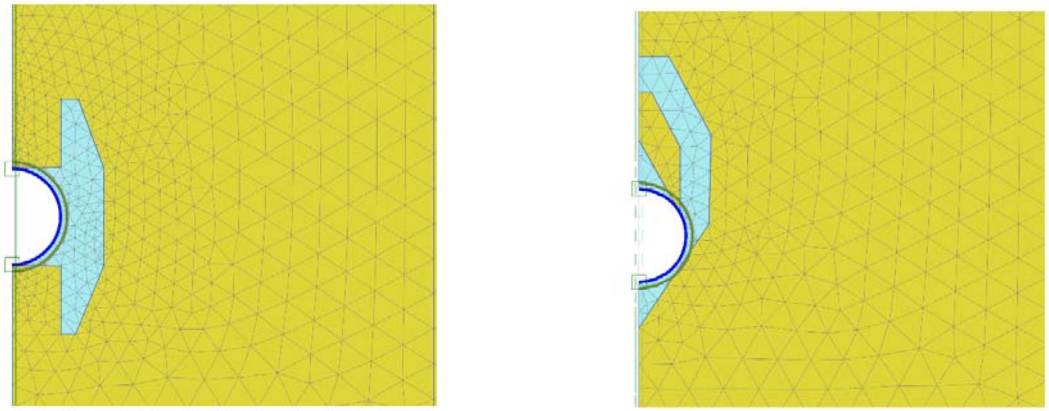

Figure 50. Plastic zones employed in the analysis with softened material (reduction of stiffness and/or strength if the host formation): (a) traditional stress relief method; (b) alternative implementation (radial pressure).

The following sets of parameters were tried for the softened zones:

- reduction of London Clay's Young's modulus to 50% of the initial value
- reduction of London Clay's undrained shear strength to 50% of the initial value
- simultaneous reduction of Young's modulus and undrained strength to 50%
- reduction of Young's modulus to 20% of the initial

It is worth mentioning that, since the value of Poisson's ratio is kept constant, the reduction in Young's modulus E_u , translates in a reduction in shear modulus G of exactly the same proportion.

The changes listed above have produced only small variations in the results and in none of the options has achieved a calculated settlement trough resembling reality.

3.2.5 Sensitivity to initial stress ratio

Considering the sensitivity of the calculated settlement to the changes in the coefficient of earth pressure at rest k'_0 reported in the literature in particular the observation by Doležalová (2002) that unrealistically low values of k'_0 produce numerical results much closer to reality a number of analysis were run progressively reducing the initial horizontal stresses.

Since the fine-grained materials in undrained conditions are modelled here in total stresses, in the following text reference will be made to the initial total stress ratio:

$$k_0 = \sigma_h/\sigma_v$$

It should be noticed that this does not coincide with the coefficient of earth pressure at rest, which is defined in terms of effective stress and, in this work, is indicated with a “dashed” notation:

$$k'_0 = \sigma'_h/\sigma'_v$$

It is always possible to convert k_0 in k'_0 if the distribution of pore-water pressure distribution is known. In the present case, the difference between the two stress ratios (total vs. effective) is small and, although confusion on their exact meaning should be avoided, one can be taken, at least in firs approximation, as a proxy of the other.

Figure 51 shows the calculated settlement trough for decreasing values of the initial total stress ratio in the stiff clay layers. These are the London Clay, which hosts the tunnel, and the Lambeth Group Clays, which lay directly underneath the London Clay. The initial stress ratio in the top layers, which are normally consolidated and have values of k'_0 well below 1.0, was kept to its best estimate value. This avoids the generation of extremely low horizontal stresses in the Made Ground and River Terrace Gravel and ensures there is no early onset of plastic deformations in these layers from the first calculation phase.

The vertical displacements at surface calculated for k_0 = 0.5 provide a satisfactory fit of the observed data. The key results for the latter analysis are shown in Figure 52 to Figure 57.

The alternative implementation of the stress relief method has been applied to the case k_0 = 0.5, without providing any significant difference in terms of vertical displacements.

The effect of reducing material stiffness and strength in the plastic zones, now significantly more extended (see Figure 55), has also proved virtually inconsequential.

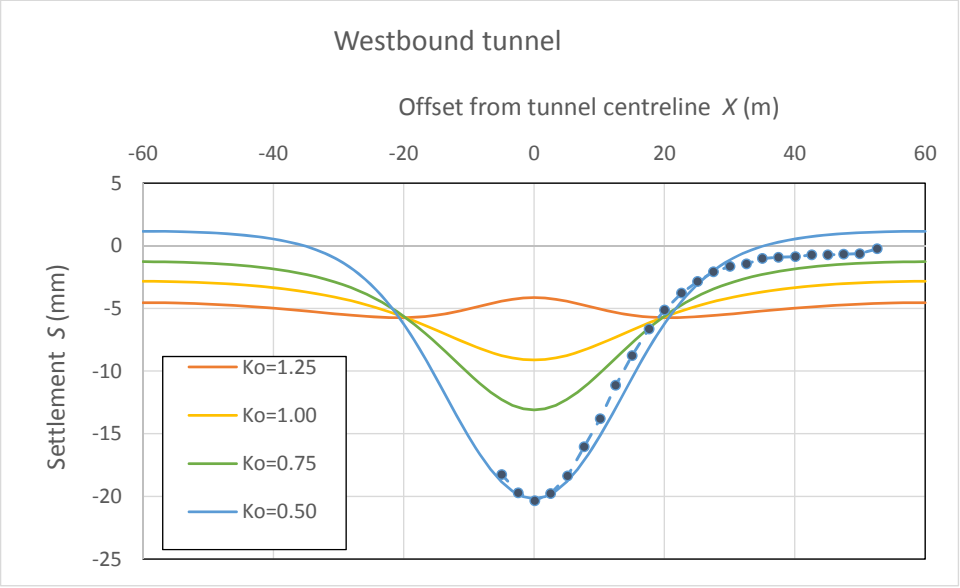

Figure 51. Settlement profile: sensitivity to initial total stress ratio in stiff clays.

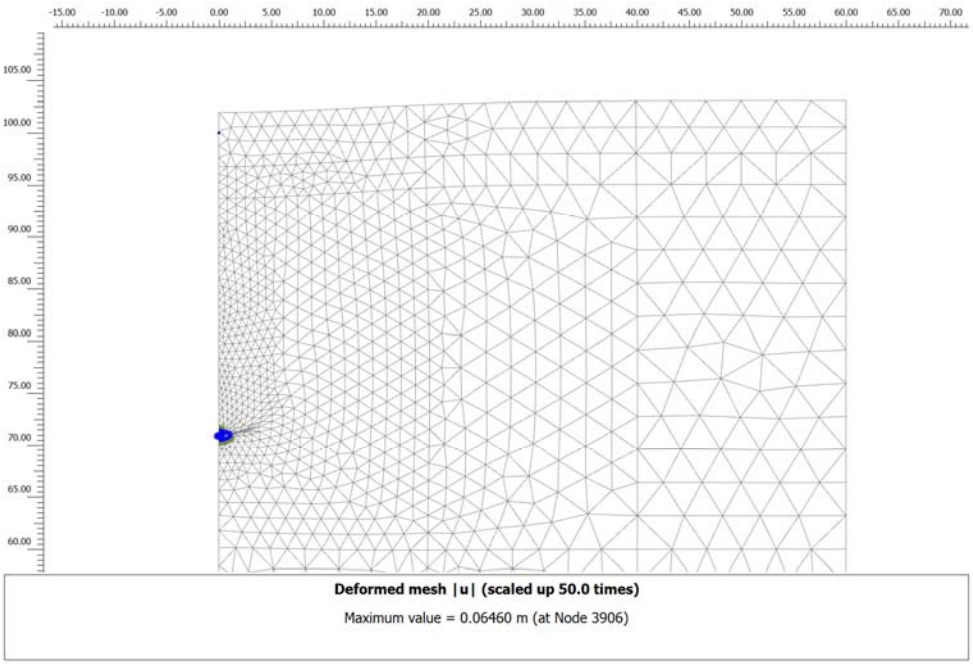

Figure 52. Stress relief method, k_0 = 0.5, deformed mesh.

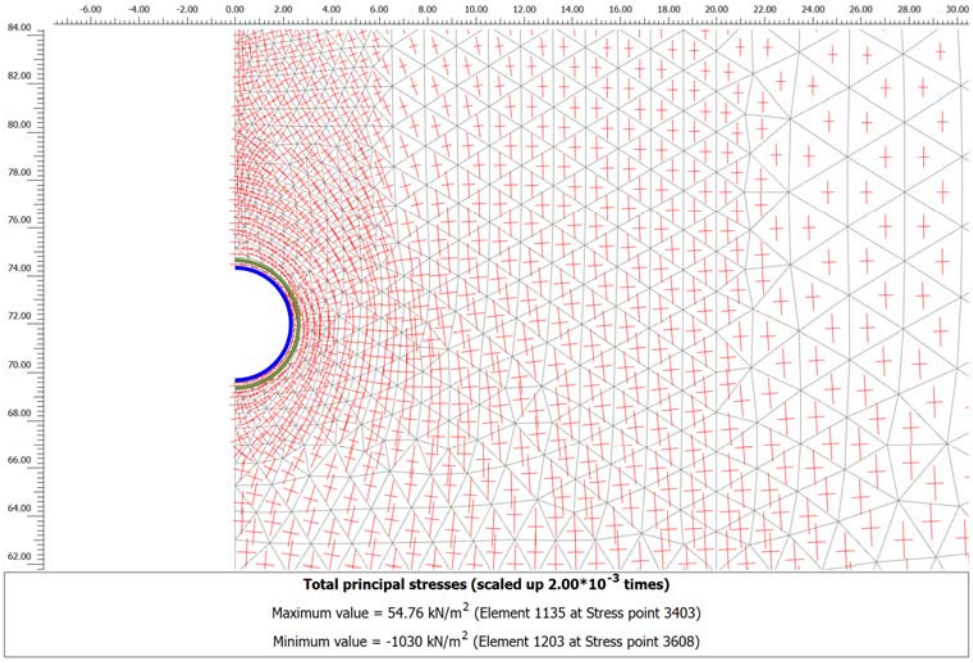

Figure 53. Stress relief method, k_0 = 0.5, principal stresses around the tunnel.

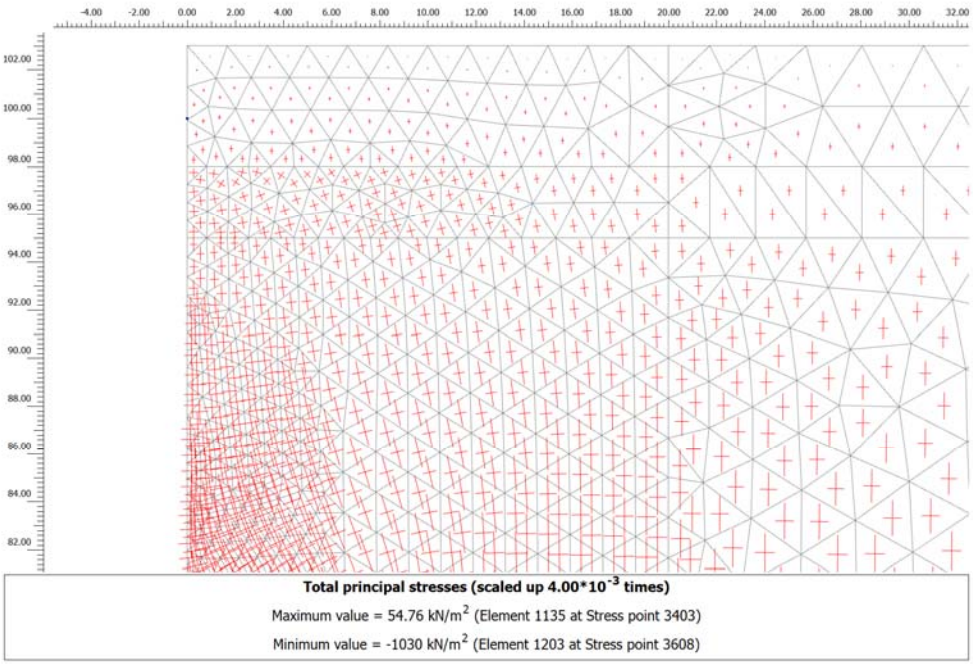

Figure 54. Stress relief method, k_0 = 0.5, principal stresses near the surface.

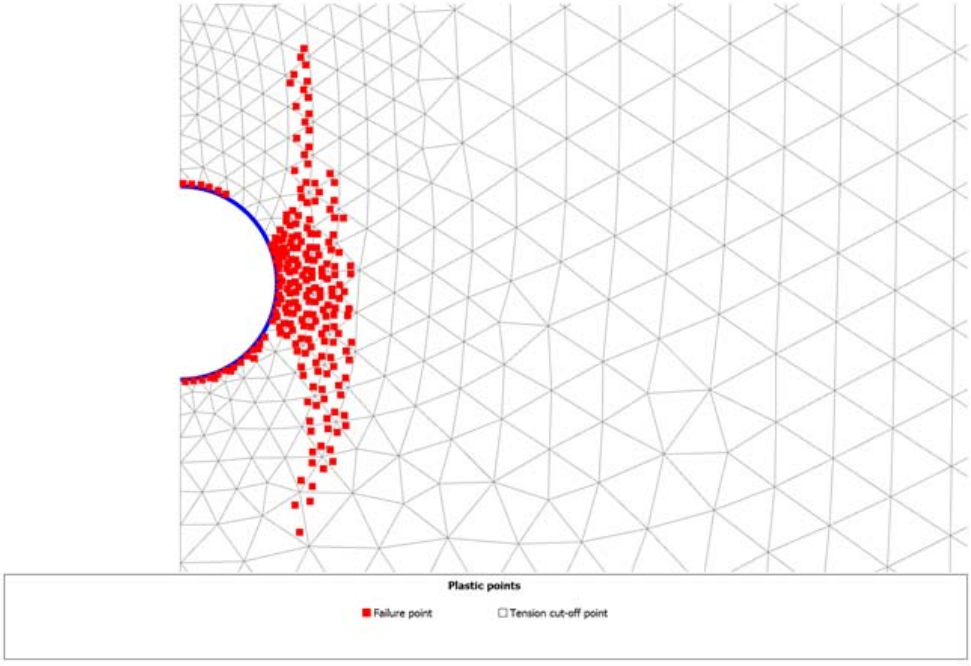

Figure 55. Stress relief method, k_0 = 0.5, plastic points.

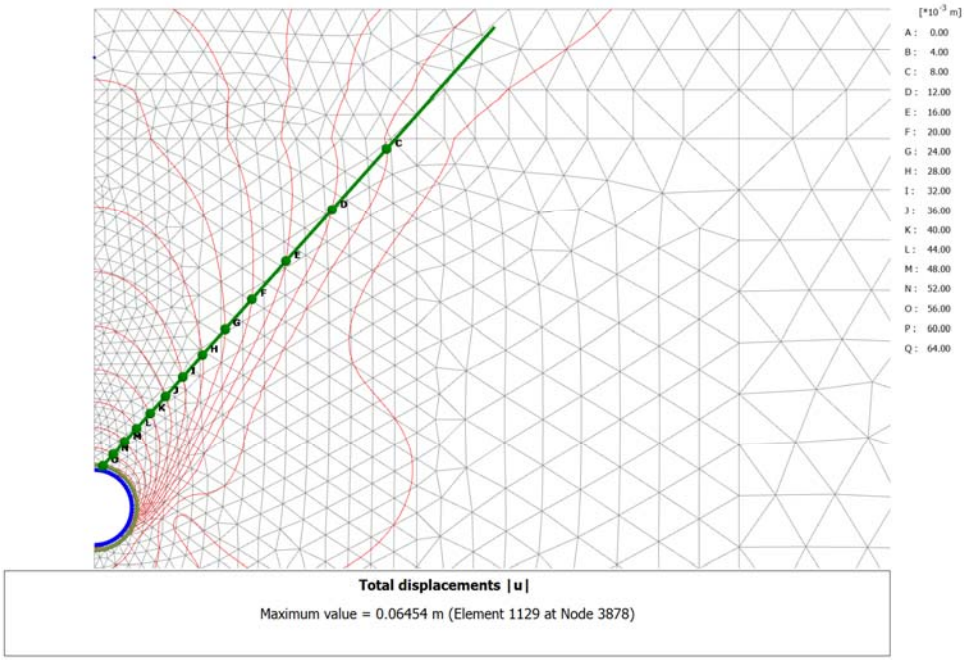

Figure 56. Stress relief method, k_0 = 0.5, total displacement.

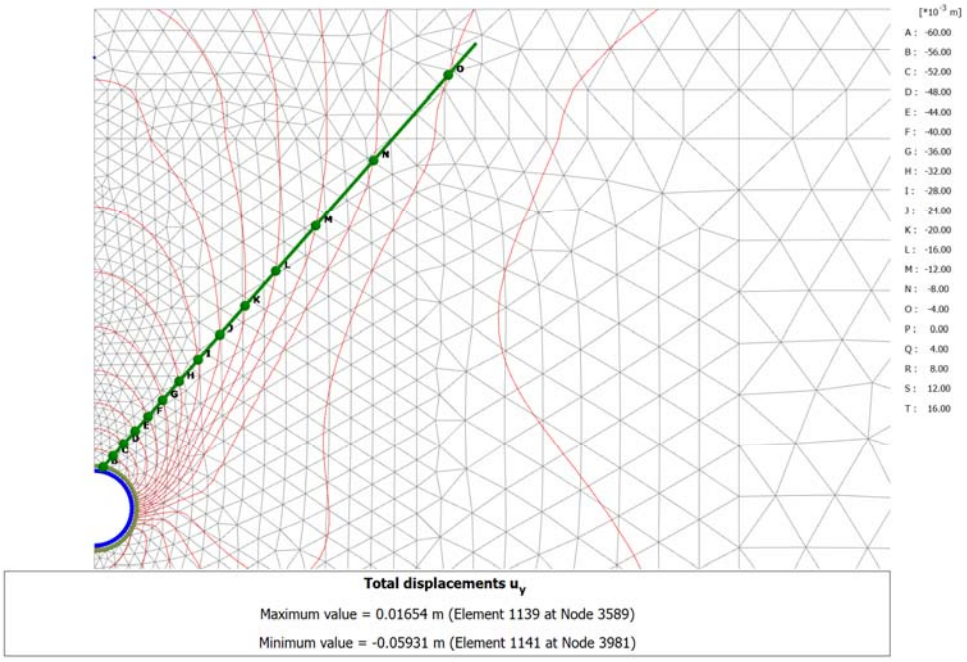

Figure 57. Stress relief method, k_0 = 0.5, vertical displacement.

3.3 Calculations for the Eastbound Tunnel

3.3.1 Introduction

This section presents the results of 2D plane strain finite element analysis of the Eastbound Tunnel of the Jubilee Line Extension at St. James's Park. The aim is to match the short-term settlements measured at the monitoring section via precise levelling at the time of construction.

The approach replicates the one adopted for the Westbound Tunnels and presented in the previous section. The calculations have been conducted with linear elastic-perfectly plastic (LE-PP) constitutive models. To simulate undrained conditions, the fine-grained soils have been modelled in total stress and with Tresca's failure criterion. The single coarse-grained material (River Terrace Gravel) has been modelled in effective stress with Mohr-Coulomb failure criterion. The calculation parameters are the same used for the Westbound tunnel.

The Eastbound tunnel is located approximately 21mBGL, which is 10m shallower than the Westbound tunnel. A maximum vertical displacement of 23.4 mm at about 1m offset from the tunnel centreline was measured. The settlement trough it is slightly asymmetrical and it has been suggested (Standing and Burland 2006) that this is due to the disturbance generated by the Westbound tunnel, which was constructed beforehand. Standing & Buralnd (2006) declare a volume loss for this profile of 2.4% and a trough width parameter K = 0.4. Considering that the excavated diameter was 4.85m (open-face shield excavated), however, the parameters mentioned above return the Gaussian curve plotted in Figure 58. In the author's view, an interpretation based on a slightly higher volume loss, V_L = 2.67% provides a better interpretation of the field data and has been adopted in this study (Figure 59).

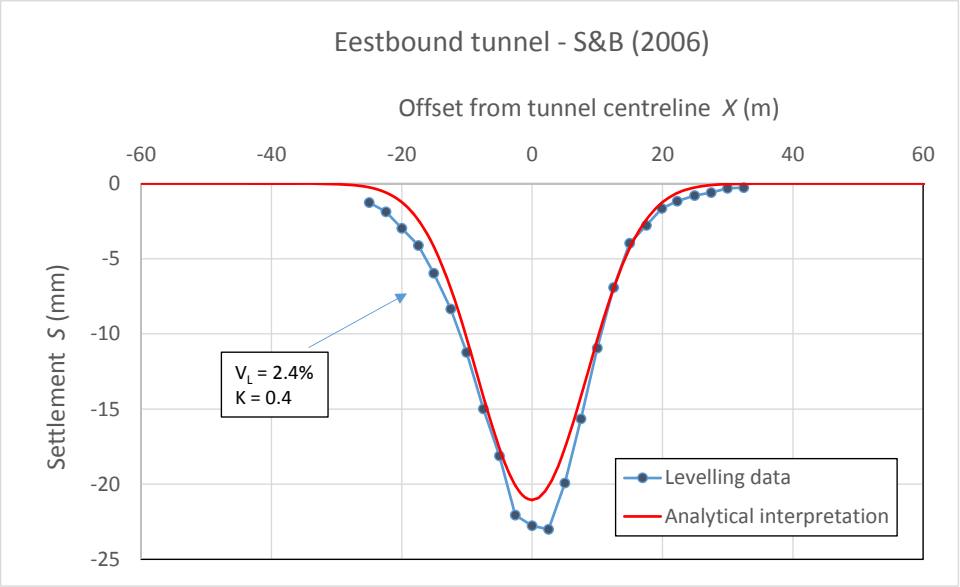

Figure 58. Gaussian settlement trough based on the interpretation proposed by Standing & Burland (2006) for the instrumented section data.

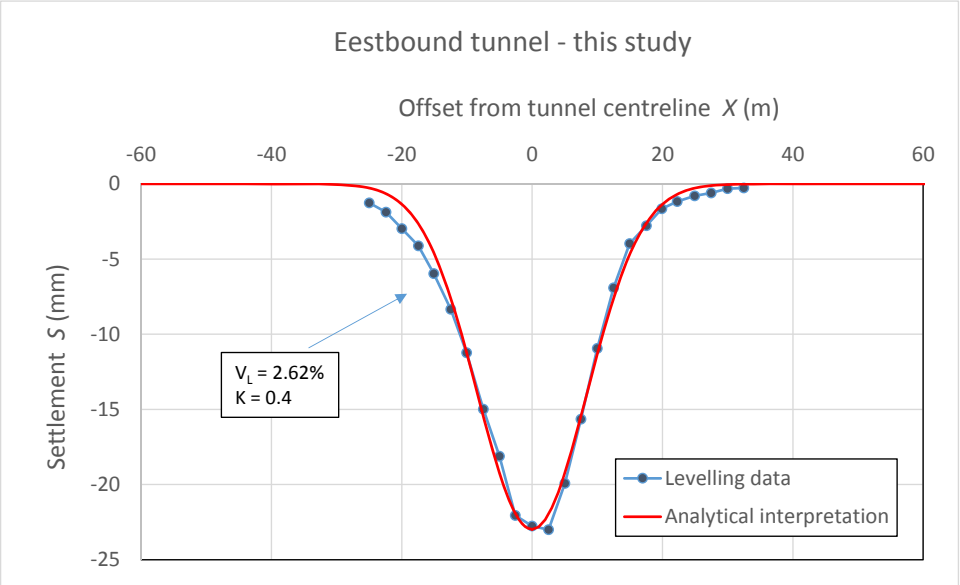

Figure 59. Gaussian settlement trough based on the interpretation adopted in this study.

As discussed for the Westbound tunnel, a correction has to be applied to the volume loss and a slightly higher value is needed in the finite element calculations to account for the lack of thickness of the lining elements in the mesh. In the specific case a corrected volume loss V_L^* = 2.85% is appropriate for the finite element calculations.

3.3.2 Stress relief method

The target volume loss (more correctly area loss, in 2D) in the finite element model has been achieved with the stress relief method (Panet & Guenot 1982; Schikora & Fink 1982), in which a portion of nodal forces at the wall, equal to (1-β), is kept in place until the activation of the lining.

The stress relief parameter needed to achieve the required area loss 0f 2.85% has been found, by trial and error, to be

(1-β) = 0.755

The key results of calculations with an initial stress ratio in the London Clay k_0 = 1.25, which is a reasonable approximation of the site conditions, are presented in Figure 60 to Figure 66.

It is obvious, from the comparison in Figure 66, that the calculated settlements bear no resemblance to what observed on site.

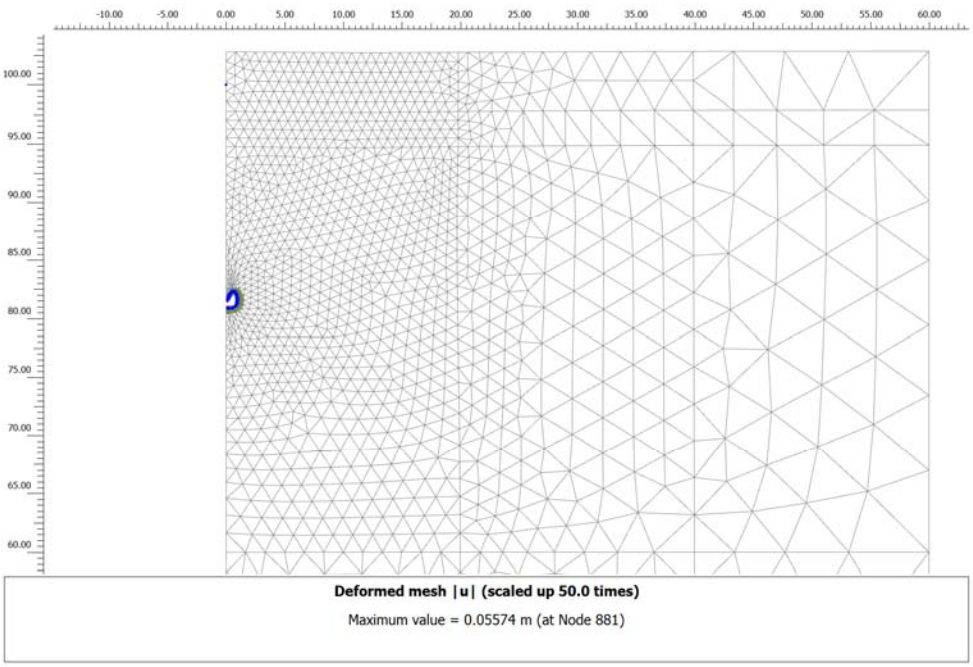

Figure 60. Stress relief method, k_0 = 1.25, deformed mesh.

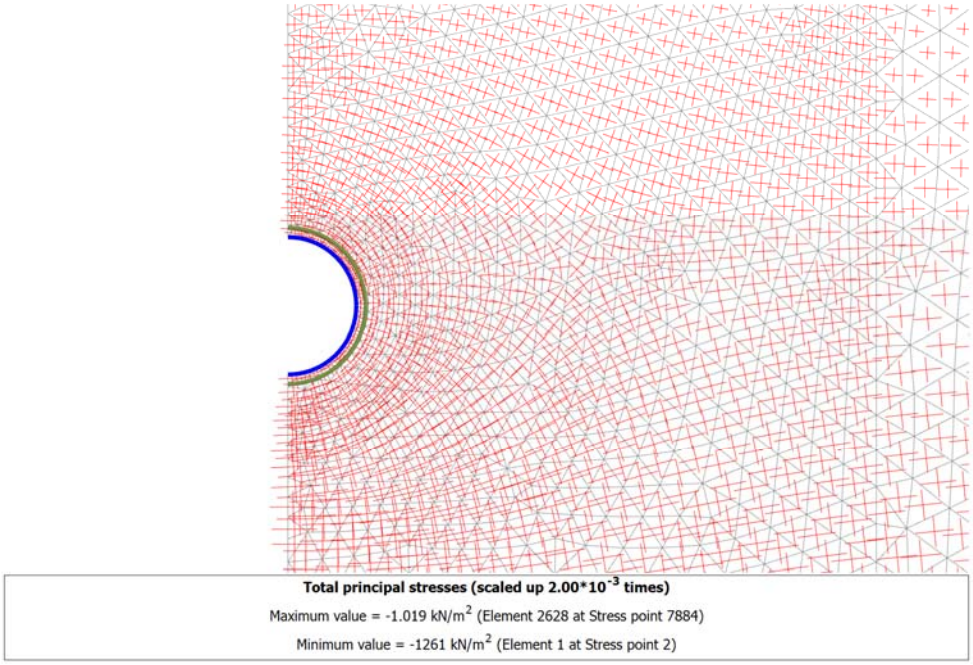

Figure 61. Stress relief method, k_0 = 1.25, principal stresses around the tunnel.

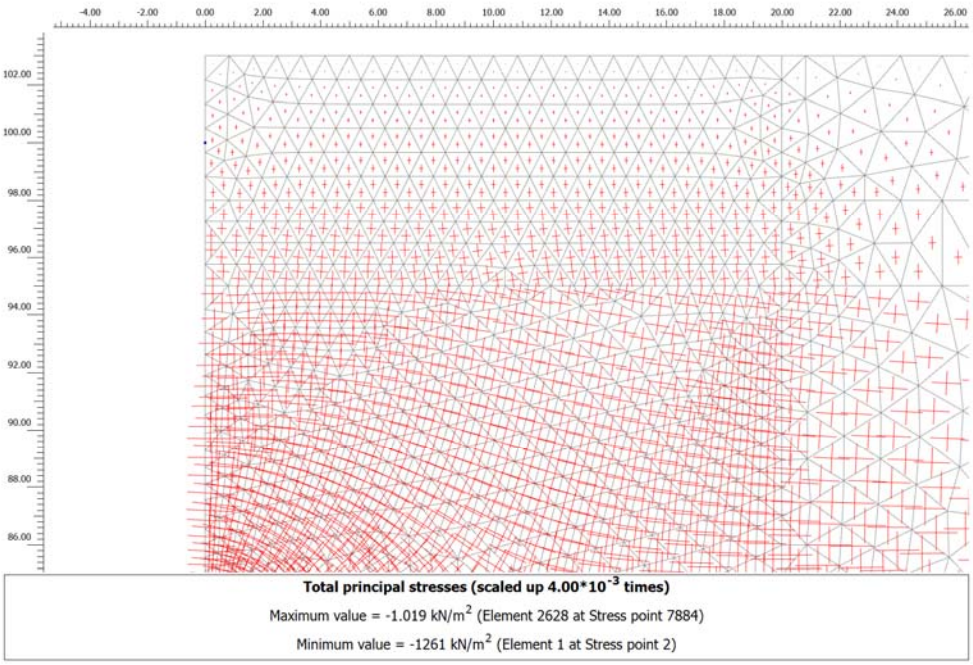

Figure 62. Stress relief method, k_0 = 1.25, principal stresses near the surface.

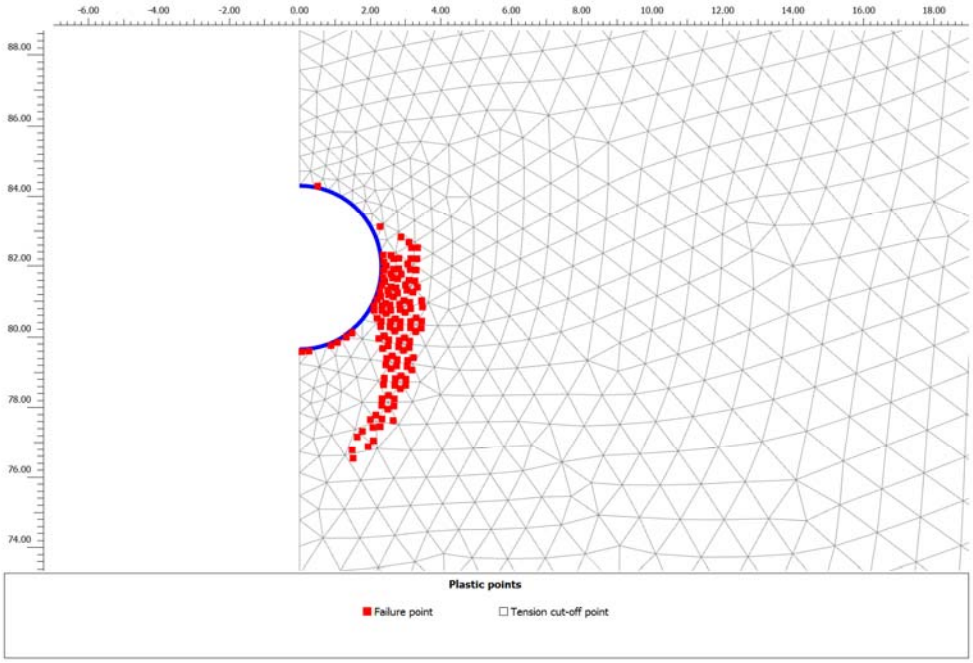

Figure 63. Stress relief method, k_0 = 1.25, plastic points.

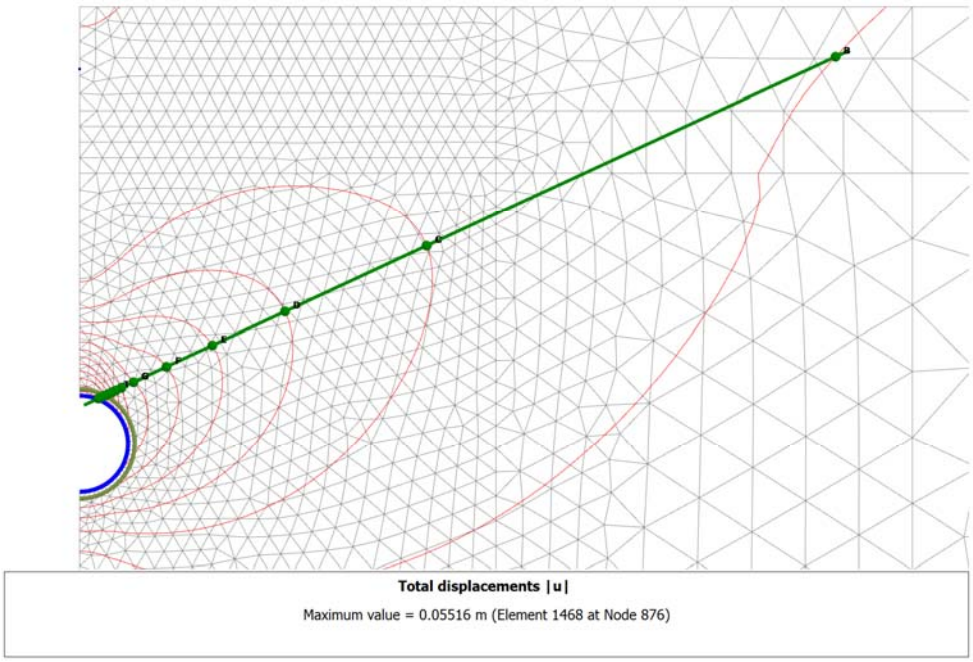

Figure 64. Stress relief method, k_0 = 1.25, total displacements.

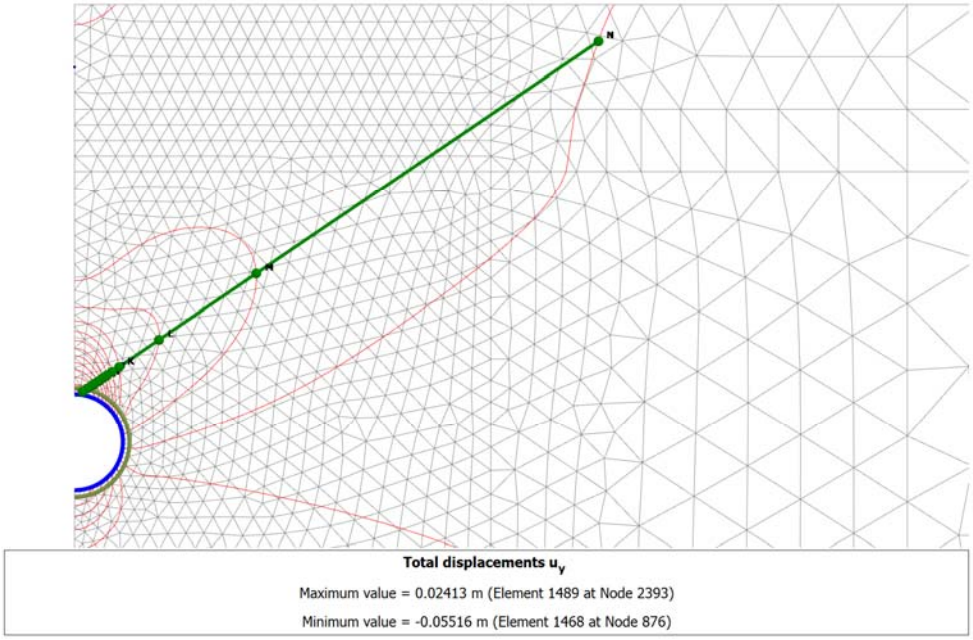

Figure 65. Stress relief method, k_0 = 1.25, vertical displacements.

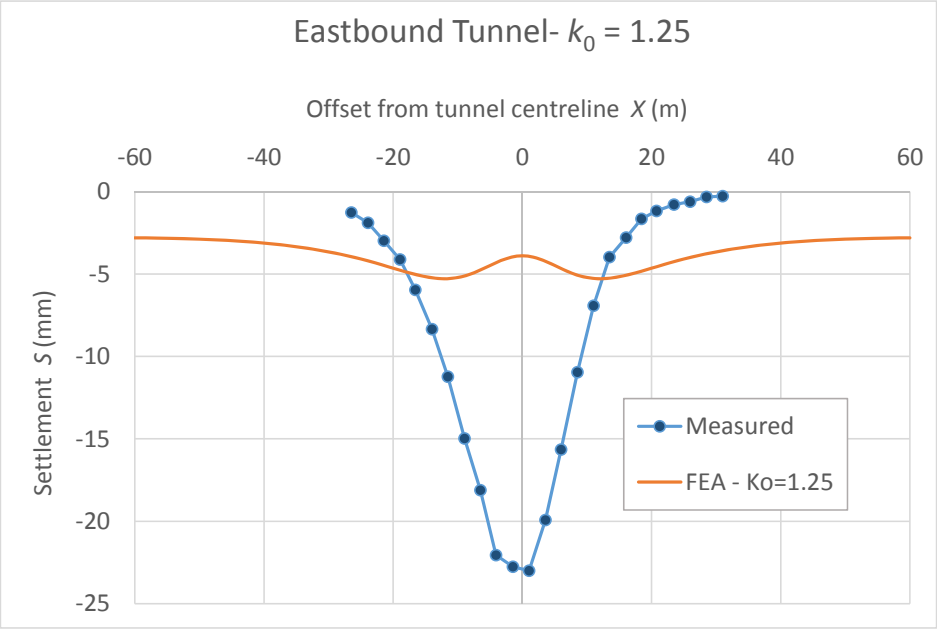

Figure 66. Stress relief method, k_0 = 1.25, vertical displacements at ground surface.

3.3.3 Alternative implementation of stress relief

As for the Westbound tunnel, an alternative approach to stress relief was also considered in this work by temporarily supporting the tunnel wall with a uniform radial pressure.

The key results of calculations with an initial stress ratio in the London Clay k_0 = 1.25, which is a reasonable approximation of the site conditions, are presented in Figure 67 to Figure 72.

The comparison between the settlement profiles calculated with the alternative method and with the traditional implementation of stress relief shows virtually no difference (Figure 73).

The main aspect differentiating the two situations is the changing in shape and extent of the area subject to plastic deformations. The use of traditional stress relief results in plastic zones that extends vertically at the sided of the tunnel, in a shape that we could define “hear shaped” (Figure 4-6). The use of the alternative method (uniform radial pressure), instead, results in a plastic zones that is predominantly above the tunnel and ha two sides joining into a dome shape.

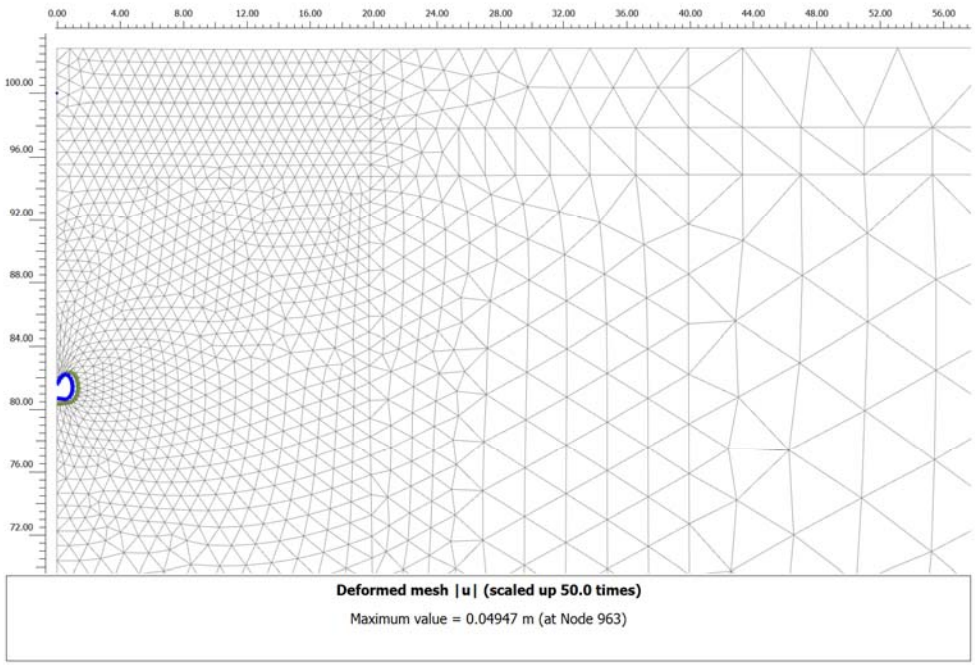

Figure 67. Alternative method, k_0 = 1.25, vertical displacements at ground surface.

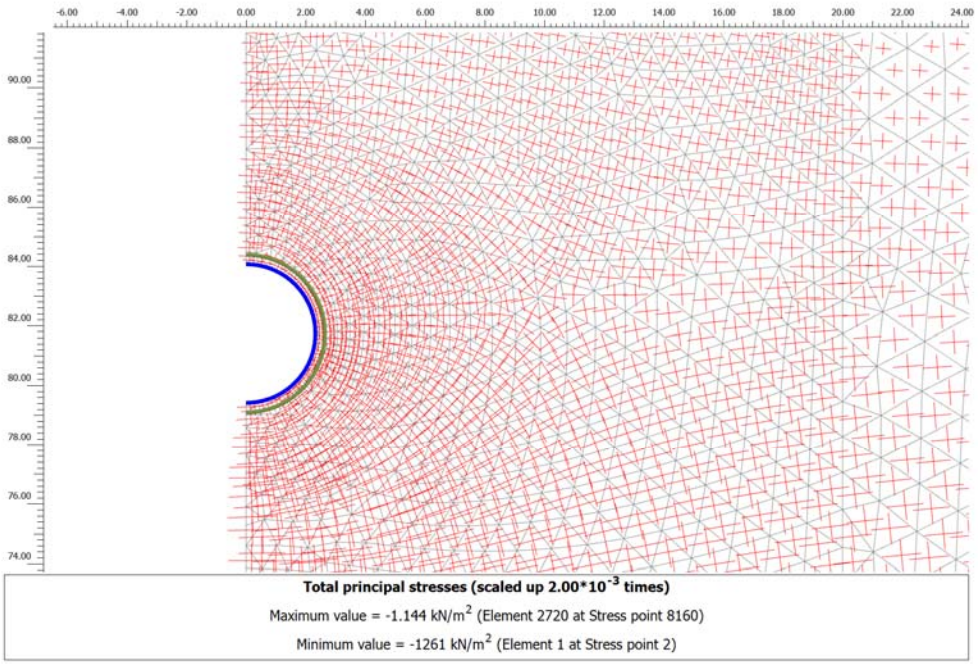

Figure 68. Alternative method, k_0 = 1.25, principal stresses around the tunnel.

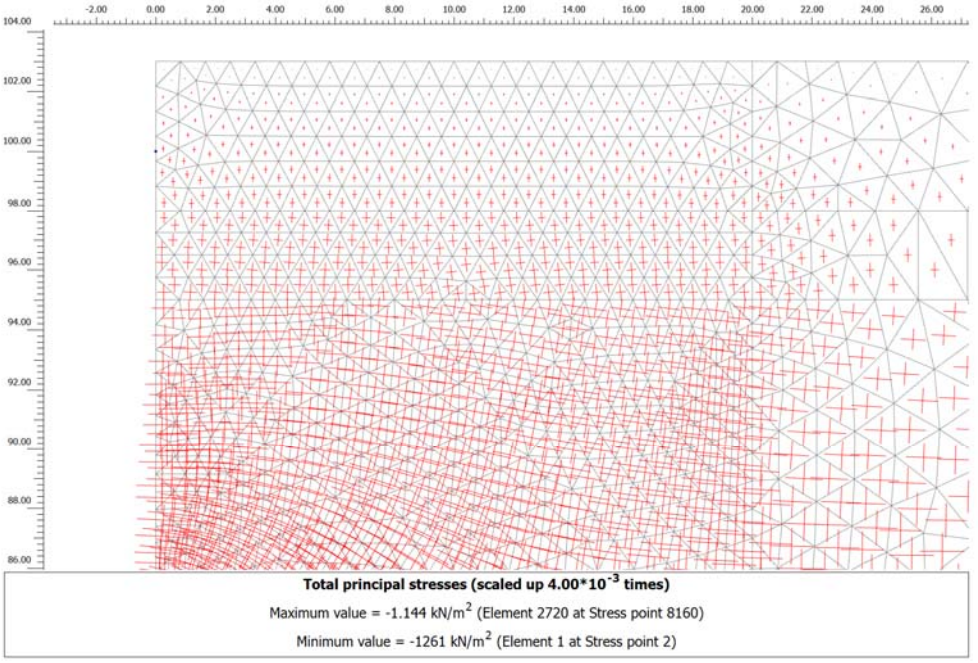

Figure 69. Alternative method, k_0 = 1.25, principal stresses near the surface.

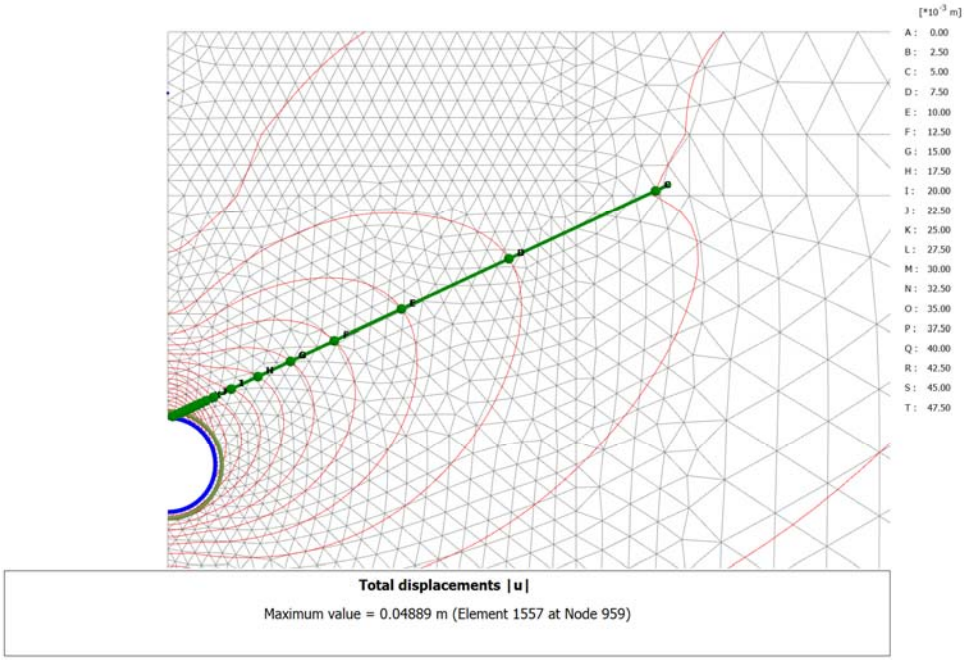

Figure 70. Alternative method, k_0 = 1.25, total displacements.

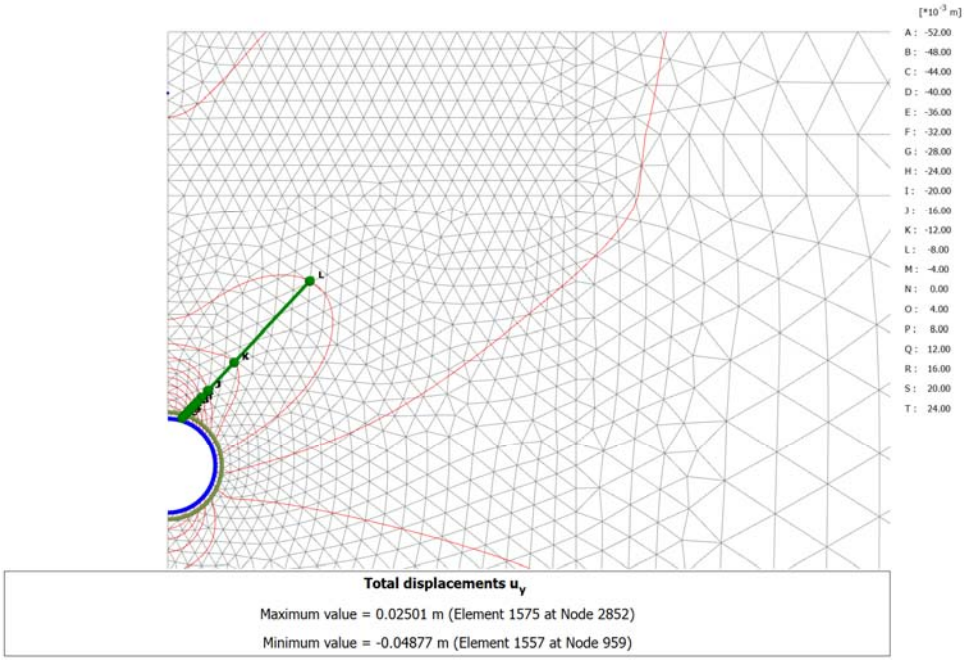

Figure 71. Alternative method, k_0 = 1.25, vertical displacements.

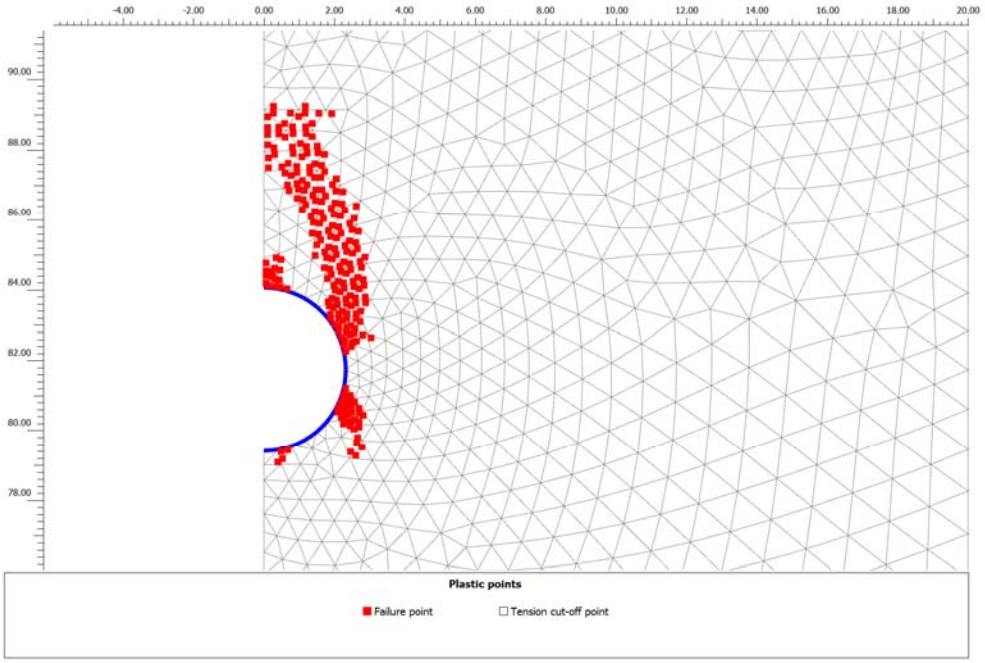

Figure 72. Alternative method, k_0 = 1.25, plastic points.

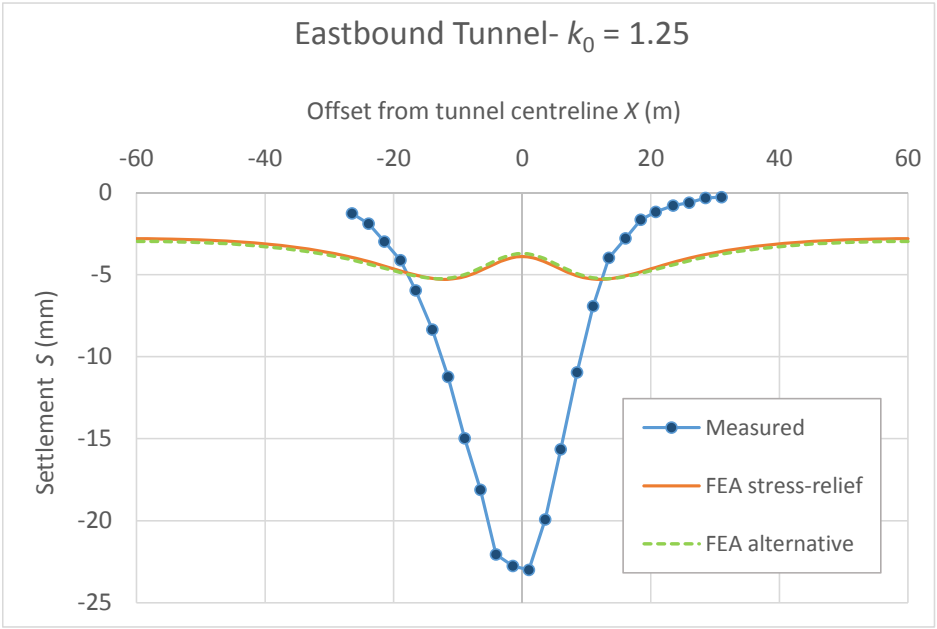

Figure 73. Settlement profile: comparison between stress relief and alternative method.

3.3.4 Use of softened zones

The attempt to use a variation of the traditional stress relief method has produced a calculated settlement profile that does not differ significantly from the one obtained with the more traditional approach and, most importantly, does not resemble the behaviour observed in reality.

However, the plastic zones obtained with the two analyses are significantly different, prompting the question of what would happen if the mechanical properties were modified in the plastic zones.

For this purposes, two meshes have been generated, in which clusters of elements inside the areas identified as subject to plasticity in the previous calculation were delimited in order to enable lower stiffness and/or strength to be assigned.

The following sets of parameters were tried for the softened zones:

reduction of London Clay's Young's modulus to 50% of the initial value
reduction of London Clay's undrained shear strength to 50% of the initial value
simultaneous reduction of Young's modulus and undrained strength to 50%
reduction of Young's modulus to 20% of the initial

It is worth mentioning that, since the value of Poisson's ratio is kept constant, the reduction in Young's modulus E_u , translates in a reduction in shear modulus G of exactly the same proportion.

The changes listed above have produced only small variations in the results and in none of the options has achieved a calculated settlement trough resembling reality.

3.3.5 Sensitivity to initial stress ratio

Considering the sensitivity of the calculated settlement to the changes in the coefficient of earth pressure at rest k'_0 reported in the literature (Doležalová 2002) a number of analysis were run, progressively reducing the initial horizontal stresses.

Again, since the fine-grained materials in undrained conditions are modelled in total stresses, reference is made to the initial total stress ratio:

$$k_0 = \sigma_h/\sigma_v$$

Figure 74. Settlement profile: sensitivity to initial total stress ratio in stiff clays.shows the calculated settlement trough for decreasing values of the initial total stress ratio in the stiff clay layers(London Clay and Lambeth Group). The initial stress ratio in the top layers, was kept to its best estimate value.

Similarly to the Westbound analysis, the vertical displacements at surface calculated for $k_0 = 0.5$ provide a satisfactory fit of the observed data. The key results for the latter analysis are shown in Figure 75 to Figure 80.

The alternative implementation of the stress relief method has been applied to the case $k_0 = 0.5$, without providing any significant difference in terms of vertical displacements.

The effect of reducing material stiffness and strength in the plastic zones, now significantly more extended (see Figure 78), has also proved virtually inconsequential.

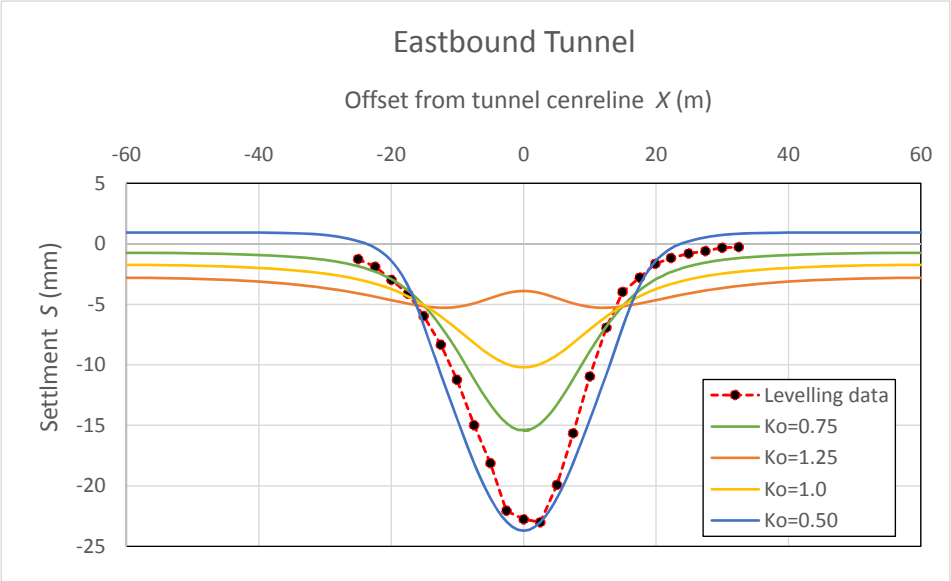

Figure 74. Settlement profile: sensitivity to initial total stress ratio in stiff clays.

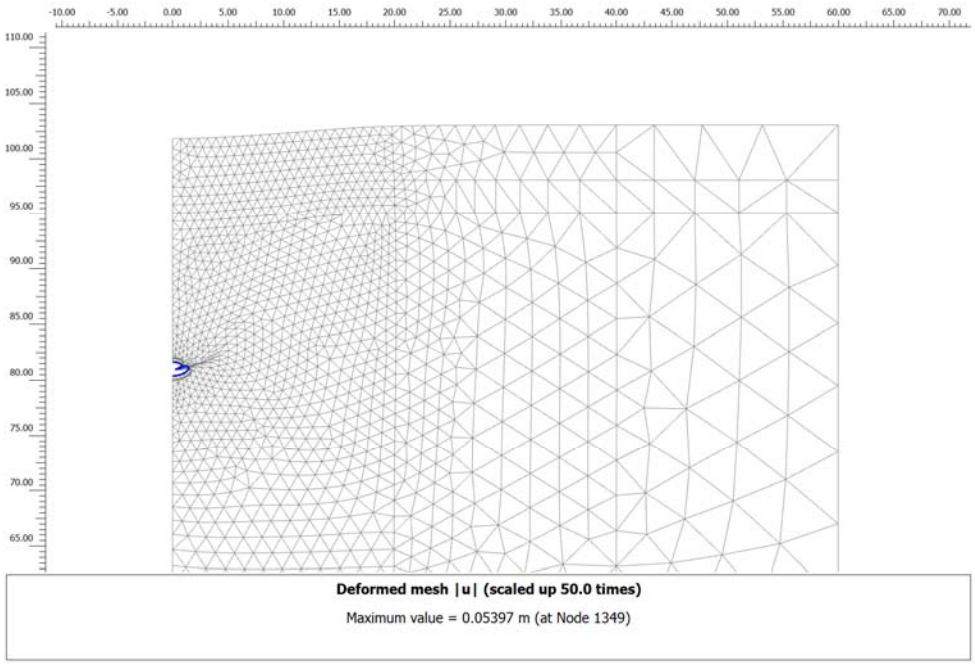

Figure 75. Stress relief method, k_0 = 0.5, deformed mesh.

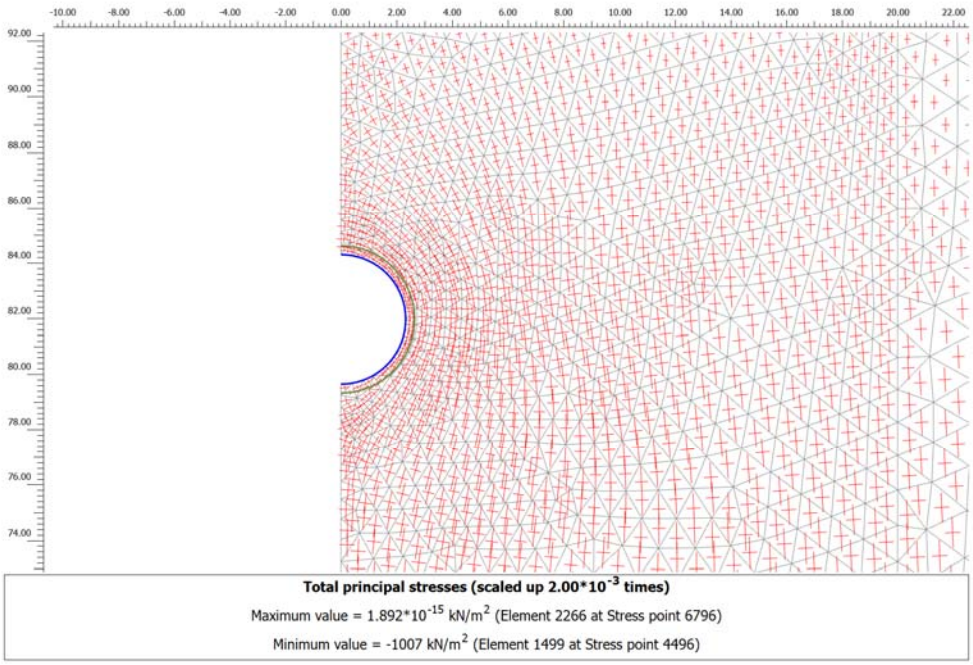

Figure 76. Stress relief method, k_0 = 0.5, principal stresses around the tunnel.

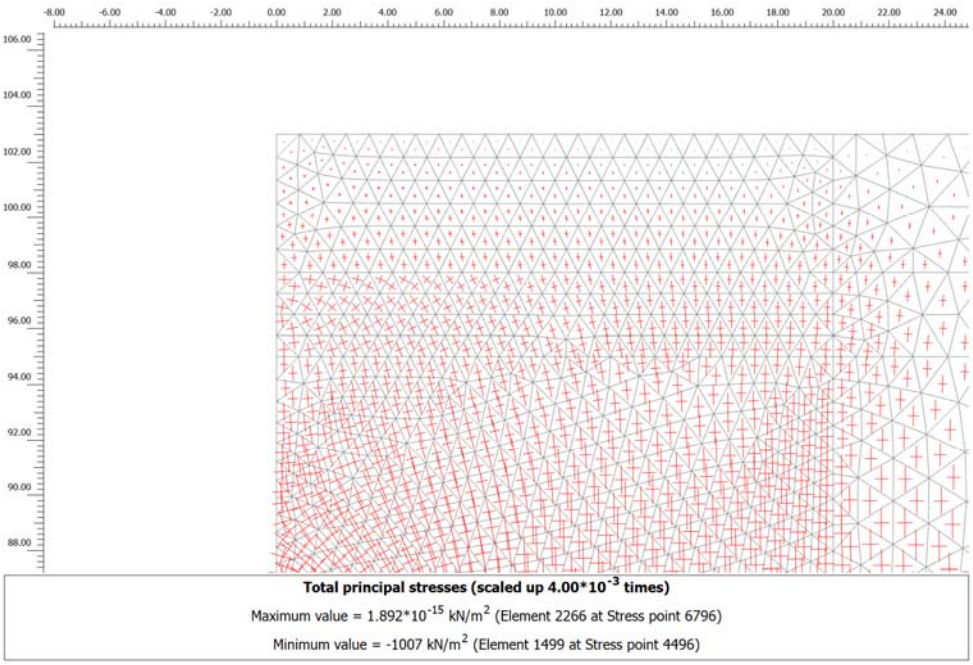

Figure 77. Stress relief method, k_0 = 0.5, principal stresses near the surface.

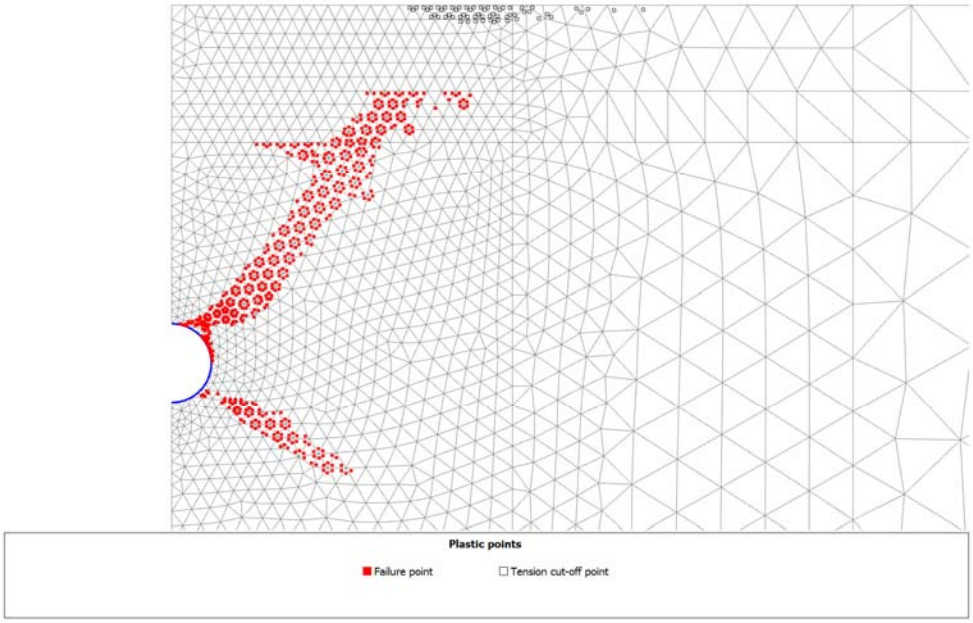

Figure 78. Stress relief method, k_0 = 0.5, plastic points.

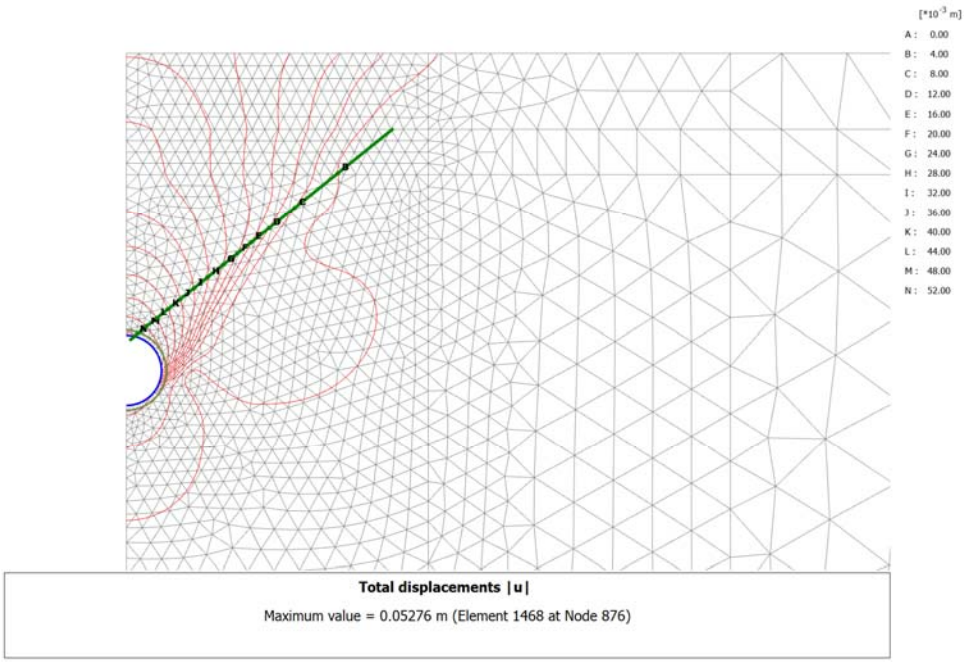

Figure 79. Stress relief method, k_0 = 0.5, total displacement.

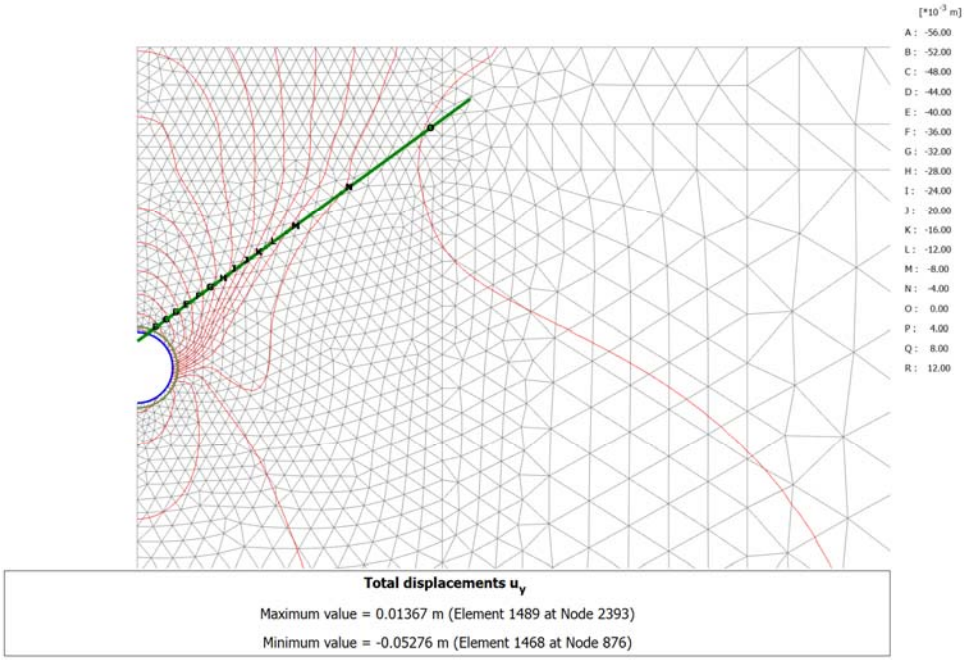

Figure 80. Stress relief method, k_0 = 0.5, vertical displacement.

3.4 Summary

3.4.1 Westbound tunnel

A set of finite element analyses of the Westbound tunnel of the Jubilee Line Extension at St. James's Park has been carried out in 2D plane strain. The aim was to verify whether it is possible to reproduce a settlement profile resembling the observed data without resorting to complex constitutive modelling and, instead employing a linear elastic perfectly plastic constitutive law. The analysis of short-term displacements with total stress modelling of the undrained response of the stiff clay layers has show that:

Calculations with a realistic initial total stresses ratio (k_0 = 1.25 in this case), performed with the stress relief (also called confinement-convergence) method, return a completely unrealistic settlement profile, which is much flatter than the real settlement trough.

The use of an alternative implementation of the stress relief method, consisting in the application of a uniform radial pressure to the tunnel wall to support it before lining activation, does not result in any significant difference in the calculated settlement profile. It generates, however, plastic zones that differ from the traditional method.

Consideration of softened material, possessing lower stiffness and/or strength, in the plastic zones does not significantly affect the calculated settlement profile.

The settlement profile is sensitive to changes in the initial total stress ratio, with values progressively lower than the actual ratio present on site returning calculated settlements that approach the observed data. The finite element analysis with k_0 = 0.5 produces a satisfactory fit with the measured settlements.

3.4.2 Eastbound tunnel

A set of finite element analyses of the Eastbound tunnel of the Jubilee Line Extension at St. James's Park has been carried out in 2D plane strain. The aim was to verify whether it is possible to reproduce a settlement profile resembling the observed data without resorting to complex constitutive modelling

and, instead employing a linear elastic perfectly plastic constitutive law. This tunnel is shallower than the previously analysed Westbound tunnel (21mBGL vs. 31mBGL) and has experienced a lower volume loss during construction (2.62% vs. 3.36%). The analysis of short-term displacements with total stress modelling of the undrained response of the stiff clay layers has shown that:

As in the case of the Westbound tunnel, calculations with a realistic initial total stresses ratio of $k_0 = 1.25$ return a completely unrealistic settlement profile, which is much flatter than the real settlement trough.

The use of traditional stress relief or of its alternative implementation (application of a uniform radial pressure) does not result in any meaningful difference in the calculated settlement profile. They generates, however, different plastic zones.

Consideration of softened material, possessing lower stiffness and/or strength, in the plastic zones does not significantly affect the calculated settlement profile.

The settlement profile is sensitive to changes in the initial total stress ratio, with values progressively lower than the actual ratio present on site returning calculated settlements that approach the observed data. The finite element analysis with $k_0 = 0.5$ produces a satisfactory fit with the measured settlements.

4 Numerical analysis - Fleet Line at Green Park

4.1 Introduction

4.1.1 Overview

This chapter presents the results of 2D plane strain finite element analysis of the Fleet Line tunnel at Green Park. The aim is to match the short-term settlements measured at the monitoring section via precise levelling at the time of construction.

Like in the previous analysis of the tunnels at St. James's Park, the calculations have been conducted with linear elastic-perfectly plastic (LE-PP) constitutive models. To simulate undrained conditions, the London Clay has been modelled in total stress and with Tresca's failure criterion. The shallow coarse-grained layer (Sand & Gravel) has been modelled in effective stress with Mohr-Coulomb's failure criterion.

The tunnel is located at a depth of 29.30 m below ground level (BGL). A maximum vertical displacement of 6.1 mm at the tunnel centreline was measured at the instrumented section when the tunnel had passed beyond the zone of influence.

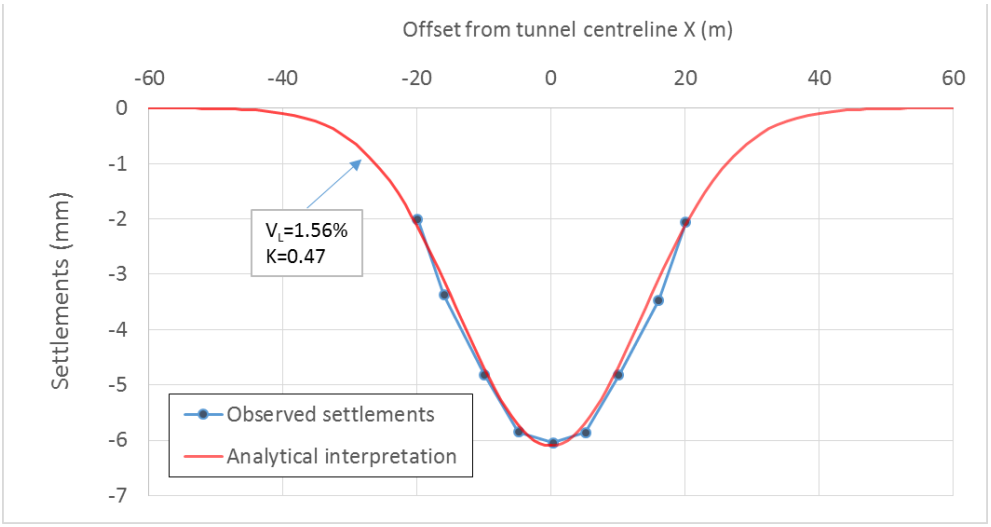

Figure 81. Analytical interpretation

Differently from the previous analyses, in which the thickness-less model lining was placed in correspondence of the real lining axis, in this case the FE beam have been placed in correspondence of the excavated diameter. This approach, which may not be ideal for estimating the structural actions in the lining, is easier to use when the focus of the analysis is the simulation of ground displacement because, firstly, there is no need to adjust the volume loss for differences between real and modelled excavation size and, secondly, the equivalent weight of the beams in the model in easier to determine.

4.1.2 Ground model

The soil profile at the site consists, form the surface, of about two meters of Sand and Gravel over a thick layer of London Clay (Attenwell & Farmer 1974, Loganathan & Poulos 1998), as summarized in Table 13. The Lambeth Group, which underlies the London Clay in this area, is sufficiently deep to have virtually no effect on the tunnel and on the ground displacements around and above the tunnel

Table 13. Ground model for Green Park.

From (mBGL)	To (mBGL)	Soil
0	2	Sand & Gravel
2	>60	London Clay

Little information is available on the layer of sand and gravel. Reasonable values for a shallow layer of coarse-grained made ground have been adopted in the calculations.

More details, understandably, are available for the host formation. In fact, the London Clay is reported to have undrained shear strength S_u increasing with depth and ranging from approximately 50 kPa at its top to 250 kPa or more toward the base of the layer - Attenwell & Farmer 1974 quote S_u = 266 kPa. Loganathan & Poulos (1998) suggest S_u = 175 kPa at tunnel axis leve. In the present calculations S_{u0} = 50 kPa has been therefore assumed as the value at the top of the layer and a gradient correposning to 125 kPa over 27.3m of London Clay thikness has then been appied. Loganathan & Poulos (1998) also suggest a E_u/S_u ratio sligltly below 250 for the London Clay. Considering the characteristic of the London Clay (overconsolidation ratio and plasticity index in particular) a value of E_u/S_u = 250 appears to be resonable and has been adopted to estimate the undrained stiffness.

The calculation parametrs are listed in Table 14. Geotechnical parameters for Green Park.. A very small effective cohesion has been assigned to the granular layer to prevent early onset of plasticity at the ground surface, withot significantly affecting the analysis results.

Table 14. Geotechnical parameters for Green Park.

Soil	γ_{sat} (kN/m^3)	c' (kPa)	ϕ' (°)	S_u (kPa)	E' (MPa)	ν' (-)	E_u (MPa)	ν_u (-)
Sand/Gravel	19.5	0.1	35	-	75	0.25	-	-
London Clay	19.0	-	-	50+4.58 z	-	-	12.5+1.15 z	0.495
Note: *z* is the depth below the top of the London Clay								

A finite element mesh of 6-nodes triangular elements has been generated to study the tunnel, as in the previous cases. The symmetry about the vertical axis passing for the centre of the tunnel has been exploited to half the size of the mesh that is 60m wide and 53m high.

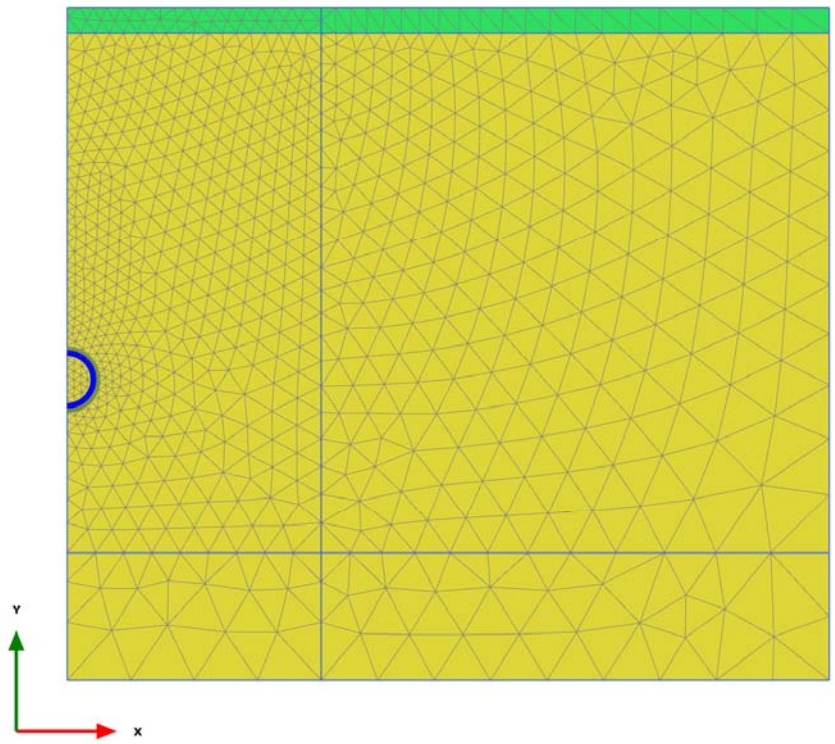

Figure 82. FEM for Fleet Line tunnel in Green Park.

Figure 82 shows the mesh composed by 1635 elements and 3413 nodes with the tunnel at 29.3 meters below the ground level. Care has been taken to sufficiently refine the mesh above the tunnel. The lower boundary of the model is fixed in the horizontal and in the vertical directions, while the nodes at the side boundaries are constrained horizontally but free to move vertically.

4.1.3 Plate parameters

The lining of the Fleet Line tunnels at Green Park is made of 7 cast iron segments. The axial stiffness of the plate representing the lining in the FE model has been calculated as:

$$E_{ca} \times A$$

Where E_{ca} is the Young's modulus of the cast iron. The bending stiffness of the plate has been estimated taking into account the behaviour of the segmental lining as described by Muir Wood (1975).

4.2 Calculations for the Fleet Line tunnel

4.2.1 Key assumptions

For the layer of Sand and Gravel a realistic coefficient of earth pressure at rest k'_0 = 0.4 has been selected. However, considering the results of the previous back analyses, a total stress ratio at rest artificially lowered to k_0 = 0.5 has been assigned to the London Clay.

The stress relief parameter needed to achieve the required area loss of 1.56% has been found, by trial and error, to be

$(1-\beta) = 0.375$

In the previous case histories the use of an alternative implementation, in which a uniform radial load is applied to the unsupported excavation, did not show any significant improvement of the modelling, only the traditional implementation of the stress relief method has been used for Green Park.

The results obtained with an initial stress ratio in the London Clay k_0 = 0.50 are presented in Figure 83 to Figure 88. It is worth noticing that the extent of the plastic zones is much smaller than the corresponding analyses for the St. James's Park tunnels.

4.2.2 Calculated settlement at ground surface

Figure 89 shows good agreement between the settlements at ground surface calculated with the reduced total stress ratio at rest and the data from measurements on site.

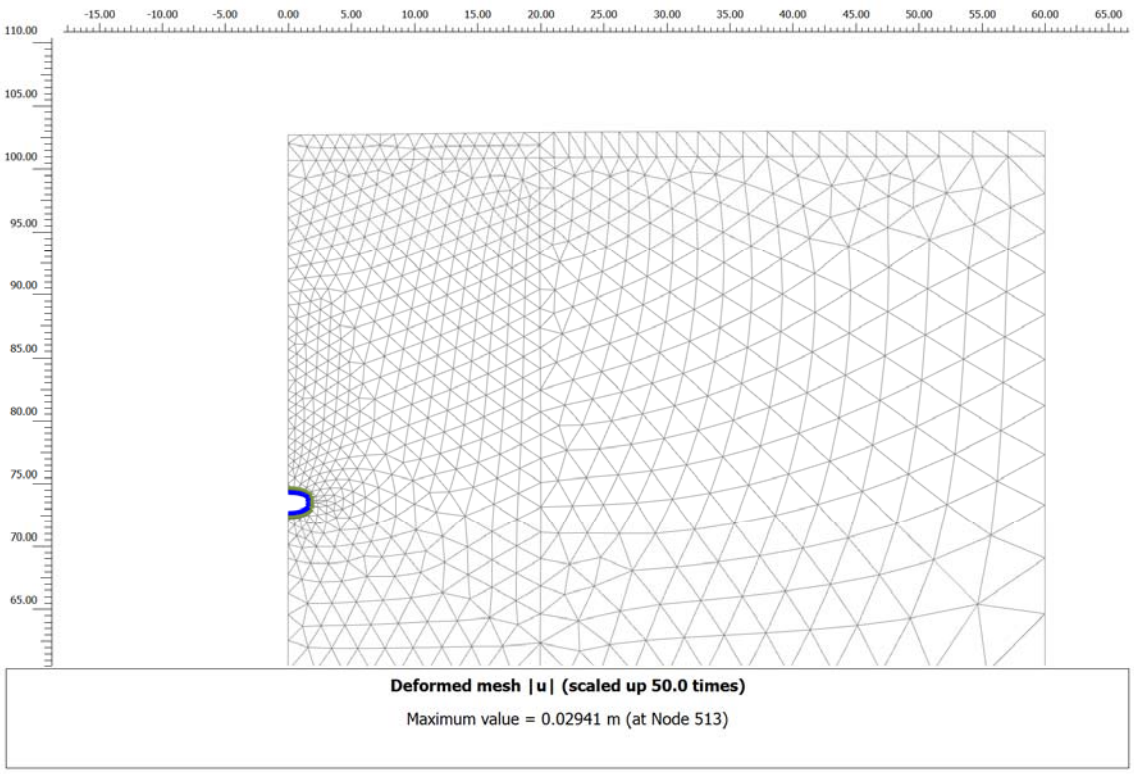

Figure 83. k_0 = 0.5, deformed mesh.

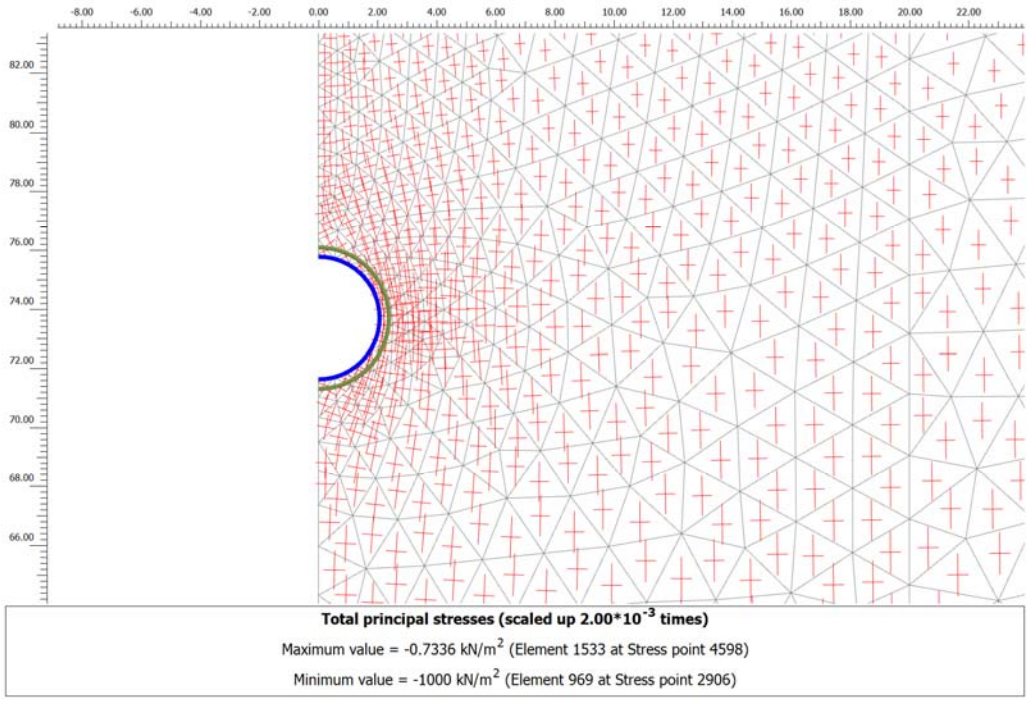

Figure 84. k_0 = 0.5, principal stresses around the tunnel.

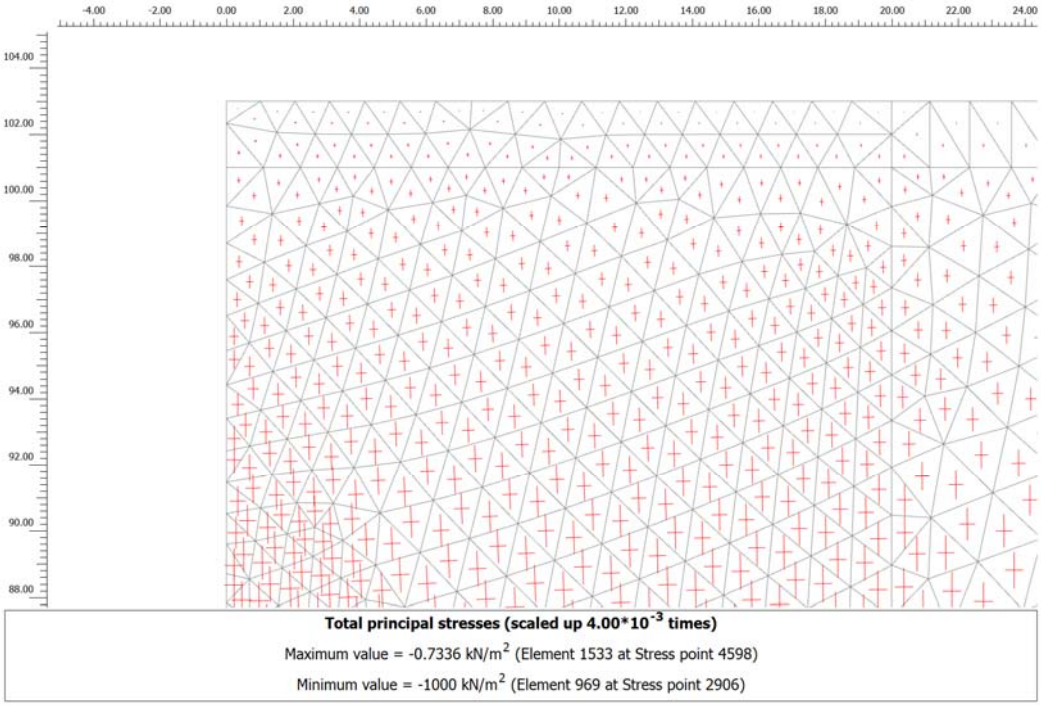

Figure 85. k_0 = 0.5, principal stresses near the surface.

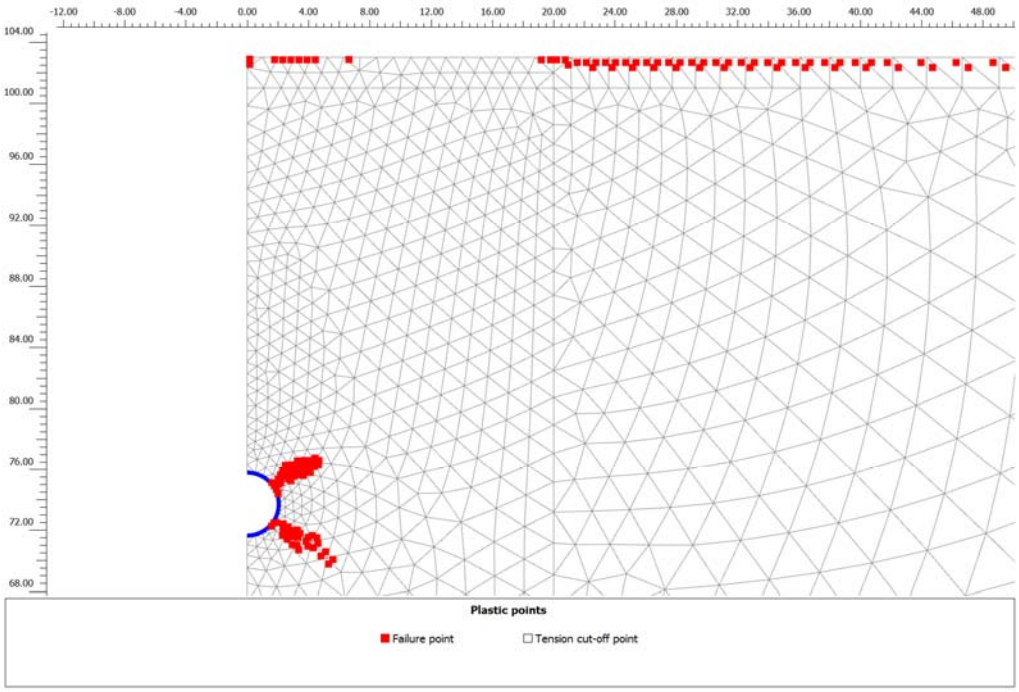

Figure 86. k_0 = 0.5, plastic points.

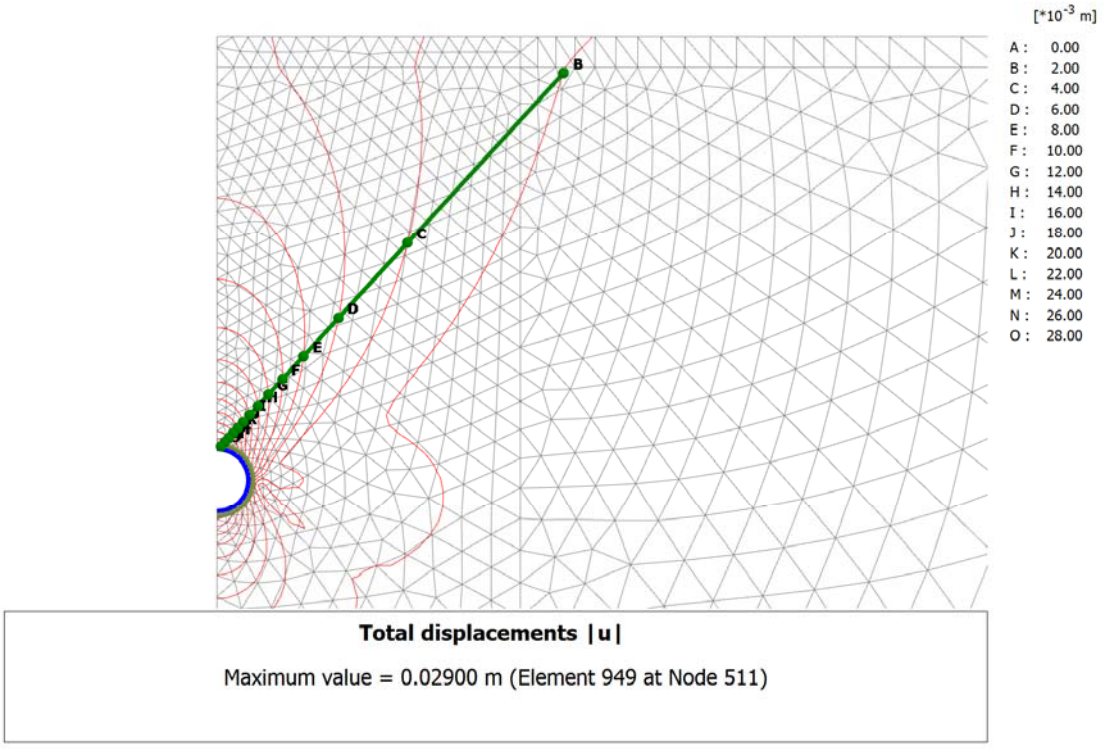

Figure 87. k_0= 0.5, total displacements.

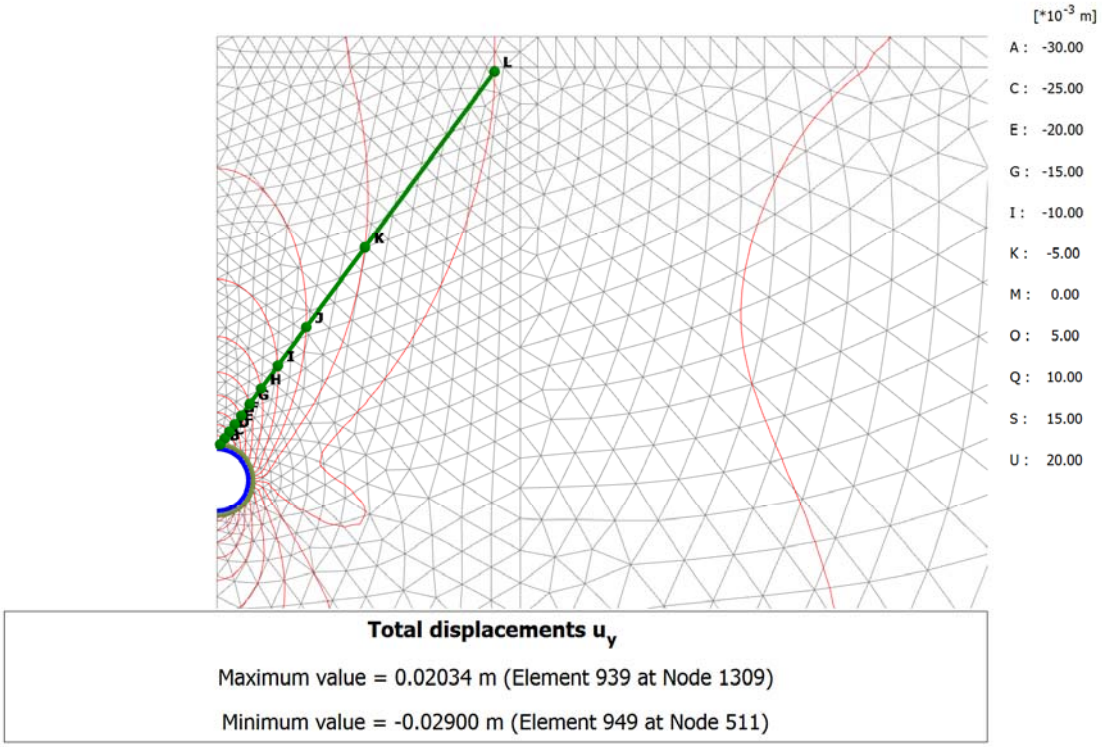

Figure 88. k_0= 0.5, vertical displacements.

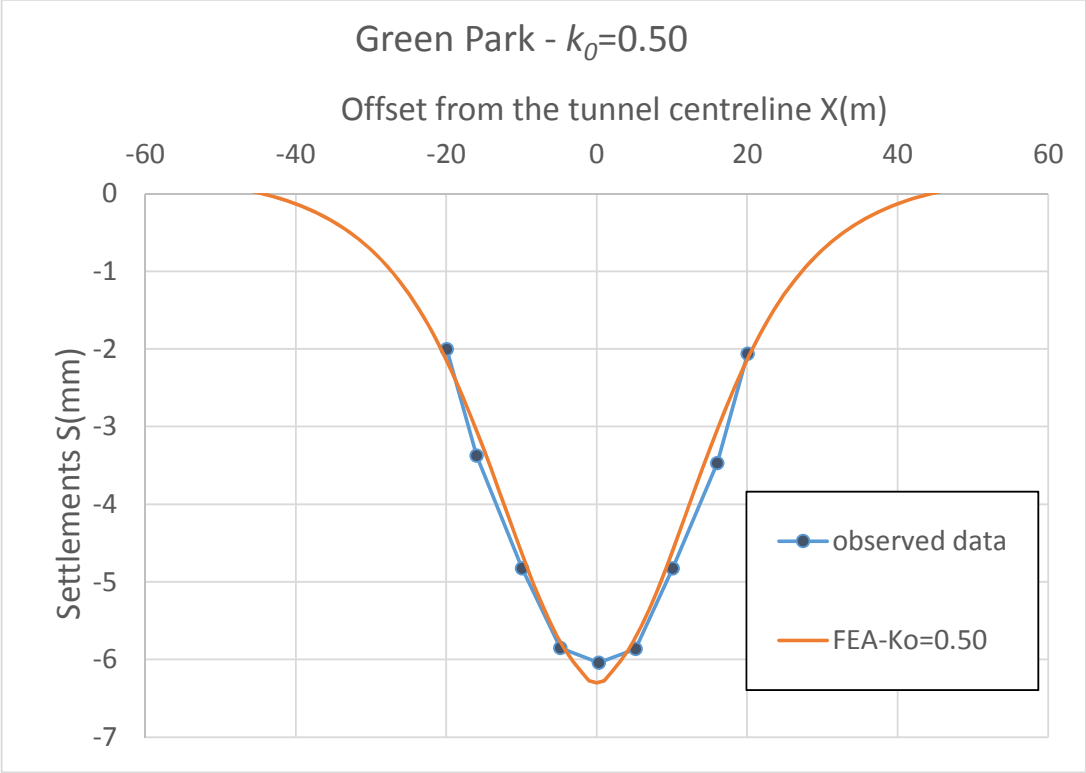

Figure 89. k_0 = 0.5, vertical displacements at ground surface.

4.2.3 Calculated settlement at depth

Figure 90 shows the comparison between the settlement calculated at various depths above the tunnel centreline and the settlement observed in the tree boreholes X1, Y1 and Z1. A good approximation of the subsurface displacements is achieved. The plot demonstrates how the finite element analysis returns a good estimate of maximum settlements for the upper 15 m, corresponding to about half of the tunnel depth. Below that level, although the quality of the results remains reasonably good, the numerical analysis tends to slightly overestimate the settlement.

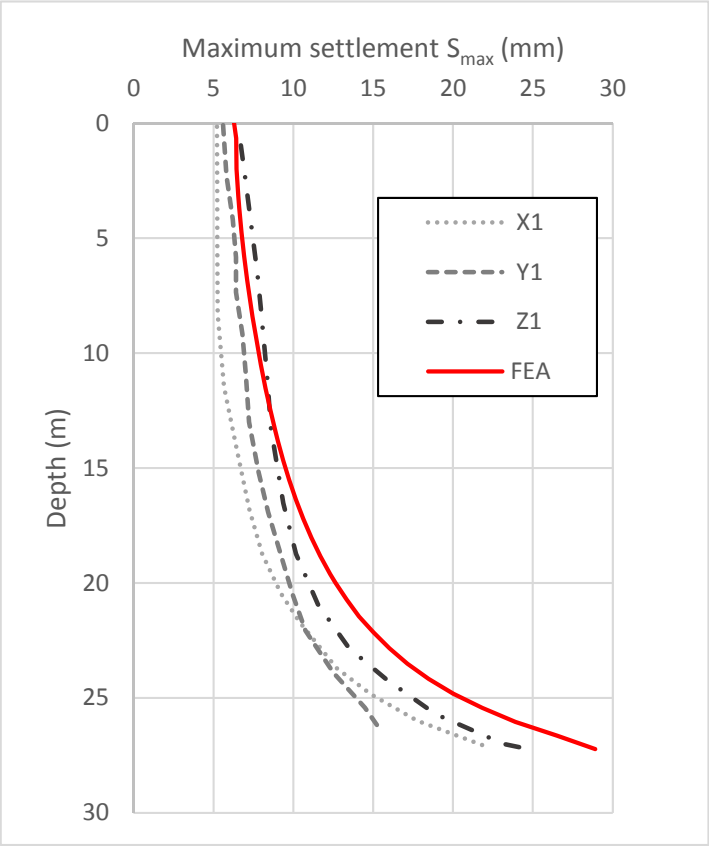

Figure 90. Maximum settlement comparison at depth.

4.3 Summary

The Fleet Line tunnel at Green Park, described in detail by Attenwell and Farmer (1974) and previously analysed by Loganathan & Poulos (1998), has been studied with a 2D plane strain finite element model. The aim was to verify whether it is possible to reproduce a settlement profile resembling the observed data without resorting to complex constitutive modelling and, instead, employing a linear elastic perfectly plastic constitutive law.

Building on the results obtained previously for the two tunnels at St. James's Park a total stress modelling of the undrained response of the stiff clay layer has been attempted with an initial total stress ratio artificially reduced to k_0 = 0.5. The results show that this approach produces a satisfactory fit with the short-term displacements measured on site at the ground surface and at depth.

5 Conclusions

5.1 Introduction

Numerical tools, and in particular the finite element method (FEM), are successfully employed to analyse soil-structure interaction problems. However, the geotechnical community is still unable to use numerical models to routinely predict with a satisfactory level of confidence the shape of the settlement trough induce by shallow in soils. The development of reliable FE modelling of tunnelling-induced ground movements would be very advantageous. In fact, empirical models based on fitting a Gaussian curve (or other suitable analytical expressions) to historical data produce good results for "green field" conditions. However, the empirical approach is not suitable to study the cases of real practical relevance, in which the presence of existing structures and infrastructures interact with the soil to modify the overall movement.

The finite element method is ideally suited to address this situations but, before attempting to model the effect of pre-existing structures, it is essential to enable the successful FE modelling of green field conditions.

To date, satisfactory results have been obtained only with extremely complex constitutive models that are outside the reach of most practicing engineers. Several studies based on the use of advanced approaches – like 3D analysis and various types of anisotropic non-linear constitutive models - have returned troughs which are much wider and flatter then the observed data (Guedes & Santos Pereira 2000; Doležalová 2002; Franzius *et al.* 2005). Recently, some more realistic results have been obtained with extremely complex constitutive models (González-Cao *et al.* 2013), which are difficult to understand and calibrate, not only for practicing geotechnical engineers but also for many academics who do not specialize in advanced constitutive models.

This dissertation has explored the possibility to calculate realistic green field short-terms settlement profiles with the finite element method without resorting to advanced constitutive models. Instead, the linear elastic-perfectly plastic model has been used in conjunction with artificially reduced initial horizontal stresses.

The approach has allowed a realistic simulation of the settlement through observed above the two Jubilee Line Extension tunnels at St. James's Park and above the Fleet Line tunnel at Green Park.

5.2 Key findings

5.2.1 Case histories

The numerical analysis of three tunnels have been carried out. The case histories were chosen among published information to avoid data confidentiality and property issues. They comprises

- the two Jubilee Line Extension (JLE) tunnels at St. James's Park, which were discussed, among others by Standing & Burland (2006)

- the Fleet Line tunnel at Green Park, which was the object of a well-documented monitoring campaign presented by Attewell & Farmer (1974)

The table below summarises the characteristics of the three tunnels; the following characteristics are listed:

- depth of tunnel axis

- diameter of the excavation

- volume loss observed on site

- geological formation in which the tunnel is excavated

- undrained shear strength of the soil estimated at tunnel level

- undrained young's modulus of the soil estimated at tunnel level

Table 15. Key characteristics of the three case studies.

Tunnel	**JLE – Westbound**	**JLE – Eastbound**	**FL at Green Park**
Depth (mBGL)	31	20.5	29.3
Excavated diameter (m)	4.85	4.85	4.146
Volume loss (%)	3.3	2.4	1.45
Host formation	London Clay	London Clay	London Clay
S_u (kPa)	180	120	170
E_u (MPa)	130	75	45

Although all three tunnels were excavated in London Clay, it can be seen that a variety of conditions is encompassed in the case studies.

5.2.2 Short-term settlement at ground surface

The author has run 2D plane strain FE analyses with linear elastic-perfectly plastic constitutive laws, with total stress modelling of the undrained response of the London Clay and of any other fine-grained layer. The ground profiles adopted in the models included relatively thin layers of coarse-grained materials near or at the surface; these materials were modelled in effective stress.

For clarity, it is work recalling that in the present study the focus is on the capability to calculate realistic settlement troughs with the finite element method. No attempt was made to use the numerical method to predict the volume loss associated to the excavation technique. In this context the volume loss (effectively an area loss in the 2D models) is an input parameter and the quality of the FE analysis is judged against the resemblance of its output, in terms of ground movements, to the actual observations.

The target area loss in the calculations was applied thought the stress-relief method (Panet & Guenot 1982, Schikora & Fink 1982). In order to control accurately the area loss in the model a simple spreadsheet developed to calculate, from the Plaxis output, the area of the tunnel cross-section in the initial, undeformed mesh and the area after the construction is completed in the model.

As expected, the use of a realistic values of the coefficient of earth pressure at rest leads to a far too wide and too shallow trough.

Alternative approaches to improve the results were tried; in particular:

a - an alternative implementation of "stress relief" in which a radial pressure is applied to the unsupported clay wall in the phase preceding the lining installation

b - the introduction of softened zones (lower strength and/or stiffness) in the regions experiencing plasticity, for both traditional and alternative stress relief implementation

These two approaches did not improved the output.

The sensitivity of the settlement profile to the initial stress state was checked varying the ratio between horizontal total stress and vertical total stress in the over-consolidated clays; these include the London Clay in all three cases and, for the two tunnels of the JLE, the underlying Lambeth Group clays. The initial horizontal stresses in the shallow, normally consolidated soils that are present on top of the London Clay were kept at realistic values.

It was found that, consistently, a stress ratio of 0.5 returns settlement profiles at ground surface that fit well the observed data.

5.2.3 Settlement at depth

For the Green Park case, measurements of vertical displacement at depth are also available and the performance of the FE model is good in this respect. The finite element analysis returns a good estimate of maximum settlements for the upper 15 m, corresponding to about half of the tunnel depth. Below that level, although the quality of the results remains reasonably good, the numerical analysis tends to slightly overestimate the settlement.

5.2.4 Summary

In the three case studies considered in this work, a good approximation of the settlement profile at ground surface was obtained with a finite element analysis in which all geo-mechanical parameters were assigned their most realistic values but total stress ratio in the overconsolidated clays – likely to be above 1 in reality – was artificially reduced to $k_0 = 0.5$.

These results were obtained for tunnels with excavated diameter between 4.146 and 4.85, at a depth ranging from 20.5 to 31 meters, which experienced volume losses between 1.45% and 3.3%.

The over-consolidated clay of the host formation had a range of undrained shear strength at tunnel level between 120 kPa and 180 kPa and a range of estimated undrained Young's modulus going from 45 MPa to 130 MPa.

The analysis of three case histories is not sufficient to demonstrate that the approach is universally valid for any stiff clay. However, considering the low sensitivity of the settlement trough to variations in soil strength and stiffness (parameters which do not appear in the analytical solutions based on Gaussian, or other, distributions), it is reasonable to expect that the approach developed here would enable realistic calculations of settlement for most stiff clays.

5.3 Limitations

The conclusions summarised in the previous section are based on three case studies in London Clay for a limited range of tunnel diameters, tunnel depths and volume losses. Although it is expected that similar results would be obtained for other stiff clays, caution should be exercised when extending the findings outside the range of originally considered circumstances.

This study did not take into account the long term response of soil to tunnelling and only focused on the short-term ground movement, which are generally considered to be critical as they induce larger differential settlements and distortions.

5.4 Recommendations

5.4.1 Recommendations to the users of the proposed approach

The author has found that the accurate implementation in the calculations of the desired area loss is not always straightforward and that automated procedure available in the software not always lead to optimal results. In this work, in order to control accurately the area loss in the model, a simple

spreadsheet was developed. The spreadsheet allows to calculate, from the FE output, the area of the tunnel cross-section in the initial phase and after the tunnel construction.

It is recommended that the user adopts this procedure or an equivalent one which offers the same level of control and reliability.

5.4.2 Recommendations for future studies

This work only encompasses three case histories in London Clay. Future studies should consider other soils and other configurations.

Importantly, once the capability to model green field displacement is ascertained, the problem of the interaction of tunnelling-induced ground movements with pre-existing structures should be studies. It is in this context that the true potential of the methodology lies.

References

Addenbrooke, T.I., Potts, D.M. & Puzrin, A.M., 1997. The influence of pre-failure soil stiffness on the numerical analysis of tunnel construction. *Géotechnique*, 47(3), pp.693–712.

Atkinson, J. H. Potts, D.M., 1977. Stability of a shallow circular tunnel in cohesionless soil. *Géotechnique*, 27(1), pp.203–215.

Attewell, P.B., 1978. Large ground movements and structural damage caused by tunnelling below the water table in a silty alluvial clay. In J. D. Geddes, ed. *Proc. Conf. Large Ground Movements and structures Cardiff*. Pentech Press, Plymouth, pp. 307–56.

Attewell, P.B. & Farmer, W.I., 1974. Ground deformations resultinf from shield tunnelling in London Clay. *Canadian Geotechnical Journal*, 11(3), pp.380–395.

Attewell, P.B. & Woodman, J.P., 1982. Predicting the dynamics of ground settlement and its derivitives caused by tunnelling in soil. *Ground Engineering*, 15(8), pp.13–22.

Attewell, P.B., Yeates, J. & Selby, A.R., 1986. *Soil movement induced by tunnelling and their effects of pipelines and structures.*,

Boscardin, M.D. & Cording, E.J., 1989. *Building Response to tunnelling, Case studies from construction of the Jubelee Line Extension, London* J. R. Burland, J. R. Standing, & F. M. Jardine, eds., Thomas Telford Publishing.

Brinkgreve, R.B.J. and V.P.A., 1998. *PLAXIS Manual* the N. R.B.J., Brinkgreve Deft University of Technology & PLaxis bv., ed.,

Brinkgreve, R.B.J., Engin, E. & Swolfs, W.M., 2014. *PLAXIS 2D: Reference, Scientific and Dynamic Manuals* B. (2002), ed.,

Bull, W.J., 2003. *Numerical Analysis and Modelling in Geomechanics*, CRC Press.

Burland, J.B. & Kalra, J.C., 1987. Queen Elizabeth II Conference Centre : geotechnical aspects. In *Proc. Instn Civ. Engrs, Part 1*. pp. 1479–1503.

Burland, J.B., Standing, J.R. & Jardine, F.M., 2001. *Building Response to tunnelling: case studies from construction of the Jubilee Line Extention*, London: Thomas Telford Publishing.

Burland, J.R. & Standing, J.B., 2006. Unexpected tunnelling volume losses in the Westminster area, London. *Géotechnique*, 56(1), pp.11–26.

Cording, E.J. & Hansmire, W.H., 1975. Displacement Around Soft Ground Tunnels. In *5th American Conference on Soil Mechanics and Foundation Engineering*. Buonos Aires, pp. 571–632.

Davies, H.R., 1999. Design and construction of the Jubilee Line Extension tunnels. In *Proc. Instn Civ. Engrs Civ. Engng, Jubilee Line Extension*. pp. 26–35.

Desai, C.S. & Gioda, G., 1990. *Numerical Method and Constitutive Modelling in Geomechanics*, Springer Limited, London.

Doležalová, M., 2002. Approaches to numerical modelling of ground movements due to shallow tunnelling. In *2nd Int. Conf. on Soil Structure in Urba Civil Engineering, ETH Zürich*. pp. 365–376.

EN, B., 1997. *Eurocodice 7: Geotechnical design-Part 1: General rules*, British Standarts, UK.

Franzius, J.N., Potts, D.M. & Burland, J.B., 2005. The influence of soil anisotropy and K0 on ground surface movements resulting from tunnel excavation. *Géotechnique*, 55(3), pp.189–199.

Gioda, G & Locatelli, L., 1999. Back analysis procedures for the interpretation od field mesasurements in geomechanics. *International Journal for Numerical and Analytical Methods in Geomechanics*, 23, pp.1407–1425.

Gonzalez, A. N., Rouainia M., Arroyo M., and Gens. A., 2012. "Analysis of Tunnel Excavation in London Clay Incorporating Soil Structure." *Géotechnique* 62, no. 12: 1095–1109.

González-Cao, J., Varas F., Bastante F.G., and Alejano. L.R., 2013. "Ground Reaction Curves for Circular Excavations in Non-Homogeneous, Axisymmetric Strain-Softening Rock Masses." *Journal of Rock Mechanics and Geotechnical Engineering* 5: 1–12.

Guedes, R.J. & Santos Pereira, C., 2000. The role of the soil Ko value in numerica analysis of shallow tunnels. In *Proc. Int. Symp Geotechnical Aspects of Underground Contruction in Soft Ground*. Tokyo, pp. 379–384.

Gunn, M.J., 1993. The prediction of surface settlements profile due to tunnelling. In *Predictive Soil Mechanics, Proc. Wroth Memorial Symposium*. Thomas Telford Publishing.

Hansmire, W.H. & Cording, E.J., 1972. Performance of a soft ground tunnel on the Washington metro. In *North American Rapid Excavation and Tunneling Conference Proceedings*. Chicago, pp. 271–289.

Higgins, K.G., Potts, D.M. & Mair, R.J., 1996. Numerical modelling of the influence of the Westminster Station excavation and tunnelling on Big Ben Clock Tower. In *Proc., Int. Symp. on Geotechnical Aspect of Underground Construction in Soft Ground*. Rotterdam: preprint vol., pp. 511–516.

King & Chris, 1981. *The stratigraphy of the London Clay and associated deposits*, Backhuys.

Lee, G.T.K. & Ng, C.W.W., 2002. Three-dimensional analysis of ground settlements due to tunnelling:role of K0 and stiffness anisotropy. In *Proc. Int. Symp on Geotechnical Aspects of Underground Construction in Soft Ground*. Toulousse, pp. 617–622.

Li, Y. & Shen, Z., 2004. Improvements on the arc-length-type method. *Acta Mechanica Sinica*, 20(5), pp.541–550.

Likitlersuang, S., Surarak C., Wanatowski D., Oh E., and Balasubramaniam. A., 2013. "Geotechnical Parameters from Pressuremeter Tests for MRT Blue Line Extension in Bangkok." *Geomechanics and Engineering* 5, no. 2: 99–118.Loganathan, N. & Poulos, H.G., 1998. Analytical Prediction for Tunnel-Induced Ground Movements in Clays. *Journal od Geotechnical and Geoenviromental Engineering*.

Mair, R.J., 2006. Tunnelling and geotechnics: new horizons. *Géotechnique*, 58(9), pp.695–736.

Mair, R.J. & Dimmock, P.S., 2007. Volume loss experienced on open-face London Clay tunnels. *Geotechnical Engineering*, 160(GEI), pp.3–11.

Mair, R.J. & Jardine, M.F., 2001. Tunnelling methods. In J. R. Burland & S. and J.B., eds. *Building response to tunnelling*. Thomas Telford Publishing.

Mair, R.J., Taylor, R.N. & Bracegirdle, A., 1993. Subsurface settlement profiles above tunnels in clays. *Geotechnique*, 43(2), pp.315–320.

Mitchell, B., 2003. *Jubilee Line Extension- from concept to completion*, London: Thomas Telford.

Muir Wood, A.M., 1975. The circular tunnel in elastic ground. *Géotechnique*, 25(1), pp.115–127.

New, B.M. & Bowers, K.H., 1994. Ground Movement Model Validation at the Heathrow Express Trial Tunnel. In *Tunneling*. pp. 301–329.

O'Reilly, M.P. New, B.M., 1982. Tunnelling induced ground movements.pdf. *Institution of Mining and metallurgy*, pp.p. 173–181.

Oasys, 2013. *Xdisp Tutorial Manual*, London, UK.

Page, D.P., 1995. Jubelee line extension. *Quarterly Journal of Engineering Geology and Hydrogeology*, 28(2), pp.97–104.

Page, D.P. & Skipper, J., 2000. The Lithological Characteristics of the Lambeth Group. *Ground Engineering*, 33(2), pp.38–44.

Panet, M. & Guenot, A., 1982. Analysis of convergence behind the face of a tunnel. In *Proceedings of the International Conference on Tunnelling,*. Brighton: The Institution of Mining and Metallurgy, pp. 197–204.

Peck, R.B., 1969. Deep Excavation and Tunnelling in Soft Soils. In *7TH International Conference on Soil Mechanics and Foundation Engineering.* Mexico City, pp. 225–290.

Potts, D.M. & Zdravkovic, L., 1999. Finite element analaysis in geotecnical engineering. Theory. , p.458.

Potts, D.M. & Zdravkovic, L., 2001. *Finite element analysis in geotechnical engineering application (vol.2)*, Thomas Telford Publishing.

Schikora, K. & Fink, T., 1982. Berechnungsmethoden moderner bergmännischer Bauweisen beim U-Bahn-Bau. *Bauingenieur*, 57, p.S. 193–198.

Schmidt B, 1969. *Settlements and ground movements associated with tunnelling in soil*. University of Illinois.

Simpson, B. Atkinson J.H. and Jovicic. V. 1989. *The engineering implicationd of rising groundwater levels in the deep aquifer beneath London*,

Simpson, B., Atkinson, J.H. & Jovicic, V., 1996. The influence of anisotropy on calculations of ground settlements above tunnels. In *Proc. of the International Symposium on Geotechnical Aspects of underground Construction in Soft Ground*. pp. 591–594.

Ward, W.H. & Thomas, H.S.H., 1965. The development of eart loading and deformation in tunnel linings in London Clay. In *Proc. 6th Int. Conf. Soil Mech and Found. Engng*. pp. 432–36.

Withers, A.D., Page, D.P. & Linney, L.F., 2001. *Geology and geotechnical properties*, Thomas Telford Publishing.

Wongsaroj, J., Soga, K. & Mair, R.J., 2007. Modelling of long-term ground response to tunnelling under St James's Park, London. *Géotechnique*, 57(1), pp.75–90.

Yeates, J., 1985. The response of buried pipelines to ground movements caused by tunnelling in soil. In J. D. G. P. P. Press, ed. *Proc. 3rd Int.Ground Movements and Structures.* Cradiff, pp. 145–60.

Zaman, M., Gioda, G. & Booker, J., 2000. *Modeling in Geomechanics*, Chichester, UK: John Wiley & Sons.

Zienkiewicz O.C., 1977. *The Finite Element Method* 3rd ed., Mc Graw-Hill.

Zienkiewicz, O.C. & Cheung, Y.K., 1967. *The finite element method in structural and continuum mechanics* McGraw-Hill, ed.,

Zienkiewicz, O.C., Taylor, R.L. & Zhu, J.Z., 2005. *The Finite Element Method Set (Sixth Edition)*, Elsevier.

Appendix A

A.1 Introduction

This appendix summarizes the basic concepts of the finite element method (FEM) and of its application to the field of geo-mechanics. Moreover, details are provided on how the method is implemented in Plaxis, the computer program that has been used to develop the numerical analyses presented in this thesis. A more detailed description of the method can be found in Zienkiewicz *et al*. (2005). A discussion of its application to geotechnical problems can be found in Desai & Gioda (1990) and Potts & Zdravkovic (2001). The implementation in Plaxis is described in the software's scientific manual (Brinkgreve *et al*. 2014).

Physical problems of all sorts can be studied through the use of mathematical models described by partial differential equations and by the appropriate boundary conditions and initial conditions. However, it is often impossible to solve the closed form of the partial differential equations associated to problems of practical relevance. The FEM provides an approximate, numerical solution to set of differential equations by dividing a continuum in a finite number of elements, defined by discrete points called nodes. The discretization of the system allows to approximate the differential equations with algebraic equations.

The FEM is, therefore a general method for the solution of any problem that can be associated to a continuous domain and described by differential equations. A fundamental contribution to the theory and application of the FEM is the work of Zienkiewicz and Cheung (1967). In Zienkiewicz's words, the FEM is "*a general discretization procedure of continuum problems posed by mathematically defined statements"* (Zienkiewicz 1977). It should be understood that there will be a discrepancy between the exact solution and the numerical results obtained with a finite element analysis. The accuracy of the approximation will depend on many factors like: the refinement of the mesh, the interpolation functions and the solution strategy that are discussed more in depth later in this appendix.

Nowadays, the finite element method is widely employed in the scientific investigation and the engineering application in many braches of fluid mechanics and solid mechanics.

In the following sections

- the general principles of the method will be concisely introduced with reference, for simplicity, to a solid mechanics framework

- some aspects that are specific to soil mechanics will be discussed

- some details of the implementation of the method in Plaxis will be provided

- the use of the method in this thesis will be briefly detailed.

A.2 The Finite Element Method

Outline

The key conceptual steps on which the numerical method is base are:

a) Element discretization

The geometrical domain of the problem is discretized in a finite number of small regions called elements. Adjacent elements exchange action only at common points called nodes.

b) Primary variable approximation

A primary variable must be selected, usually displacement is the unknown variable selected for geotechnical problems. Then the variation over the finite element of the variable must be established.

c) Formulation of element equations

Using an appropriate variation principle (e.g. minimum potential energy or others) the element equations are derived in the form:

$$\boldsymbol{K}\,\Delta v = \boldsymbol{f}$$

Where $\boldsymbol{K}$ is the stiffness matrix**,** Δv is the vector of incremental element nodal displacements and $\boldsymbol{f}$ is the vector of incremental element nodal forces.

d) Formulation of global equations

Combine element equations to form global equations by assembling all the previous

$$\boldsymbol{K}_g\,\Delta v_g = \boldsymbol{f}_g$$

e) Definition of boundary conditions

Establish appropriate boundary conditions that represent the boundary value problem to be solved.

f) Solve the global equation

The global equations are in the form of a large number of simultaneous equations, solving those the displacements will be obtained at all nodes. The secondary variable of engineering relevance, like stresses and strain, will be evaluated from displacements.

Discretization

The first step will be to transform a continuum problem to a discrete model subdividing the geometry in several small regions called finite elements, interconnected by points common to two or more elements and by boundary lines. For two dimensional problems, the finite elements are usually triangular or quadrangular in shape. Based on the geometry of the problem, the right finite elements can be chosen. For geotechnical problems, the main requirement is that the elements should be applicable to all the geometric situation such as curved boundary (very common when dealing with tunnel excavation). The number of elements and the size of these depend on the material behavior. Zones where the unknown variable varies rapidly need to be refined, with smaller elements and, hence, more dense nodes, as well as zones with point load or zone around structural elements. Elements with irregular or extreme geometries should be avoid. For example, quadrangular elements that appear particularly long and narrow may not perform well in the calculation. Similarly, triangular elements with particularly acute angles may generate numerical problems. In general, a “smooth” result, in terms of variation in space of the primary variable, is a good indication of sufficiently fine mesh.

Displacement approximation

Each element has a number of nodes, each with some degrees of freedom that correspond to the discrete values of the displacement components.

To describe the behavior on a single element it is adopted a local coordinate system (ξ, η, ς) that will be discerned from the global one (*x,y,z*).

Within a local element the displacement field $\underline{u}(\xi, \eta, \varsigma)$ is obtained from the discrete nodal values in a vector $\underline{v}(\xi, \eta, \varsigma)$ using interpolating functions, called shape functions $\underline{\underline{N}}(\xi, \eta, \varsigma)$.

$$u = \boldsymbol{N}_i v_i$$

In other words once the position ξ of a point within the element i is known, the displacement of that point can be calculated as interpolation of the displacements of the nodes in the elements v_i:

$$u(\xi) = \sum_{i=1}^{n} N_i(\xi) v_i$$

The shape functions or interpolation functions N_i describe how these displacements vary over the domain under investigation. Those shape functions satisfy continuity between two contiguous elements.

If the geometry of the global element can be derived from the local element using the same shape functions the element is called *isoparametric*. Strains are derived from the displacements. Once the strain has been calculated for the local element, the strain in the global system can be defined.

$$\varepsilon(x, y, z) = B_i v_i$$

The matrix B contains the derivatives of N_i with respect to the global coordinates. The relationship between local and global derivative involves the Jacobian matrix J.

Low order polynomials are typically chosen as shape functions in practice. In particular, the shape functions are polynomial depending on the number of nodes within the element and will affect the approximation of the finite element method. In a 3-node triangular element the shape functions will be linear. This implies linear variation of the displacements across the element. To have a better, smoother representation of the displacement is a single element it is necessary to increase the number of nodes in the element. The overall accuracy of the method over a geometrical domain can also be improved increasing the number of elements and, therefore, generating a finer mesh with smaller elements.

Requirement for a general solution

In general, the theoretical solution must satisfy equilibrium, compatibility, the constitutive model (stress-strain or force-displacement law) and boundary conditions. The contemporary satisfaction of all the conditions leads to the solution of the mathematical problem. In the Finite Element Method equilibrium and compatibility are not satisfied everywhere in the domain but only at discrete nodes. The solution of the partial derivative equations does not have to hold in absolute terms, what is sought is the solution of the weak or integrated form of it. The solution of the weak form satisfy the differential equations only on average, it does not satisfy it in all the points.

The solid body equilibrium can be imposed by means of a number of equivalent criteria, including the principle of minimum potential energy and the principle of virtual work.

Numerical integration

The explicit evaluation of the partial differential equation cannot be performed, therefore a numerical integration scheme is employed. Essentially, the integration of a function is replaced by the weighted sum of the function evaluated in certain points, internal to the element, called integration points or Gauss points. The values of the weight and the location of the integration points depend on the integration scheme used.

Global equations

The global equations are formed by assembling all the separate element equations.

The terms of the global stiffness matrix are obtained by summing the individual element contributions whilst taking into account the degrees of freedom which are common between elements. The global stiffness matrix K_g, it is symmetric and normally shows a band width depending on the global numbering.

$$K_g \, \Delta v_g = f_g$$

The same procedure is followed for the right hand side of the equation (f_g), where the load vector is obtained by summing the individual loads acting on each node.

Careful arrangement of the nodal numbering can results in more efficient calculations thanks to a reduced bandwidth of the global stiffness matrix.

Boundary conditions

The relevant set of boundary conditions has to be imposed to the global system of equations. In general terms, tree different kinds of boundary conditions can be modeled (Potts & Zdravkovic 1999).

The first kind affects only the left hand side $(\boldsymbol{K}_g)$ of the system equations. These boundary are loading conditions such as point loads, boundary stresses, body forces, construction and excavation (i.e. elements activation or deactivation).

The second kind of boundary conditions affects only the left hand side $(\boldsymbol{f}_g)$ of the system of equations. These are kinematic conditions such as prescribed displacements (including the various types of fixities generally established at the sides and base of most meshes).

The third and final kind of boundary conditions are more complex, since they affect the whole structure of the system equations. Those include local axes, which require a transformation of the stiffness matrix and the right hand side load vector, tied freedoms and springs, which affect the numbering of the degrees of freedom and the stiffness matrix assembly procedure(Potts & Zdravkovic 2001).

A.3 Application to geomechanics

Overview

The finite element method provides a powerful tool for the analysis of geotechnical problems. In fact, this numerical approach can capture the essence of soil-structure interaction problems, in which relative movement of the structure with respect to the soil can occur and has a fundamental impact on the system's performance. The possibility to model excavations and construction stages through the deactivation or activation of elements is also advantageous.

There are several specificities that set the geomechanical calculations apart from other solid mechanics applications.

A notable aspect is the need to often treat the soil a bi-phase material, in which solid skeleton and pore water interact and the soil behavior is governed by the components of effective stress (important exceptions are completely dry soils and the total stress modelling of fully saturated fine-grained soils in undrained conditions).

A second typical characteristic of finite element modelling in geotechnics is the frequent need to account for a considerable amount of non-reversible displacement, which results in highly non-linear calculations. For this reason, elastic-plastic behavior is discussed more in detail in the following sections.

It is worth remembering, at this stage, that the complexity of the soil behavior is also caused by various other phenomena: particles interactions, compaction and dilatancy, anisotropy, consolidation, viscosity and other forms of time-dependent behavior. These considerations prompted Brinkgreve (2013) to remind his reders that despite the development of easy-to-use finite element programs, it may still be challenging to create a good model that enables a realistic analysis of the physical processes involved in a real project and that provides realistic quantities of design quantities. For the sake of briefness, however, reference is made, with regards to the advances aspect mentioned above to the texts by Desai & Gioda (1990) and Potts & Zdravkovic (2001). In the following section, instead, a short description of the elasto-plasticity framework is provided.

Elasto-plasticity

Elastic-plastic calculations

Most geotechnical problems invoke the necessity to model the possibility that the soil develop significant irreversible strain. In this problems, it is essential to use an elastic-plastic constitutive model, Three elements are needs to be included in elastic-plastic calculations: a yield function, a plastic potential function and a flow rule.

Yield function

In its simplest form the yield function if a scalar function of the stress components that define when plastic strain occurs:

$$F(\sigma') = 0$$

For stress states where $F < 0$ the material behavior is elastic, $F = 0$ identify the onset of plastic strain; stress states with $F > 0$ are not allowed. Mohr-Coulomb criterion is often used as the yield function in geotechnical modelling.

In this case, the yield function is a fixed surface in the principle stresses space and the material behavior is described as perfectly plastic. However, in a more advanced form of modelling, the yield function may expand or shrink in relation to a variable selected as hardening parameter *k*

$$F(\sigma', k) = 0$$

Now the variation of deformation can be divided into an elastic and a plastic component as follow:

$$\delta\varepsilon = \delta\varepsilon^e + \delta\varepsilon^p$$

The elastic increment is calculated knowing the elastic constitutive matrix, while the plastic increment is necessary to define a plastic potential and a flow rule.

Plastic potential and flow rule

The direction of the plastic vector $\delta\varepsilon^p$ is specified through a flow rule:

$$\delta\varepsilon^p = \Lambda\frac{\delta P}{\delta\sigma_i}$$

Where $\frac{\delta P}{\delta\sigma_i}$ in normal vector to the plasticity condition, P is a function of the stress state called plastic potential, and Λ is a negative scalar multiplier that controls the magnitude of the incremental strain components. When the plastic potential coincides with the yield function the flow rule is called associated and the plastic strain is normal to the yield surface. When this happens the normality condition is said to be applied. When the potential and the yield function differ the flow rule is said to be non associated. The flow rule is of great importance since controls the dilatancy of the soil, which in turn has a significant influence on volume changes and strength.

Non-linear solution methods

If the soil is modelled and an elastic-plastic material (or even a non-linear elastic material), the equivalent constitutive matrix is no longer constant, but varies with the stress and/or strain. It therefore changes during a finite element analysis.

The finite element method can be adapted to deal with nonlinear constitutive models and several strategies have been formulated to do this. All these solutions involve applying the boundary conditions incrementally. Depending on the solution strategy adopted the accuracy of the results is strongly influenced (Potts & Zdravkovic 1999).

When the relation between stress increments and strain increments is non-linear, a global iterative procedure is required to satisfy both the equilibrium and the constitutive relation. To tackle this problem the finite element equations are reduced to an incremental form:

$$K^j \delta v^j = f_{ex}^i - f_{in}^j$$

The superscript j refers to the iteration number, δv is a vector containing sub-incremental displacements and where n is the number of iterations within step i. The final solution is obtained by summing the results of each increment.

$$\Delta v^i = \sum_{j=1}^{n} \delta v^j$$

This method is also known as *initial stress method*, consist in subdividing the total load in a sum of increments, the stress and strain resulted from the increment of load are calculated with an iterative process. The iteration starts with the calculation of the increments in stress $\Delta\sigma'_1$and strain in every finite element. Commonly the stress increment $\Delta\sigma_1{}'$will violate the condition imposed by the yield criterion. So based on the strain increment and the constitutive matrix it is calculated a new stress increment $\Delta\sigma_1$ that fulfil the requirement of the yield surface. To do so on each element it is applied a set of nodal force $(\Delta\sigma'_1 - \Delta\sigma_1)$ so that the incremental stress acting on the node is now actually respecting the yield criterion. Now this extra set of forces as to be removed allowing the structure to deform further. New incremental stress and strain are calculated and the iteration keep going until the extra nodal forces are so little that can be ignored. A tolerance is set and this will regulate what is the acceptable value of "out-of- balance" forces. When the initial stress method converge the solution will respect the equilibrium and the yield criterion. This method has the advantage to

This iteration is performed without updating the stiffness matrix during the iteration. This is assumed to be constant that is an advantage since is not required the calculation of a whole new matrix. But in some nonlinear static analysis, for instance when softening is present, this might be a problem since the tangent stiffness matrix may become singular causing several convergence difficulties. For such situations the arch-lengh method is useful to avoid bifurcation points and track unloading.

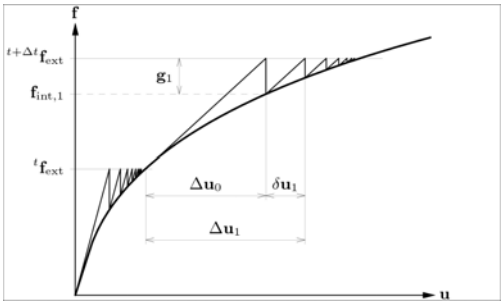

Figure A-1

The arch-length method brings the iterations to converge along an arc. Ordinary solution techniques lead to instability near the limit points and also have problems in case of snap-through and snap-back. Thus they fail to predict the complete load-displacement response. In the case no failure occurs there will be no differences between the results obtained with the arc-length control and the one obtained using another method. But when failure occurs the failure load will be determined at the end of the calculation with the arc-length method.

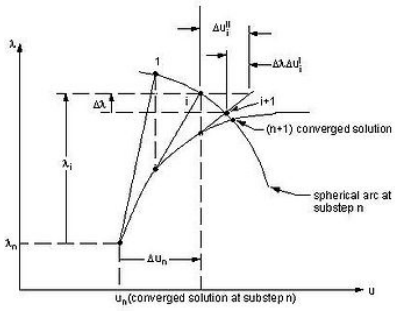

Figure A-2

A.4 Implementation in PLAXIS 2D

Overview

Plaxis 2D can solve bi-dimensional plane strain and axisymmetric problems. In 2D plane-strain analyses, the displacements and strain in *z*-direction are assumed to be zero. However, normal stresses in z-direction are fully taken into account. An axisymmetric model is used for circular structures with a uniform radial cross section and loading scheme around the central axis, where the deformation and stress state are assumed to be identical in any direction (Brinkgreve et al. 2014).

Basic equations of continuum deformation

In PLAXIS the equilibrium of the body is imposed through the use of the principle of virtual work (PVW). The PVW is a necessary and sufficient condition for the equilibrium. This principle states that the equilibrium of the body requires that for any compatible, small virtual displacements imposed onto the body, the total internal virtual work is equal to the total external virtual work.

$$\int \delta\varepsilon^T * \sigma \; dV = \int \delta u^T b \, dV + \int \delta u^T t \, dS$$

Where t is the vector containing the forces on the boundary, while b is the vector of the volumetric forces acting on the body examined.

Implementing the strain-displacement relation as follow:

$$\varepsilon = \boldsymbol{B}\, v$$

Where $\boldsymbol{B}$ is the matrix that contains the derivatives of the shape functions. As the strain and the stress vector have 6 components in a three dimensional problem, $\boldsymbol{D}$ must be a 6x6 matrix.

The development of the stress state σ can be regarded as an incremental process:

$$\sigma^i = \sigma^{i-1} + \Delta\sigma$$

$$\Delta\sigma = \int \dot{\sigma}\, dt$$

Considering all the definitions above the pwv becomes:

$$\int \delta\varepsilon^T * \Delta\sigma \; dV = \int \delta u^T b^i \, dV + \int \delta u^T t^i \, dS - \int \delta\, \varepsilon^T \sigma^{i-1} \, dV$$

Using the compatibility and the constitutive law the equilibrium equation can be written as:

$$\int (B\delta v)^T * \Delta\sigma \; dV = \int (N\delta v)^T b^i \, dV + \int (N\delta v)^T t^i \, dS - \int (B\delta v)^T \sigma^{i-1} \, dV$$

The discrete displacement can be placed outside the integration as:

$$\delta v^T \int B^T * \Delta\sigma \; dV = \delta v^T \int N^T b^i \, dV + \delta v^T \int N^T t^i \, dS - \delta v^T \int B^T \sigma^{i-1} \, dV$$

$$\int B^T * \Delta\sigma \; dV = \int N^T b^i \, dV + \int N^T t^i \, dS - \int B^T \sigma^{i-1} \, dV$$

Implementing the constitutive model and the definition of matrix of stiffness:

$$\dot{\sigma} = D\,\dot{\epsilon} \qquad\qquad K = \int B^T D B \det(J) dV$$

The equilibrium for each element is obtained:

$$K^i \Delta v^i = f_{ex}^i - f_{in}^{i-1}$$

Where f_{ex}^i is the vector of the external forces and f_{in}^i is the vector of the internal reaction vector. The superscript *i* refers to the step number. However, because the relation between stress increments and strain increments is generally non –linear, the stiffness matrix cannot be formulated exactly beforehand.

Elements

The elements available in Plaxis are 6-nodes and 15-nodes triangular elements. The 15-nodes triangle provides a fourth order interpolation for displacement and the integration involves twelve stress points. The 6-node triangle provides a second order interpolation for displacements and the numerical integration involve three stress points. Structural elements are available as well as well as interfaces elements. The first are similar to the 6-nodes element but instead of tree degrees of freedom they have six degrees of freedom per node: tree displacements and tree rotation. The interface elements have pairs of nodes instead of single nodes.

In terms of Gaussian integration the number of Gauss points depends on the type of element. In PLAXIS the 6-nodes element has three integration points. Here an example of the numerical integration:

$$\int_{-1}^{1} \int_{-1}^{1} f(\xi, \eta) \, d\xi \; d\eta = \sum_i \sum_j f(\xi_i, \eta_i) \, w_i \, w_j$$

The structural elements formulated in Plaxis are obtained by essentially collapsing one, or more dimensions to zero.

Integration method

The integration procedure implemented in PLAXIS use the elastic stiffness matrix, and it gives a robust iterative procedure as long as the material stiffness does not increase, even when using non associated plasticity models. The arc-length control (Li & Shen 2004) is used to facilitate and accelerate convergence, over relaxation and extrapolation are also used to improve the iteration process. Plaxis also implement an automated step size selection (Brinkgreve et al. 2014).

Use of method and software in this thesis

The analysis presented in this thesis are all in plain strain conditions and were carried out using 6-node triangular elements. A tunnel excavation is a markedly tree-dimensional problem and dedicated techniques, described in Section 2 have been adopted to reflect the 3D effects in the 2D calculations.